EXPERIMENTAL INVESTIGATION AND RHEOLOGICAL MODELLING OF THE FINE AGGREGATE MATRIX (FAM) PHASE IN THE MULTISCALE TRANSITION FROM BINDER TO ASPHALT MIXTURE

Dissertation

submitted to and approved by the

Faculty of Architecture, Civil Engineering and Environmental Sciences
Technische Universität Braunschweig

and the

Department of Civil and Environmental Engineering
University of Florence

in candidacy for the degree of a
Doktor-Ingenieurin (Dr.-Ing.) /
Dottore di Ricerca in Civil and Environmental Engineering*)
by

Chiara Pratelli
born 03/11/1989
in Lucca, Italy

Submitted on	23 January 2020
Oral examination on	22 April 2020
Professorial advisors	Prof. Michael P. Wistuba Prof. Massimo Losa

2020

*) Either the German or the Italian form of the title may be used.

Experimentelle Untersuchung und rheologische Modellierung der FAM-Phase (Fine Aggregate Matrix) in dem mehrskaligen Übergang vom Bindemittel zum Asphaltgemisch

Forschungsprojekt von Chiara Pratelli

Doctoral Candidate Dr. Chiara Pratelli

Supervisors Prof. Michael P. Wistuba
(TU Braunschweig)

Prof. Massimo Losa
(Università di Pisa)

ABSTRACT (in English)

In the last decades, the multi-scale approach has gained wide attention for studying and understanding the mechanisms affecting the performance of asphalt mixtures. According to such approach, the asphalt mixture could be seen as an assemblage of components of different length scales, each with its own mechanical properties, and thanks to the investigation on these lower scales a scale-wise insight can be gained and used to capture phenomena not considered in continuum approaches.
This Thesis is focused on the interrelation between the Fine Aggregate Matrix (FAM) the asphalt mixtures.

Fine aggregates, filler, binder and air voids compose the FAM, which represents the intermediate scale between mastic and asphalt mixture. This phase has a critical role in the overall performance evaluation of asphalt mixture and the simplicity, efficiency and the lower costs/times required to study the FAM make it a very attractive specification-type approach. However, despite the growing interest on FAM testing, there are some concerns about proper FAM mix design. Moreover, there are many lacks in predicting the performances of asphalt mixtures from the FAM phase.

The primary objective of this Thesis was the identification of a design method for FAM, which allows recreating the FAM phase, as it exists within the asphalt mixture. The selected design method has shown promising results and seems quite accurate in reproducing the FAM within the asphalt mixture.

The second issue which is pursued in this Thesis, is a multi-scale approach based on the rheological 2S2P1D model, allowing to interrelate the four material scales (from binder to asphalt mixture). Firstly, it was verified that the 2S2P1D model remains valid for FAM in the Linear ViscoElastic (LVE) range and that it could adequately fit experimental data of FAM. Then, it was possible to relate the different phases thanks to the definition of interrelationships between one model parameter.
The interrelation between the asphalt mixture and the corresponding FAM could be used to predict the rheological properties of the asphalt mixtures starting from FAM tests.

This methodology allows making reliable forecasts of the LVE behaviour of the asphalt mixtures, as demonstrated by the results of validation tests. Future developments will

investigate other volumetric compositions of mixes, to study the influence of microstructural and volumetric characteristics on the model parameters.

Keywords: *Multi-scale approach, Fine Aggregate Matrix-FAM, torsion bar, LVE range, rheology, 2S2P1D model, SHStS transformation.*

ABSTRACT (in Italian)

Il cosiddetto approccio "multi-scala" è utilizzato per lo studio e la comprensione dei meccanismi che influenzano le prestazioni dei conglomerati bituminosi. Secondo tale approccio le miscele possono essere viste come assemblaggi di componenti (sottofasi) e grazie allo studio, su scala ridotta, delle prestazioni di queste è possibile ricavare indici prestazionali delle miscele bituminose ed informazioni circa le loro performance in sito. Questa tesi si focalizza in particolare sulla comprensione dell'interrelazione tra la cosiddetta sottofase FAM e i conglomerati bituminosi.

Questa fase, intermedia tra i mastici e le miscele, ha un ruolo fondamentale nella valutazione complessiva delle prestazioni delle miscele bituminose, e la semplicità, l'efficienza e i minori costi e tempi dei test sui FAM li rendono ancor più interessanti. Ciononostante, esistono ancora delle riserve sul loro impiego per i test di caratterizzazione e classificazione delle miscele, dovute al mancato accordo sul loro corretto mix design e sulla fabbricazione di campioni rappresentativi delle miscele. Esistono inoltre delle carenze circa la modellazione delle prestazioni delle miscele a partire da test di laboratorio sui FAM.

Il primo obiettivo della presente Tesi consisteva nell'identificazione di un metodo per la corretta progettazione del mix design dei FAM. L'accuratezza del metodo selezionato è stata poi verificata empiricamente, risultando sufficientemente elevata.

Successivamente, per interrelazionare le quattro fasi analizzate (bitume, mastice, FAM e conglomerato bituminoso) è stato utilizzato un approccio multi-scala, basato sul modello reologico 2S2P1D. Dopo aver verificato che il modello fosse valido per la modellazione dei dati sperimentali dei FAM, si è proceduto alla ricerca di un'interrelazione di un parametro del modello (tempo caratteristico) tra le diverse fasi. In particolare, la determinazione della relazione tra il tempo caratteristico delle miscele e quello del corrispondente FAM può essere utilizzata per prevedere il comportamento delle miscele a partire dai dati sperimentali dei FAM.

La presente ricerca costituisce un importante riferimento per studi futuri, fornendo linee guida per la progettazione del mix design dei FAM e per la realizzazione dei campioni. Inoltre, fornisce alcuni interessanti spunti di approfondimento, legati allo studio

dell'influenza della composizione volumetrica e della microstruttura della miscela sui parametri del modello 2S2P1D.

Parole chiave: *Approccio Multi-Scala, Fine Aggregate Matrix-FAM, test con barra di torsione, ambito linear-viscoelastico, reologia, modello 2S2P1D, trasformazione SHStS.*

KURZFASSUNG (in German)

Der sogenannte "Multi-Skala" -Ansatz wird verwendet, um die Mechanismen zu untersuchen und verstehen, die die Leistung von bituminösen Konglomeraten beeinflussen. Nach diesem Ansatz können die Gemische als Baugruppen von Bauteilen (Teilphasen) angesehen werden, und dank der Untersuchung ihrer Leistung in kleinem Maßstab, ist es möglich Leistungsindizes der bituminösen Gemische und Performance-Informationen vor Ort zu erhalten.

Diese Arbeit konzentriert sich insbesondere auf das Verständnis der Wechselbeziehung zwischen der sogenannten FAM-Subphase und die bituminösen Konglomeraten.

Diese Phase zwischen Kitten und Gemischen spielt eine grundlegende Rolle bei der Gesamtleistungsbewertung von bituminösen Gemischen, und die Einfachheit, Effizienz und geringeren Kosten und Zeiten von FAM-Tests machen sie noch interessanter. Trotzdem bestehen weiterhin Vorbehalte gegen ihre Verwendung zur Charakterisierung und Klassifizierung von Gemischen, da keine Übereinstimmung über deren korrektes Mischungsdesign und über die Herstellung repräsentativer Proben der Gemische besteht. Es gibt auch Mängel bei der Modellierung der Leistung von Gemischen aus Labortests an FAMs.

Das erste Ziel dieser Arbeit war es, eine Methode für das korrekte Design des FAM-Mix-Designs zu identifizieren. Die Genauigkeit der ausgewählten Methode wurde dann empirisch verifiziert, was zu einem ausreichend hohen Ergebnis führte.

Anschließend wurde ein mehrskaliger Ansatz basierend auf dem rheologischen 2S2P1D-Modell verwendet, um die vier analysierten Phasen (Bitumen, Mastix, FAM und bituminöses Konglomerat) miteinander in Beziehung zu setzen. Nachdem wir überprüft hatten, ob das Modell für die Modellierung der experimentellen FAM-Daten gültig war, suchten wir nach einer Wechselbeziehung eines Modellparameters (charakteristische Zeit) zwischen den verschiedenen Phasen. Insbesondere kann die Bestimmung der Beziehung zwischen der charakteristischen Zeit der Gemische und der des entsprechenden FAM verwendet werden, um das Verhalten der Gemische ausgehend von den experimentellen Daten der FAMs vorherzusagen.

Diese Forschung stellt eine wichtige Referenz für zukünftige Studien dar und liefert Richtlinien für das Design des Mix-Designs der FAMs und für die Realisierung der Proben. Darüber hinaus bietet es einige interessante Einblicke in die Untersuchung des

Einflusses der volumetrischen Zusammensetzung und der Mikrostruktur des Gemisches auf die Parameter des 2S2P1D-Modells.

Schlüsselwörter: *Mehrskalenansatz, Feinaggregat-Matrix-FAM, Torsionsstab, LVE-Bereich, Rheologie, 2S2P1D-Modell, SHStS-Transformation.*

ACKNOWLEDGEMENTS

I would like to express my special thanks to my two supervisors, Prof. Michael P. Wistuba, from TU Braunschweig and Prof. Massimo Losa, from University of Pisa, who gave me the opportunity to do this incredibly instructive experience and for their guidance and support during these years. Despite my research path has been characterized by many ups and many downs, it has trained me to face difficulties, challenges and tough moments with a renewed trust in my skills.

I would like to thank Prof. Pietro Leandri for his inestimable support and encouragement, without forgetting his precious advices. He has been for me an example of passion for research and teaching, as well as a Friend.

I would like to thank Ing. Chiara Riccardi and her beautiful family, for their hospitality and support and for becoming my "second family" in Braunschweig.

I would like to thank all the members of the laboratory staffs, both in Italy and in Germany. Thank you for supporting and helping me in the most varied ways (from laboratory problems to electrical ones and so on).

I would like to thank more in general all the ISBS team, for involving me in many activities and experiences (from trekking in die Harz to Christmas party organization), making my stay in Braunschweig special.

I would like to thank all my friends, the old and the new ones, and my incredible colleagues for their unconditional encouragement during these years.

A special thanks also to my Lorenzo, for his love and patience during all my best times such as during the worst ones. Thanks for staying close to me even when I would have liked to run away from myself.

Lastly, I would like to thank all my beautiful family. We have been faced many terrible moments in these years. We lost many important "parts", but we are closer and stronger than ever.
Your support, example and unconditional love is my fundamental pillar.
This Thesis is dedicated to You and to our missing "parts".

INDEX

LIST OF ABBREVIATIONS AND VARIABLES

Abbreviations

DFAIB	*Fine Aggregate Initial Break Sieve*
DMA	*Dynamic Mechanical Analyzer*
DSR	*Dynamic Shear Rheometer*
FAIB	*Fine Aggregate Initial Break*
FAM	*Fine Aggregate Matrix*
LOE	*Line of Equality*
LVE	*Linear ViscoElastic*
MIX	*Asphalt Mixture*
NMAS	*Nominal Maximum Aggregate Size*
PCS	*Primary Control Sieve*
PG	*Performance Grading*
PMB	*Polymer Modified Binder*
PTTSP	*Partial Time-Temperature Superposition Principle*
RAP	*Recycled Asphalt Pavement*
RAS	*Recycled Asphalt Shingles*
RMSP	*Root Mean Squared Error in Percentage*
RTFO	*Rolling Thin-Film Oven*
RVE	*Representative Volume Element*
SBS	*Styrene Butadiene Styrene*
SCS	*Secondary Control Sieve*
SGC	*Superpave Gyratory Compactor*
T-f sweep test	*Temperature Frequency sweep test*
TRS	*Thermorheologically Simple*
TTSP	*Time-Temperature Superposition Principle*
WMA	*Warm Mix Asphalt*

Standards and protocols

AASHTO	*American Association of State Highway and Transportation Officials*
ASTM	*American Society for Testing and Materials International*
EN	*European Norm*
FGSV	*Forschungsgesellschaft für Straßen und Verkehrswesen*
NCHRP	*National Cooperative Highway Research Program*
SHRP	*Strategic Highway Research Program*

Models

2S2P1D	*2 Springs, 2 Parabolic elements, 1 Dashpot*
CAM	*Christensen-Anderson-Marasteanu*
MCF	*Moon-Cannone Falchetto*
SHStS	*Shift-Homothety-Shift in time-Shift*
WLF	*Williams-Landel-Ferry*

Variables

ρa	*Apparent Specific Density of aggregates*
ρrd	*Bulk Specific Density of aggregates*
ρssd	*Bulk Saturated Surface Dry Density of aggregates*
W_{A24}	*Water Absorption of aggregates*
Gsa	*Apparent Specific Gravity of aggregates*
Gsb	*Bulk Specific Gravity of aggregates*
Gse	*Effective Specific Gravity of aggregates*
Gb	*Specific Gravity of asphalt binder*
Gmb	*Bulk Specific Gravity of the asphalt mixture*
Gmm	*Theoretical Maximum Specific Gravity of the asphalt mixture*
VC%	*Mastic Volumetric Concentration*
at	*Time-Temperature Shift Factor*
bt	*Normal Shift Factor correction of Cole-Cole diagram*
J	*Radial Instrument Compliance*
Tg	*Glass Transition Temperature*
ε	*Axial Strain*
σ	*Axial Stress*
γ	*Shear Strain*
τ	*Shear Stress*
|E*|	*Complex Modulus*
E’	*Storage Modulus*
E’’	*Loss Modulus*
|G*|	*Complex Shear Modulus*
G’	*Storage Shear Modulus*
G’’	*Loss Shear Modulus*
δ	*Phase Angle*
fr	*Reduced Frequency*
ν	*Poisson’s Ratio*
τ_0	*Characteristic Time*
α	*Transformation Parameter*

CHAPTER 1

1. INTRODUCTION

Asphalt pavements are widely employed in different fields of public and private construction, including roadways, airport runways, parking lots, driveways and many more. A lot of money is spent every year on materials, machines and manpower for their construction and maintenance. Indeed, in addition to the cost of the materials, the process of constructing and maintaining these pavements is also very expensive and time-consuming. One of the most effective parameters to minimize these costs is the selection of appropriate materials for road construction.

The study on the fundamental properties of asphalt materials could be used to improve and maximize the performance potential of asphalt pavements. Indeed, the performance characteristics of asphalt mixtures, which behave in a viscoelastic manner, play the most influential role in designing asphalt pavements and the knowledge gained from these studies supports the design process and the development of longer-lasting and better-performing materials.

Asphalt mixtures must resist many distresses over their service lives, such as rutting, fatigue cracking, and moisture damage. The conventional and typical method to evaluate the performance properties of asphalt mixtures is by performing macro-scale mechanical tests under controlled laboratory conditions on asphalt mixture specimens. The advantages of this approach are that it considers the combined effect of all the constituent components of the asphalt mixtures and their overall interactions in terms of performance. Thus, it allows an efficient ranking of the candidate mixtures based on their performance properties. However, such laboratory tests are very time-consuming and require expensive equipments and skilled personnel to fabricate and test asphalt mixtures specimens.

Recently, several research studies have been undertaken to investigate the performance properties of asphalt mixtures using the so-called “multi-scale approach”. Such approach defines the asphalt mixture as an assemblage of components of different characteristic length scales, each with its own mechanical and engineering properties, and involves targeted experiments to gain scalewise insight. Indeed, many of the critical behaviors that affect asphalt mixtures performance are affected by localized behaviors that cannot be completely captured using traditional continuum modelling approaches.

The asphaltic mixtures can be considered as heterogeneous mixtures, a combination of various sizes of aggregates particles, which are bound together with asphalt binder. It is commonly modelled from a different length scales perspective as a composite material consisting of three constituents: air voids, asphalt binder and aggregates of different size and shape. Different research efforts have conventionally identified the following phases within the asphalt mixtures; namely, from the smallest scale (binder) to the largest (asphalt mixture itself):

- Binder: obtained from the distillation of crude oil. It composed primarily of hydrocarbons, but it may contain other constituents, including oxygen, nitrogen, sulphur and traces of metallic elements (e.g. vanadium, nickel and iron).

- Mastic: composed by mineral filler, ranging from 1 µm to 75-63 µm, in a binder matrix.

- Fine Aggregate Matrix (FAM): constitutes by fine aggregate particles usually smaller than 2 mm, with a specific gradation, in a mastic matrix (Arshadi & Bahia, 2015).

- Asphalt Mixture: which results from the combination of coarse aggregate particles at sizes up to 31.5 mm in a FAM matrix.

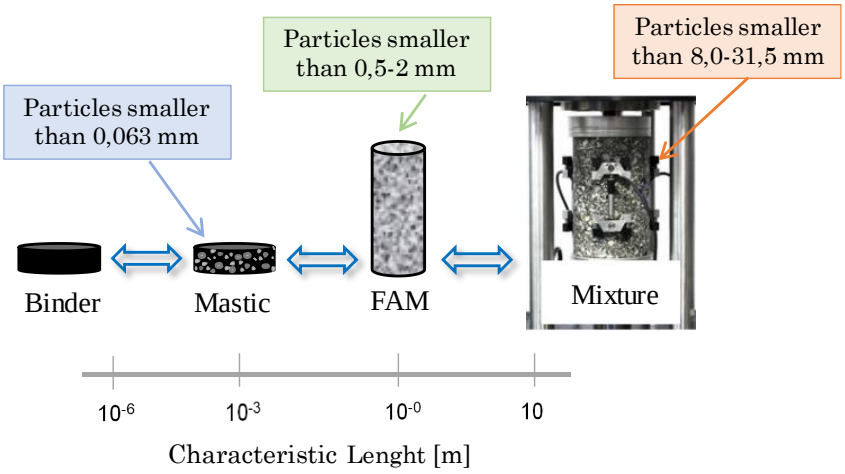

Fig. 1 *Multiscale framework of asphalt mixture.*

Many researchers investigated the fundamental behavior of asphalt mixtures through experiments on the asphalt binder only. However, a primary drawback to experiments on asphalt binder is that this material constitutes only approximately 4-6% of the total asphalt mixture mass (10-15% by volume) and interacts within the composite in a complex and

not completely understood manner. Thus, any observations made on asphalt binder must be tempered with the fact that the observed behaviors may be insignificant for the total response of the mixture (Underwood & Kim, 2013a).

More recently, several studies have highlighted the potentialities of laboratory tests on Fine Aggregate Matrix (FAM) to evaluate the performance of asphalt mixtures. The Fine Aggregate Matrix was introduced and identified as a more homogeneous (Masad et al., 2006) and viscoelastic phase (Kim, 2003) (Kim et al., 2003a) (Kim et al., 2003b) for asphalt mixture evaluation. It is composed of fine aggregates, filler, binder and entrained air voids and represents the intermediate scale between the asphalt mastic and asphalt mixture (Figure 2). It is considered the most representative phase of the mixture response, because it takes into account the binder-filler interaction.

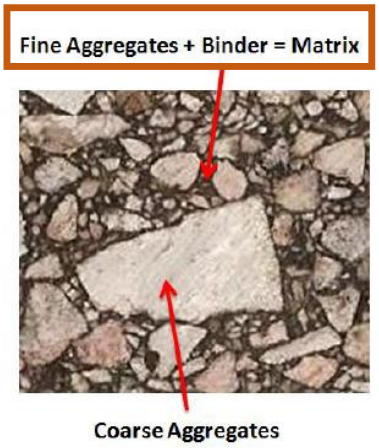

Fig. 2 *Phases of asphalt mixture: Fine Aggregate Matrix (FAM) and coarse aggregates* (Karki, 2010).

Several studies demonstrated that FAM phase acts as a critical phase in evaluating the performance characteristics of asphalt mixtures, including viscoelastic, fatigue damage, permanent deformation and healing characteristics (Kim et al., 2003) (Bhasin et al., 2008) (Palvadi, 2011) (Palvadi et al., 2012) (Motamed et al., 2012) (Izadi, 2012) (Coutinho, 2012) (Gudipudi & Underwood, 2015) (Nabizadeh, 2015) (Haghshenas et al., 2016) (Gundla et al., 2017) (Im et al., 2017) (Riccardi et al., 2018).

A strong relationship between FAM and asphalt mixtures was observed and it suggests that tests on FAM samples can provide deep insight in the behavior of asphalt mixtures. Thus, tests with FAM could provide direct indications of how different factors affect the performance of asphalt mixtures and play a crucial role in the pavements design process.

Furthermore, FAM specimens can be created with much smaller geometries, and that can improve considerably testing repeatability and reduce testing time/cost. Hence, the simplicity, repeatability and efficiency of FAM testing, in comparison to the testing of asphalt mixtures, make it a very attractive specification-type approach for evaluating the performance characteristics of the asphalt mixtures.

1.1 Objectives of this Thesis

The key objectives of this Thesis are:

- Identify and verify the accuracy of a proper design method to produce Fine Aggregate Matrix (FAM) specimens, which could accurately represent the aggregate gradation and asphalt content of the FAM fraction within the full graded asphalt mixture.

- Define an accurate test procedure for the rheological characterization of FAM cylindrical specimens within the linear viscoelastic (LVE) range, by means of a solid torsion bar fixture in a dynamic shear rheometer (DSR). Such test procedure, given the actual absence of standards and protocols, could provide guidelines for the full rheological characterization of FAM specimens.

- Verify if the rheological 2S2P1D model remains valid for the FAM phase, such as for other bituminous materials and if it accurately fits the experimental data collected by testing the FAM specimens within the LVE range.

- Examine and model the relationships of mechanical responses between an asphalt mixture and its corresponding FAM phase and identify significant parameters to link their performance in the LVE range. The influence of different types of binders on FAM properties and characteristics shall also be investigated.

- Explore a simple, reasonable and practically efficient FAM-based testing-analysis method that can evaluate linear viscoelastic characteristics and performance of asphalt mixtures.

- Check if FAM testing-analysis can be used as a specification-type tool to evaluate the performance characteristics of the overall asphalt mixtures and if needed, provide recommendations to enhance the FAM testing protocols with torsion bar.

1.2 Overview of the Methodology

This Thesis investigates the link between performance characteristics of asphalt mixture and its corresponding sub-phases, binder, mastic and especially FAM phase, in LVE range and the possibility to forecast the mechanical properties of the asphalt mixtures from these multi-scale relationships. To reach such objective the linear viscoelastic characteristics of the different phases (from binders to asphalt mixtures) need to be identified, modelled and linked.

The methodology followed in the present research is summarized in Figure 3. The blue arrow identifies an already known relationship between the binder phase and the mixture phase, while the orange and red arrows indicat new links between the different material phases (Binder-FAM; Mastic-FAM and FAM-Mixture).

Particularly, the link between FAM and asphalt mixture has been evaluated.

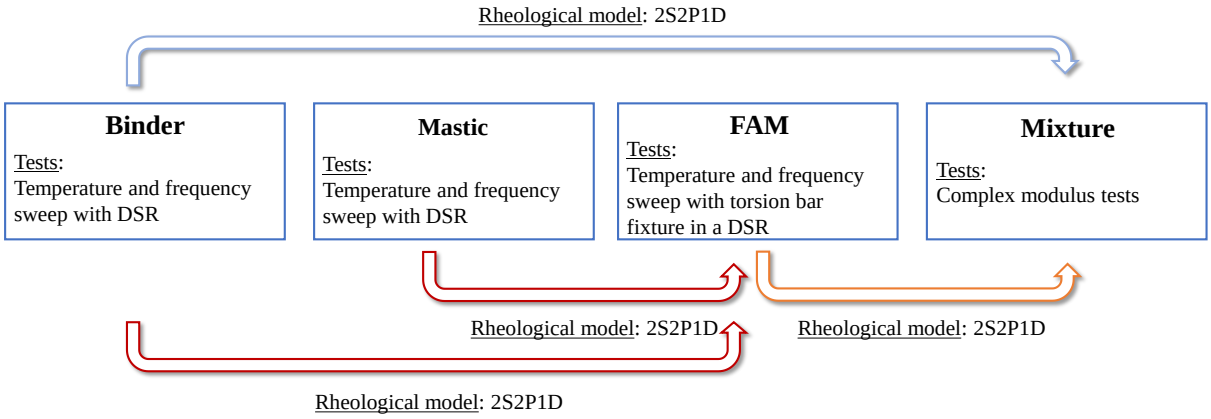

Fig. 3 *Research's methodology.*

In the present study the rheological 2S2P1D model, developed by Olard and Di Benedetto (Chapter 2, Paragraph 2.2.1) to link the mechanical properties of mixtures to those of binders (Olard et al., 2003b) (Olard, 2003) (Di Benedetto et al., 2004), is extended to the prediction of the rheological properties of FAM and to forecast the response of asphalt mixtures from experimental results in LVE of FAM tests.

Specifically, the two following passages have been studied:

- Firstly, it is investigated the possibility to link all the phases (from binder to asphalt mixture), introducing the FAM phase as intermediate phase between mastic and mixture (Figure 4) and using the same values for the δ, h, k and β

parameters of the 2S2P1D model (which values are imposed from the binder phases) (Olard & Di Benedetto, 2003) (Di Benedetto et al., 2004) (Delaporte et al., 2009). The 2S2P1D model will be extended to the FAM phase, verifying its accurateness in fitting its experimental data in LVE range. It is used to link the characteristic times of the phases, which are the parameters that govern the temperature dependency of the respective material phase and that represent the time needed to relax.

- Finally, it is evaluated the possibility to determine the mechanical properties of asphalt mixtures employing only the experimental results of FAM rheological properties (Figure 5).

The results of the back-calculated rheological properties of the asphalt mixture will finally be compared with experimental data and discussed.

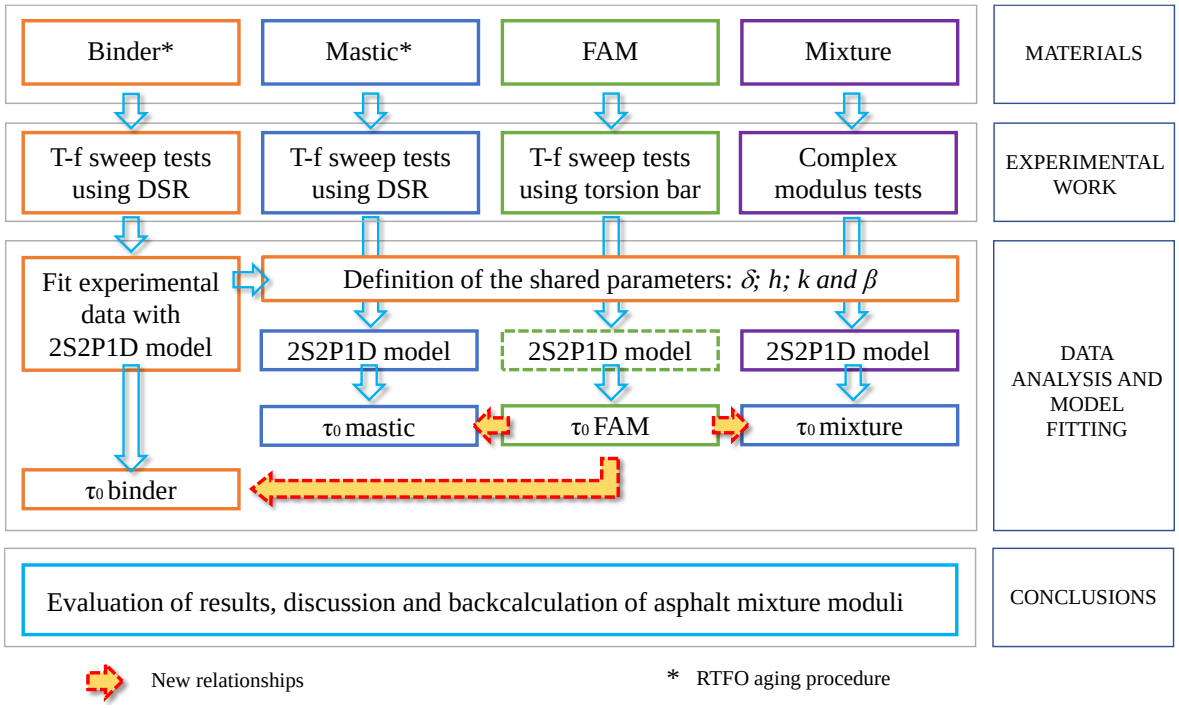

Fig. 4 *Flowchart of the first step of the PhD research.*

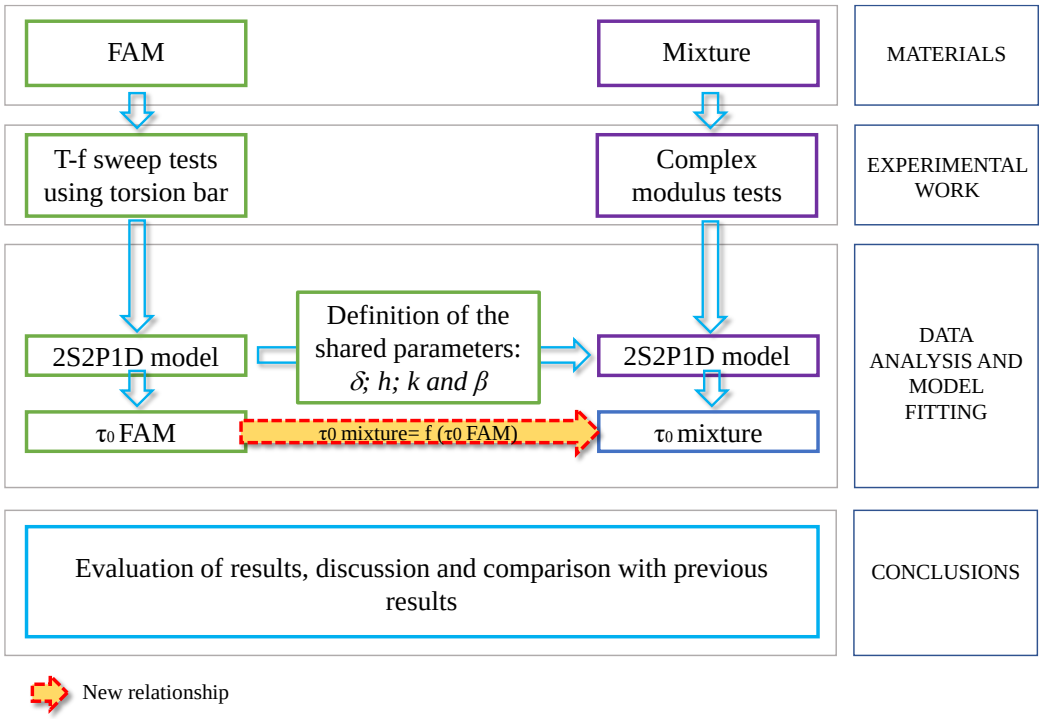

Fig. 5 *Flowchart of the second step of the PhD research.*

Moreover, an appropriate procedure for FAM mix design and for FAM specimen fabrication, to ensure a proper representativeness of the FAM phase, and a FAM testing protocol in LVE range are developed.

1.3 Outline of the Thesis

This Thesis is organized in six chapters, as follows:

- CHAPTER 1: Chapter 1 provides the introduction of the Thesis background, the motivations for the research conducted, an overview of the methodology and on the innovative aspects.

- CHAPTER 2: Chapter 2 presents the outcome of a detailed literature review, summarizes the State-of-the-Art related to FAM, and introduces first efforts to test and evaluate the rheological and performance properties of FAM, which reflect asphalt mixture performance. A summary from the literature review on FAM sample fabrication is also presented. Finally, a brief introduction on some of the existing models in LVE range is provided, which are used in the Thesis.

- CHAPTER 3: Chapter 3 introduces and describes the experimental program of the research. All the materials, the mix designs and the fabrication methods of the

tested samples are presented. Test methods, test protocols and machines used in the Thesis and the data analysis tools are described in detail. The results of the full rheological characterization in linear-viscoelastic (LVE) range of each tested material phase, in terms of complex shear moduli and phase angles mastercurves, are reported and the mechanical properties of all the material phases are finally compared.

- CHAPTER 4: In Chapter 4 the multi-scale approach for prediction of the mechanical response of asphalt mixtures within the LVE range is presented. The 2S2P1D model is extended to the FAM phase, to establish new links between the characteristic times of four material scales (binder-FAM, mastic-FAM and FAM-mixture). Then, these relationships are validated by comparing the experimentally obtained data with the modelled ones.

- CHAPTER 5: In Chapter 5 the relationship between the characteristic times of the FAM and of the asphalt mixture is defined, starting from the fitting of the FAM phase with the 2S2P1D model. The defined relationship between the characteristic times of these two phases allows the backcalculation of the complex modulus of the mixture from FAM experimental data.

- CHAPTER 6: Chapter 6 summarizes the main findings of the Thesis and the contributions of this research. Finally, it provides some proposals and outlooks on future developments.

CHAPTER 2

2. LITERATURE REVIEW

2.1 Fine Aggregate Matrix- FAM

2.1.1 Background and state of the art

The Fine Aggregate Matrix (FAM) phase, composed by fine aggregates (usually smaller than 2 mm), filler, binder and entrained air voids, one length scale below the asphalt mixture (Kim, 2003), is a homogeneous and viscoelastic material, and was verified to be responsible for creating the more compliant phase in the mixture (Masad et al., 1999) (Kim et al., 2003a) (Abbas et al., 2007) (Kim et al., 2007) (Elseifi et al., 2008) (Vasconcelos et al., 2011) (Underwood & Kim, 2011) (Palvadi et al., 2012) (Kim and Aragao, 2013) (Underwood & Kim, 2013).

Tests on FAM samples could provide direct indications of how this phase affects the performance characteristics of the corresponding asphalt mixture. The quality of FAM mostly influences the mechanical characteristics of the entire asphalt mixture, as the damages related to fatigue cracking and moisture damage initiate and propagate through the FAM phase (Kim & Little, 2005) (Montepara et al., 2011). In addition, testing of FAM is generally more repeatable, quicker, cheaper and more efficient than the testing of the corresponding asphalt mixture.

FAM materials are characteristically similar to asphalt mixtures with the primary difference that the maximum aggregate size is usually smaller than 1.19 mm or than 2.36 mm (Underwood & Kim, 2013b) and so test samples can be created with small geometries and still meet Representative Volume Element (RVE) requirements (Hashin, 1983). The maintenance of the RVE requirements ensures that measured properties are not functions of the test geometry and that they represent the fundamental characteristics of the material. Being able to fabricate and test small geometries means that mechanistically viable experiments can be carried out using less costly equipment and in less time than would be required for larger geometries (Underwood & Kim, 2013b).

As FAM test specimens contain fine aggregates only, they can be created with small and simple geometries, e.g. FAM samples generally have about 12 mm in diameter and 45-50 mm in height. This represents a considerable reduction in material consumption and laboratory work, in comparison to the high amount of material needed to prepare asphalt

mixture samples. Hence, FAM tests significantly improve testing repeatability (Martono et al., 2007) and exponentially reduce the experimental costs and the time necessary for the characterization and the performance investigation of asphalt mixtures.

The term Fine Aggregate Matrix (FAM) was introduced by Kim in 2002 (Kim, Little, & Lytton, 2002), to define thephase which is a single characteristic length scale below asphalt mixture and where many interesting phenomena occur between the coarsest aggregate particles. Several studies on FAM samples tested in torsional shear mode were performed to provide direct indications of how this phase affects the corresponding asphalt mixture performance. Testing FAM materials lead to the conclusion that FAM scale may account for most of the physicochemical interactions and aggregate stiffening.

Thus, FAM testing can be used for material characterization and ranking mixtures, playing a significant role in estimating the resistance to damage of the asphalt mixture.

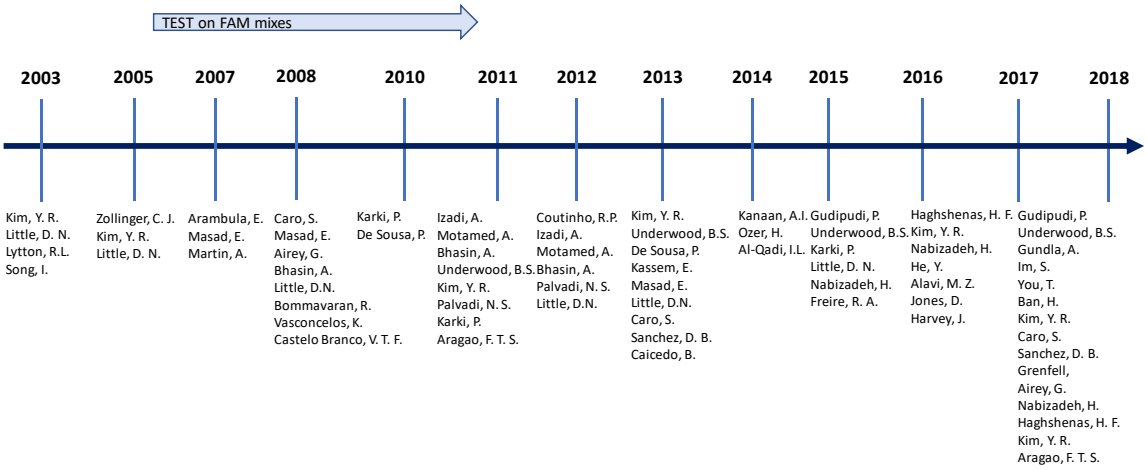

Fig. 6 *Timeline of the research studies on FAM.*

Studies on FAM have gathered wide interest since a good agreement between the FAM phase and asphalt mixture properties was observed based on rheological tests (Kim, Little, & Lytton, 2002) (Kim, 2003) (Kim et al., 2003a) (Kim et al., 2003b) (Kim & Little, 2005) (Underwood & Kim, 2013), on moisture tests (Zollinger, 2005) (Masad et al., 2006) (Arambula et al., 2007) (Caro et al., 2008) (Vasconcelos et al., 2010), fatigue (Kim et al., 2003a) (Kim et al., 2003b) (Kim & Little, 2005) (Motamed et al., 2012) (Izadi, 2012) (Coutinho, 2012) (Gudipudi & Underwood, 2015) (Nabizadeh, 2015) (Haghshenas et al., 2016) (Im et al., 2017) (Gudipudi & Underwood, 2017b), and on permanent deformation characterization (Im et al., 2015) (Im et al., 2017) (Riccardi et al., 2018). Other

researchers used the FAM to evaluate the effect of healing on fatigue properties of asphalt materials (Bhasin et al., 2008) (Izadi et al., 2011) (Palvadi, 2011) (Palvadi et al., 2012) (Karki et al., 2015) (Karki, Bhasin, & Underwood, 2016).

In addition to these experimental and analytical studies, it was also shown that mechanical and fatigue properties of FAM and asphalt mixture are linked (Karki, 2010) (Aragão et al., 2010) (Aragão et al., 2011) (Underwood & Kim, 2013b) (You et al., 2014) (Im and Kim, 2014) (Karki et al., 2015) (Im et al., 2017) (Gudipudi & Underwood, 2015).

Using cohesive zone models, Aragão and Kim (Aragão et al., 2011) simulated fracture growth in mixture using FAM and coarse aggregate properties as input parameters. FAM properties form an important component involving multiple-scale numerical and computational simulations (Aragão et al., 2010) (Karki, 2010) (You et al., 2014) (Karki et al., 2015) (Im et al., 2017). Im et al. (Im et al., 2017) found a link in the deformation characteristics between an asphalt mixture and its corresponding FAM phase. A simple test procedure was designed, and a creep-recovery test was conducted at various stress levels on a mixture and its corresponding FAM. The obtained results shown that there is a link between asphalt mixture and FAM in linear and nonlinear viscoelastic and viscoplastic deformation characteristics, and FAM could successfully predict viscoelastic stiffness properties and viscoplastic hardening of mixtures. Another recent study on the FAM phase (Gudipudi & Underwood, 2017b) showed that asphalt mixture phase properties can be predicted within 10% to 20% of the asphalt mixture experimental data by using an analytical upscaling procedure.

In all the previous cited studies, the comparison between asphalt mixtures and the corresponding FAM results revealed a strong interrelationship between the two lenght scales.

The Dynamic Mechanical Analyzer (DMA) to test small FAM cylindrical specimens was successfully used to characterize mechanical and fatigue performance in several studies, and for characterizing blended binders in asphalt mixtures with Recycled Asphalt Pavement (RAP) and Recycled Asphalt Shingles (RAS) content.

Recently, has been investigated the suitability of testing FAM instead of an asphalt mixture containing recycled asphalt material as an alternative method. Kanaan et al. (Kanaan et al., 2014) studied the viscoelastic, strength and fatigue cracking properties of FAM mixes with different amount of recycled asphalt shingles (RAS), while only recent

research works tested FAM containing reclaimed asphalt pavements, also known as RAP (Nabizadeh, 2015) (Alavi et al. , 2016) (Haghshenas et al., 2016) (He et al., 2016) (Sánchez et al., 2017). Nabizadeh et al. (Nabizadeh et al., 2017), used FAM tests to investigate the effect on fatigue life when using various rejuvenating agents in asphalt mixtures produced with RAS and RAP. FAM mix testing resulted an appropriate procedure for evaluating the properties and performance of blended asphalt mixes containing relatively high quantities of RAP and RAS (Nabizadeh, 2015) (He et al., 2016) (Alavi et al., 2016) (Sánchez et al., 2017) (Zhu et al., 2017).

2.1.2 FAM mix design

Researchers claim for careful FAM fabrication, as FAM phase must reproduce the internal structure of the fine portion of the aggregate gradation of the corresponding full graded asphalt mixture and the physicochemical interactions between aggregates and binder should be suitably replicated in FAM specimens. Once the constituents of the fine portion are selected to achieve desirable behavior, the FAM mix can be tested in order to evaluate the effect of mixture design on performance.

Despite the growing number of investigations in this area, there is no consensus among researchers about a proper design method that could represent the FAM fraction within the mixture and that can be applied to most materials. The FAM sample fabrication, the mix design (binder content, aggregate gradation and maximum nominal aggregate size of the FAM), compaction methods and density levels are major issues in performing FAM-based evaluations.

2.1.2.1 Binder content

The asphalt binder content of FAM samples strongly influences their engineering properties. A study by Underwood and Kim (Underwood and Kim, 2013) showed that a 1% increase in FAM asphalt binder content can produce a 20 to 35% decrease in complex shear modulus |G*| and a 25 to 40% increase in strain tolerance. Considering the hypothesis that FAM represents the fine matrix of the full mixture, the binder content of the fine matrix of the asphalt mixture should be directly proportional to the binder content of the full asphalt mixture (Ng et al., 2018).

Various methods were proposed to investigate this issue. Earlier studies used a standard aggregate gradation and a fixed percentage of asphalt binder to prepare FAM samples,

irrespective of the gradation of the aggregate or asphalt content of the full mixture (Kim, Little, & Lytton, 2002) (Kim, 2003) (Kim et al., 2003a) (Zollinger, 2005). These researchers fabricated samples with a binder content of 8% by total mass, chosen on the assumption of an average asphalt film thickness of 10μm within the asphalt mixture. Castelo Branco (Castelo Branco, 2008) proposed a procedure to define the binder content based on the assumption that FAM binder content must be equal to the binder content of the fine aggregate matrix of the full mixture. First, the amount of binder absorbed by the coarse aggregate (following the standard of the American Association of State Highway and Transportation Officials, AASHTO T85, 2014) was subtracted from the total binder content of the full asphalt mix. Then, all the remaining binder was considered to be part of the FAM.

Underwood and Kim (Underwood & Kim, 2013b) used gravimetric experiments with FAM extracted directly from compacted asphalt concrete (AC) mixtures to find the binder content of FAM. They assumed that all the effective asphalt binder in the mixture exists in a mastic form, and this mastic coats all the aggregates with a constant thickness. Under this microstructural hypothesis, asphalt content was calculated based on the film of mastic within the mixture coating the FAM aggregates; not including the mastic that coats particles larger than FAM-sized particles. Their data also suggested that FAM phase consists of aggregates with 100% passing to the 0.3 to 2.36 mm sieve, depending on the maximum aggregate size of the corresponding asphalt mixture.

Other researches suggested experimental methods to evaluate the asphalt binder content of the FAM samples. Coutinho (Countinho, 2012) determined the FAM binder content using the solvent extraction binder method (AASHTO T164, 2014), while Sousa et al. (Sousa et al., 2013) proposed an empirical determination based on ignition extraction (AASHTO T308, 2014) on sieved loose mix to determine the effective asphalt binder content of FAM. Freire (Freire, 2015) introduced a correction in the calculation presented by Countinho, in order to include the fine matrix adhered to the coarse aggregate particles in the calculations.

Ng et al. (Ng et al., 2018) evaluated the applicability of some of these design methods of fine aggregate matrices, also considering FAM produced with modified asphalt binders. They proposed a procedure to define the binder content of the FAM sample produced with both neat and modified binders. This procedure is based on the concept of specific surface and introduces a multiplier to account the modified asphalt binder content

(specific for each modified asphalt binder). The specific surface method and the ignition method proposed by Sousa (Sousa et al., 2013) yielded to equivalent asphalt binder contents. The latter procedure is based on the hypothesis that the FAM represents the fine matrix of the full mixture and the binder content of the FAM sample should be directly proportional to the binder content of the full asphalt mixture.

Some shortcomings were identified in the replication of some of the previously mentioned experimental methods. The procedure proposed by Castelo Branco (Castelo Branco, 2008) defined a high binder content for FAM mixes, and it was not possible to extract the samples from the Gyratory compacted specimens. While the procedure proposed by Countinho (Countinho, 2012) adapted by Freire (Freire, 2015) determined a low binder content for the mixes, and during the mixing process the aggregates particles were not completely covered by asphalt binder, which resulted in an inadequate densification of the samples.

2.1.2.2 Aggregate gradation

Concerning aggregate gradation and its composition, the main assumption in studies with FAM is that the FAM should represent the fine portion of the aggregate gradation of the full asphalt mixture. Izadi et al. (Izadi et al., 2011) highlighted that engineering properties of FAM are less influenced by gradation parameters when compared to binder content, air voids percentage and compaction variables.

Usually the proportion of the fine aggregates is kept the same as in the full mixture aggregate gradation, but normalized with respect to the largest sieve of aggregate in the FAM. To define it most researchers utilized their own technique. Zollinger (Zollinger, 2005) proposed a FAM design involving the normalization of the gradation so that the 100% of the FAM aggregate would pass the sieve of nominal size 1.19 mm (No. 16). The material passing sieve No. 16 is commonly used to represent FAM in international studies.

In a study conducted by Aragão et al. (Aragão et al., 2010) an image treatment process was used to capture digital images of asphalt mixtures, in order to define the nominal maximum aggregate size of FAM. The particles smaller than 0.30 mm were considered as part of the FAM phase, because the portion of the aggregate gradation smaller than 0.30 mm is not distinctively captured by the digital image processing.

Many Brazilian researchers used the material passing the sieve of nominal size 2.00 mm (No. 10) as the fine portion of the aggregate gradation of the full asphalt mixture. This sieve was chosen, instead on Sieve No. 16, because it is part of the sieve series of the Brazilian standards for asphalt mixtures. Freire et al. (Freire, et al., 2014) demonstrated that fatigue characteristics if the samples made with particles passing Sieves No. 10 and 16 are not affected by aggregate size, and both sizes can be used to represent the FAM properly.

One pragmatic approach is to set the largest size of aggregate in FAM based on resolution limitations with digital image analysis (2.36-2 mm) (Kim et al., 2008) (Valenta et al., 2018). Underwood (Underwood & Kim, 2012) defined the delineation between coarse and fine aggregate as mixture dependent and proposed to use fine aggregate particles passing the 0.3 - 2.36 mm sieves, depending on the Nominal Maximum Aggregate Size (NMAS) of the mixture. This NMSA-FAM definition is based on the packing principle proposed by Vavrik (Vavrik et al., 2001) (Vavrik et al., 2002), the Bailey method of gradation determination.

The Bailey method which is used for analysis and developing aggregate gradations in asphalt concrete mixtures and is rooted in packing theory, provides a theoretically justified concept using the definition of the Primary Control Sieve (PCS) (Vavrik et al., 2001). This sieve is computed based on the ideal aggregate diameter that would just fit inside the void space created by three of the nominally largest sized coarse particles touching in the most optimal arrangement.

According to Bailey method the maximum aggregate size of FAM materials occurs at Fine Aggregate Initial Break (FAIB) sieve, it corresponds to the Secondary Control Sieve (SCS), which depends on the Nominal Maximum Aggregate Size (NMAS), and is defined as the result of the following formula shown in Equation [1]:

$$FAIB = SCS = PCS \cdot 0.22 = NMAS \cdot 0.22^2 \quad [1]$$

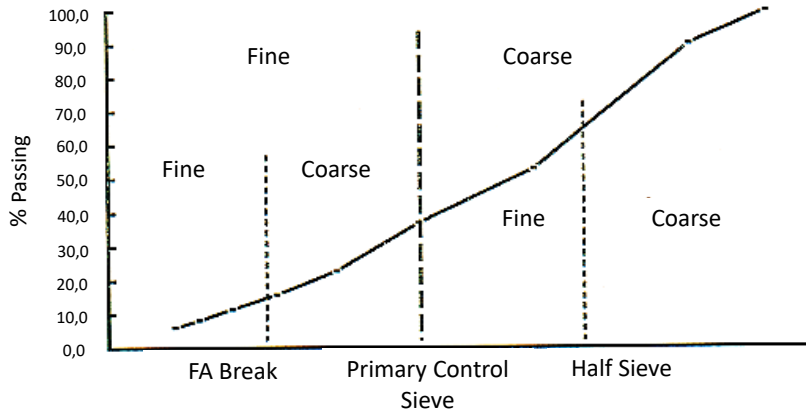

Fig. 7 *Division points in coarse and fine aggregate fractions* (Vavrik et al., 2001).

Where:

- *PCS*, is the Primary Control Sieve and represents the size of intergranular voids and it is proportional to that of the coarse particles;

- $FAIB = SCS$ is the Fine Aggregate Initial Break sieve, that separates the fine aggregate into coarse and fine portions;

- *NMAS* is the Nominal Maximum Aggregate Size for the overall blend. It is defined according the Superpave terminology as one sieve larger than the first sieve that retains more than 10%, or according to the European standards it corresponds to the upper dimension D sieve size; the total passing from sieve size D should always be above 90% (EN 13043, 2013) (EN 13108-1, 2016).

The value of 0.22 used in the control sieve equation is an empirically derived quantity, determined from 2-D (Vavrik et al., 2001) (Vavrik et al., 2002) and 3-D (Bourbie et al., 1987) (Reed, 1988) analysis of the aggregates packing. It represents the particle size that will just fit inside the volume created by three same-sized angular particles. Several researches showed that the packing of particles follows different models when the characteristic diameter ratio is above or below 0.22 (Aim & Le Goff, 1967) (Toufar et al., 1976) (Toufar et al., 1977). The definition of fine and coarse aggregates is more specific and related to their volumetric function inside an aggregate blend, to determine the packing and aggregate interlock provided by the combination of aggregates in various sized mixtures. Equation [1] was found to represent average conditions of asphalt mixtures, which are composed by particles having different shape, texture and strength.

The fine aggregate initial break sieve D_{FAIB}, corresponding to the NMAS of the FAM mixture, is the closest sized sieve to the results of the Equation [1].

Kim et al. (Kim et al., 2004) recommended a ratio between aggregate size and sample diameter higher that 1:3.

The percentage of aggregates of the FAM is determined by Equation [2]:

$$Percent\ passing\ sieve\ No.ii\ in\ FAM = \frac{Mass\ of\ aggregate\ passing\ Sieve\ No.ii\ \ in\ full\ mixture}{Mass\ of\ aggregate\ passing\ the\ maximum\ Sieve\ in\ full\ mixture}\ x\ 100\% \quad [2]$$

According to the research of Underwood and Kim (Underwood and Kim, 2013) the mass of the aggregate passing the break sieve must be correct, considering that part of the filler-sized particles coats the coarse aggregate particles. The aggregate gradation is calculated considering only the filler-sized particles, within the mastic that coats FAM aggregates. The results of a study conducted by Izadi et al. (Izadi et al., 2011) demonstrated that a change in fine aggregate fraction of the aggregate do not significantly influence the engineering properties of the FAM specimens, which are instead more strongly influenced by the binder content, percentage of air voids and compaction variables.

2.1.2.3 Air voids content

Underwood and Kim (Underwood & Kim, 2013a) showed that a one percentage increase in air void content results in a 5 to 8% decrease in complex shear modulus |G*| for the 9.5 mm FAM and a 10 to 12% decrease in complex shear modulus |G*| for the 19 mm FAM, and a 10% decrease in strength and a 0-5% increase in strain tolerance. Moreover, they completed a series of gravimetric experiments on FAM extracted from asphalt mixtures with analysis of computed tomography images and estimated that 40 to 75% of the air within the asphalt mixtures exists in the FAM (Underwood & Kim, 2013a). The values of air voids contents in this range are considered acceptable and representative of the air voids present in the fine portion of the corresponding asphalt mixture.

2.1.2.4 Compaction

Sample compaction plays a fundamental role in determining the significance of FAM-based experimental results.

In the earliest works (Kim, Little, & Lytton, 2002) (Kim, 2003) (Kim et al., 2003a) (Kim et al., 2003b) premixed FAM samples were pressed into specially fabricated cylindrical molds, by applying impact loads. However these samples showed high voids content on their top, that could result in cracks at sample edges. Zollinger (Zollinger, 2005) introduced the use of gyratory-based compaction (Superpave Gyratory Compactor, SGC), followed by the coring of the FAM samples. This compaction method produced more uniform specimens in terms of compaction and air voids distribution. Izadi et al. (Izadi et al., 2011) evaluated the influence of compaction methods on the engineering properties of FAM specimens. In most cases the SGC compacted FAM specimens had a microstructure that most closely resembled the microstructure of the FAM in the corresponding asphalt mixtures.

Gudipudi and Underwood (Gudipudi & Underwood, 2015) found through a trial and error procedure, that a mostly uniform air void distribution can be obtained across the test specimen height by compacting the gyratory specimen to a height of 95 mm.

2.2 Models in LVE range

The behaviour of asphalt materials is viscoelastic, and thefore it depends on loading time and temperature and can be defined through the definition of complex modulus (|G*|) and phase angle (δ). This technique is based on the Time-Temperature Superposition Principle (TTSP). In the linear viscoelastic range, they can be considered thermorheologically simple (TRS) materials, and the effects of time of loading and temperature can be expressed through one joint parameter, named shift factor a_T (Williams, Landel, & Ferry, 1955) (Ferry, 1980).

Through the use of mastercurves and shift factor relationships it is possible to interpolate the complex modulus at an expanded range of frequencies and temperatures, describing the linear viscoelastic (LVE) rheological properties of bituminous materials. The models proposed in this literature review are able to describe these curves and have been employed in the present work.

2.2.1 The 2S2P1D Model

The rheological 2S2P1D model (an abbreviation of the combination of 2 Springs, 2 Parabolic creep elements and 1 Dashpot) is able to describe the linear viscoelastic properties of binders and asphalt mixtures, was proposed by Olard and Di Benedetto

(Olard et al., 2003b) (Olard, 2003) (Di Benedetto et al., 2004) (Pouget et al., 2010) (Tiouajini et al., 2011) (Yusoff et al., 2013) (Yusoff et al. , 2014) as a modification of the Huet-Sayegh model (Sayegh, 1965).

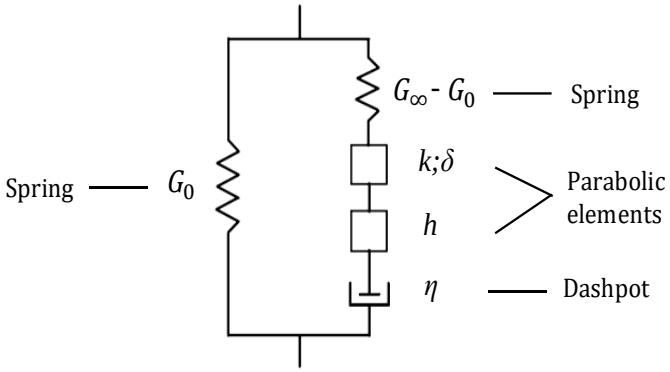

Fig. 8 *2S2P1D analogical model, valid for both bituminous binders and asphalt mixtures.*

According to this model, at a reference temperature T_0, the complex modulus can be expressed as:

$$G^*(\omega,T) = G_0 + \frac{G_\infty - G_0}{1 + \delta(i\omega\tau)^{-k} + (i\omega\tau)^{-h} + (i\omega\beta\tau)^{-1}} \quad [3]$$

Where i is the complex number ($i^2 = -1$); ω is the angular frequency, defined as $\omega = 2\pi f_r$, where f_r is the reduced frequency; G_0 is the static asymptotic shear modulus when $\omega \to 0$; G_∞ is the glassy asymptotic shear modulus when $\omega \to \infty$; k and h are dimensionless exponents such as $0 < k < h < 1$, while δ and β are dimensionless constants, in particular η, which is the Newtonian viscosity of the material, can be defined as $\eta(T) = (G_\infty - G_0)\beta\tau(T)$, where $\tau(T)$ is the characteristic time (depending on temperature).

In Figure 9, the parameters of the 2S2P1D model are described in more details. The parameter h controls the slope at low values of G'', while k governs the slope at high values of G'' in the Cole-Cole diagram (G' vs G''). The constant δ is correlated to the slope at the low temperatures/high frequencies in the mastercurve of the complex modulus, and the height of the maximum point in the Cole-Cole diagram, while β is linked to the slope of the curve at high temperatures/low frequencies of the $|G^*|$ mastercurve, where the higher the value of β, the higher the values of η and $|G^*|$.

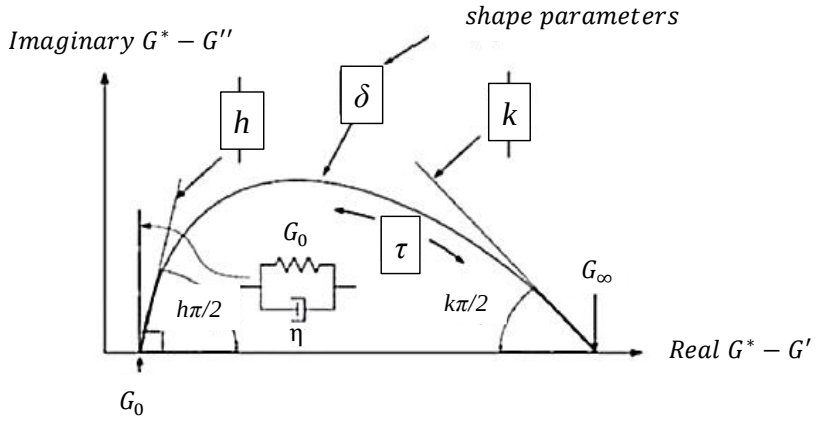

Fig. 9 *Graphical visualization of the parameters of the 2S2P1D model in the Cole-Cole diagram* (Mangiafico, Di Benedetto, Sauzéat, & Olard, 2013).

Based on the Time-Temperature Superposition Principle (TTSP), τ is defined as:

$$\tau(T) = a_T(T) \cdot \tau_0 \quad [4]$$

Where a_T is the time-temperature shift factor at the temperature T; and $\tau_0 = \tau(T_0)$ is the characteristic time at the reference temperature T_0.

The time-temperature shift factor a_T can be defined as the horizontal shift that must be applied to material properties at any temperature to determine the same properties at a reference temperature T_0.

Based on this Time-Temperature Superposition Principle (TTSP) the reduced frequency can be expressed as:

$$f' = f \cdot a_T \quad [5]$$

The shift factor $a_T(T)$ can be determined using the Williams-Landel-Ferry (WLF) equation for bituminous materials (Equation [6]) (Williams, Landel, & Ferry, 1955) (Ferry, 1980), it is used in the model to express the time-temperature shift factor a_T, in the range of temperature observed in laboratory, at a specific reference temperature T_0:

$$log\frac{a_T(T)}{a_T(T_0)} = -\frac{C_1(T - T_0)}{C_2 + (T - T_0)} \quad [6]$$

where C_1 and C_2 are empirical constants depending on the material.

According to the 2S2P1D model only seven parameters ($G_0, G_\infty, \delta, h, k, \beta$ and τ_0) are needed to entirely determine the linear viscoelastic (LVE) behavior of the specific

material at a given temperature. Moreover, for binders, the experimental static modulus G_0 is close to zero, and can be assumed equal to zero, reducing the number of constants of the model to six.

The main advantages of the 2S2P1D model are that it has been demonstrated able to describe the linear viscoelastic (LVE) properties for any bituminous material (binders, mastics, mortars and asphalt mixtures) over a wide range of temperatures and frequencies and that four of the seven parameters, δ, h, k and β, remain the same for every phase, i.e. for binders and the corresponding mastics, mortars and mixtures, since, according to the literature, these parameters depend only on binder source (Olard & Di Benedetto, 2003) (Di Benedetto et al., 2004) (Delaporte et al., 2009).

Several studies demonstrated that there is a good linear correlation between the binder and the corresponding mixture characteristic time parameters in the log-log scale (Olard & Di Benedetto, 2003) (Di Benedetto et al., 2004) (Pouget et al., 2010):

$$\tau_{mix} = 10^{\alpha}\tau_{binder} \quad [7]$$

Where α, known as the transformation parameter, probably depends on mix design and/or ageing during mixing (Di Benedetto et al., 2004).

Hence, writing Equation [3], for binders and mixtures, the following expressions are obtained:

$$G^*_{binder}(i\omega\tau_{binder}) = G_{0_{binder}} + \frac{G_{\infty_{binder}} - G_{0_{binder}}}{1 + \delta(i\omega\tau_{binder})^{-k} + (i\omega\tau_{binder})^{-h} + (i\omega\beta\tau_{binder})^{-1}} \quad [8]$$

$$G^*_{mix}(i\omega\tau_{mix}) = G_{0_{mix}} + \frac{G_{\infty_{mix}} - G_{0_{mix}}}{1 + \delta(i\omega\tau_{mix})^{-k} + (i\omega\tau_{mix})^{-h} + (i\omega\beta\tau_{mix})^{-1}} \quad [9]$$

Where only τ_{binder} and τ_{mix} are functions of the temperature.

Combining Equations [7], [8] and [9] and considering that, in accordance to literature, the constants δ, h, k and β are the same for the binder and the corresponding mixture, the following relationship between the complex modulus of the mixture $G^*_{mix}(\omega, T)$ and the complex modulus of the binder $G^*_{binder}(\omega, T)$ can be obtained:

$$G^*_{mix}(\omega, T) = G_{0_{mix}} + (G^*_{binder}(10^{\alpha}\omega, T) - G_{0_{binder}})\frac{G_{\infty_{mix}} - G_{0_{mix}}}{G_{\infty_{binder}} - G_{0_{binder}}} \quad [10]$$

This equation corresponds to three geometrical transformations: a negative translation along the the real axis (i), a homothetic expansion from the origin (ii) and a final positive translation of the binder curve in the Cole-Cole plane (iii), to obtain the mixture curve, as depicted in Figure 10 (Olard & Di Benedetto, 2003) (Di Benedetto et al., 2004). Equation [10] is known as the Shift-Homothety-Shift in time-Shift (SHStS) transformation and allows the calculation of the asphalt mixture complex modulus at the temperature T if the complex modulus of the binder is known at the same temperature. Moreover, if the TTSP is verified for binders the following property can be added for both binders and mixes:

$$G^*(\omega, T) = G^*(\omega \cdot a_T(T), T_0) \qquad [11]$$

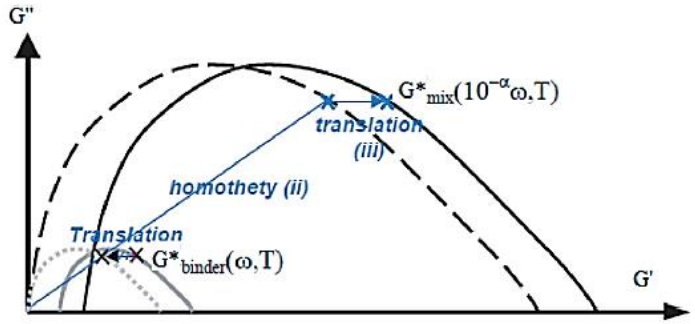

Fig. 10 *The SHStS transformation in the Cole-Cole plane- the prediction of the mixture modulus from binder one* (Di Benedetto et al., 2004).

Recent studies have demonstrated that the same expression allows to efficiently predict the complex modulus of mastics from the binder complex modulus (Riccardi et al., 2018), the complex modulus of mortars from the binder one (Riccardi et al., 2016) and the complex modulus of the mixture from the mortar one and vice versa (Riccardi, 2017).

2.2.2 The Christensen Anderson Maresteanu (CAM) model

The behaviour of the asphalt mixture and its material phases, which behave in a viscoelastic manner, depends on loading time and temperature.

Mastercurves provide a fundamental rheological understanding of viscoelastic materials and allow to estimate the mechanical properties over a wide range of temperatures and frequencies that could be verified in field, but that are not practical to simulate in laboratory. In the present Thesis the model presented in NCHRP 459, 2001 (NCHRP-459, 2001) is used, in order to plot the mastercurves of the complex modulus and of the phase angle. The CAM model (Anderson et al., 1994) (Marasteanu, 1999), and its more recently proposed generalization (Zeng et al., 2001) are universal models, valid for

binders, mortars, FAM, and asphalt mixtures, and which allow to calculate the complex modulus E^* (or complex shear modulus G^*) and phase angle δ mastercurves by using the following equations and parameters:

$$G^* = G_e^* + \frac{G_g^* - G_e^*}{[1 + (f_c/f')^k]^{m_e/k}} \quad [12]$$

Model parameters are graphically depicted in Figure 11:

- $G_e^* = G^*(f \to 0)$ is the equilibrium complex modulus ($G_e^* = 0\ GPa$ for binders);
- $G_g^* = G^*(f \to \infty)$ is the glassy complex modulus ($G_g^* = 1\ GPa$ for binders);
- k and m_e are two dimensionless shape parameters;
- f_c is the location parameter, also called crossover frequency, with dimensions of frequency, it corresponds to the frequency at a given temperature where G_g^* and m_e asymptotes interception;
- $f'_c = f_c \left(\frac{G_e^*}{G_g^*}\right)^{1/m_e}$ is the frequency where G_g^* and m_e asymptotes intercept;
- f' is the reduced frequency (in Hz), function of both temperature and strain.

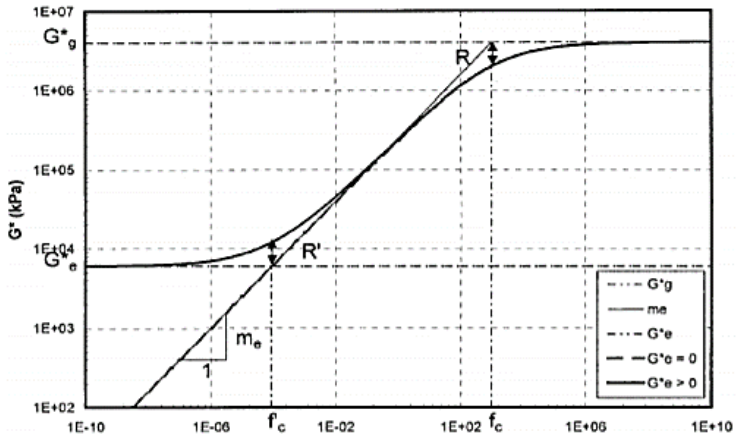

Fig. 11 *Typical schematic representation of a mastercurve* (NCHRP 459, 2001).

$$\delta = 90I - (90I - \delta_m)\left\{1 + \left[\frac{\log(f_d/f')}{R_d}\right]^2\right\}^{-m_d/2} \quad [13]$$

Where:

$$I = \begin{Bmatrix} 1 \ for\ mixtures \\ \begin{Bmatrix} 0\ if\ f' > f_a \\ 1\ if\ f' \leq f_a \end{Bmatrix} for\ binders \end{Bmatrix} \quad [14]$$

The results of these tests on FAM samples for determining the linear viscoelastic (LVE) characteristics of FAM will be compared with the LVE results (mastercurves and linear parameters) obtained for the different phases (binders, mastics and asphalt mixtures) analyzed in the LVE range.

2.2.3 The Sigmoidal Model

Another frequently used model is the sigmoidal model. The sigmoidal model equation is:

$$log\ E^* = \delta + \frac{\alpha}{1 + e^{(\beta + \gamma \cdot log f')}} \quad [15]$$

Where δ is the minimum value of $log\ E^*$, α is equal to $log\ E_{max} - log\ E_{min}$, β and γ are shape parameters and f' is the reduced frequency, function of both temperature and strain, with dimensions of frequency.

CHAPTER 3

3. EXPERIMENTAL INVESTIGATION AND RHEOLOGICAL MODELLING IN THE LVE RANGE OF THE FAM PHASE – *Materials and Tests*

In the first part of this Chapter the experimental program of the Thesis is introduced. Then, the four investigated material scales (from binder to asphalt mixture) and the tests details (testing devices and procedures) are presented. Particularly, an extensive effort is made to identify a proper mix design method and sample fabrication procedure for the FAM phase, in order to guarantee to the laboratory specimens an accurate resemblance to the phase as exists between the coarse aggregate particles in the full-graded asphalt mixture. Indeed, one of the main goals of this research was the identification of guidelines to achieve a proper mix design for FAM, which accurately represents this phase, with its characteristics and properties.

Test protocols and testing machines are also described in detail. Given the actual absence of standards and protocols for FAM testing, a test procedure for the investigation of the rheological behavior of FAM over a wide range of temperatures and frequencies in the LVE range is established.

The results of the experimental investigation of the different material scales are analyzed, modelled and graphically reported in terms of isotherm mastercurves, at the reference temperature of 20°C, in order to provide a simple visual understanding of the viscoelastic rheological properties of the material phases in LVE range and allow the comparison of their mechanical properties over a wide range of temperatures and frequencies.

The results of the experimental investigation presented in the present Chapther are also employed in both Chapter 4 and Chapter 5, where the 2S2P1D model is implemented for the FAM phase and used in the multiscale transition from binder to asphalt mixture.

Riccardi found that the transformation parameter α, used to link the characteristic times of different material scales, depends both on binder content and aggregate gradation (Riccardi, 2017). For this reason, four asphalt mixtures, characterized by the same mix design and different types of binders, and the corresponding sub-phases will be analized.

3.1 Description of the Experimental Plan

The main purpose of the research is to investigate the possibility to back-calculate the complex modulus of the asphalt mixture in the LVE range with this simple and effective expression, knowing the complex modulus of the corresponding FAM phase.

To establish the relationships between the asphaltic materials the sub-phases of the asphalt mixtures must be representative. They must be designed as they exist within the full-graded asphalt mixture. Hence, the production of the mastic and FAM phases originates directly from the mix design (aggregate gradation and binder content) of the asphalt mixture.

In the mastic phase is represented the aggregates portion passing through the 63 µm Sieve, referred as filler, in a binder matrix. While the combination of filler and "matrix" aggregates forms the aggregate gradation of the FAM phase, which simulates the fine-portion of the full-graded asphalt mixture.

One of the main issues of the present research regards the choice of a suitable protocol for the definition of a reference sieve size to define these matrix aggregates and more in general the proper mix design of this phase (binder content, air voids content). As reported in the following sections an extensive literature review has been carried out to investigate this topic and succeed in this purpose.

Besides the production of FAM samples, the experimental plan includes the following tasks:

- The determination of the rheological properties of binders in LVE range using a DSR device in strain-controlled mode for high temperatures, and in stress-controlled mode for intermediate and low temperatures (see Paragraph 3.2.3);
- The determination of the rheological properties of the mastics in LVE range as they exist in the corresponding asphalt mixtures, using a DSR device in strain-controlled mode for high temperatures, and in stress-controlled mode for intermediate and low temperatures (see Paragraph 3.2.4);
- The determination of the rheological properties of the FAM in LVE range as they exist in the corresponding asphalt mixtures, using a solid torsion bar fixture in a DSR in strain-controlled mode (see Paragraph 3.2.5);

- The determination of the rheological properties of the asphalt mixtures in LVE range using uniaxial tension-compression test apparatus in strain-controlled mode (see Paragraph 3.2.1);

- The definition of the interrelations between material scales (from binder to asphalt mixture) in the LVE range by fitting the experimental data with the 2S2P1D model and linking their characteristic times (see Chapters 4 and 5);

- Validation of the results and comparison between experimental data and modelled values and final discussion.

Test methods and parameters used for the four investigated material scales are reported in Figure 12.

Material phase	Testing machine	Test Schematic *	Temperatures [°C]	Frequencies [Hz]
Binder	DSR machine	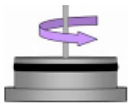	-30, -20, -10, 0, 10, 20, 30, 40, 50, 60, 70, 80, 90	10, 9, 8, 7, 6, 5, 4, 3, 2, 1.59, 1, 0.9, 0.8, 0.7, 0.6, 0.5, 0.4, 0.3, 0.2, 0.1
Mastic	DSR machine		-10, -5, 0, 5, 10, 20, 30, 40, 50, 60, 70, 80, 90	10, 9, 8, 7, 6, 5, 4, 3, 2, 1.59, 1, 0.9, 0.8, 0.7, 0.6, 0.5, 0.4, 0.3, 0.2, 0.1
FAM	Torsion bar fixture in a DSR		-10, 0, 10, 20, 30, 40	30, 25, 20, 15, 10, 9, 8, 7, 5, 3, 1, 0.5, 0.3, 0.1
Mixture	Uniaxial tension-compression test		-10, 0, 10, 15, 20	10, 5, 3, 1, 0.3, 0.1

* TEST GEOMETRIES ARE NOT SHOWN TO SCALE

Fig. 12 *Test methods and parameters used in the experimental plan.*

3.2 Materials and Tests

In the following sub-sections are introduced the analyzed materials and tests performed on them. The materials' part follows this order: firstly, asphalt mixtures are presented, then followed by a deepening on the aggregates and asphalt binders that constitute them (asphalt binders are tested materials too), and finally, asphalt mastics and FAM mixes. This order has been chosen considering that both mastic and FAM mix designs are bindingly related to the mixture one, and for this reason the selection of the mixtures is preliminary. The same order was followed in the "test results, data elaboration and modelling" section (Paragraph 3.3).

3.2.1 Asphalt Mixtures

Four different asphalt mixtures, with the same aggregate gradation curve reported in Figure 13, were produced. The mixtures were blended from five stockpiles of Gabbro with the following aggregate sizes in different proportions: 0/2, 2/5, 5/8 and 8/11, and limestone filler, to meet the target gradation, and four different asphalt binders, two unmodified binders of the types PEN 50-70 and PEN 70-100, and two polymer modified binders (PMB) with a thermoplastic elastomer modification named styrene butadiene styrene (SBS), of the types PMB 25-55-55 A and PMB 45-80-65 A.

The four asphalt binders were provided by the active research project VEGAS, FFG-Project Nr. 863063.

Table 1 *Tested materials.*

Asphalt mixture	**MIX_111**	**MIX_211**	**MIX_321**	**MIX_421**
Corresponding FAM	FAM_ 111	FAM_ 211	FAM_321	FAM_421
Corresponding mastic	M_111	M_211	M_321	M_421
Corresponding binder	B_11	B_21	B_32	B_42
Type of binder	PEN 50-70	PMB 25-55-55A	PEN 70-100	PMB 45-80-65A

The mixtures were labelled as MIX_"ABC", where "A" defines the type of binder, "B" stands for the binder supplier and "C" is referred to the asphalt mixture mix design. The mix design (gradation curve and binder content) was the same for all asphalt mixtures

(C=1) and consisted of 6.0 w.-% of binder and 94.0 w.-% of aggregates, with a distribution typical of a main course commonly used in Germany.

The four mixtures are henceforth labelled as MIX_111, MIX_211 (provided by Total, B=1), MIX_321 and MIX_421 (provided by OMV, B=2).

The target air voids content of the asphalt mixture samples was 3.5 ± 1%.

The Nominal Maximum Aggregate Size (NMAS) of the mixtures was 11.2 mm.

Asphalt mixture aggregate gradation and mix properties are shown in Table 2.

Table 2 *Summary of aggregate gradation and mix properties of asphalt mixtures.*

	Sieve size [mm]	**% Passing [M-%]**
Aggregate gradation	**22.4**	100
	16.0	100
	11.2	97.50
	8.0	81.23
	5.6	65.00
	2.0	40.30
	1.0	29.19
	0.5	22.13
	0.25	15.07
	0.125	10.89
	0.063	8.04
Binder content [M-%]	5.9%	
Air void content [%]	3.5 ±1.0%	

The gradation curve of the aggregates used for the asphalt mixtures and the grading band limits of main courses, according to the German standards (FGSV), are reported in Figure 13-(a), while the 0.45 power gradation graph and the corresponding maximum density line are reported in Figure 13-(b) (Roberts et al., 1996).

The specific gravities of the aggregates and asphalt binder are reported in Table 3.

a)

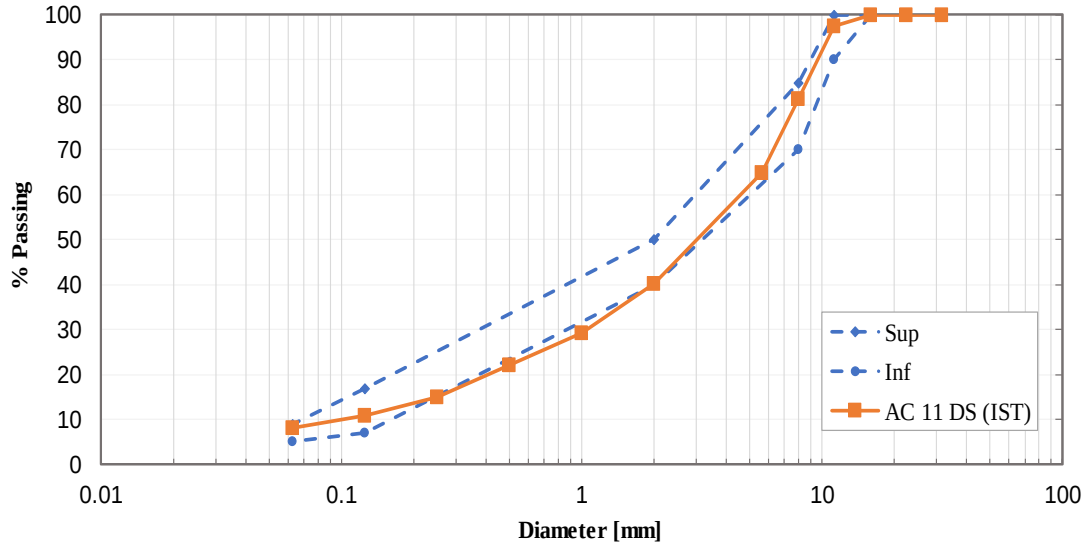

b)

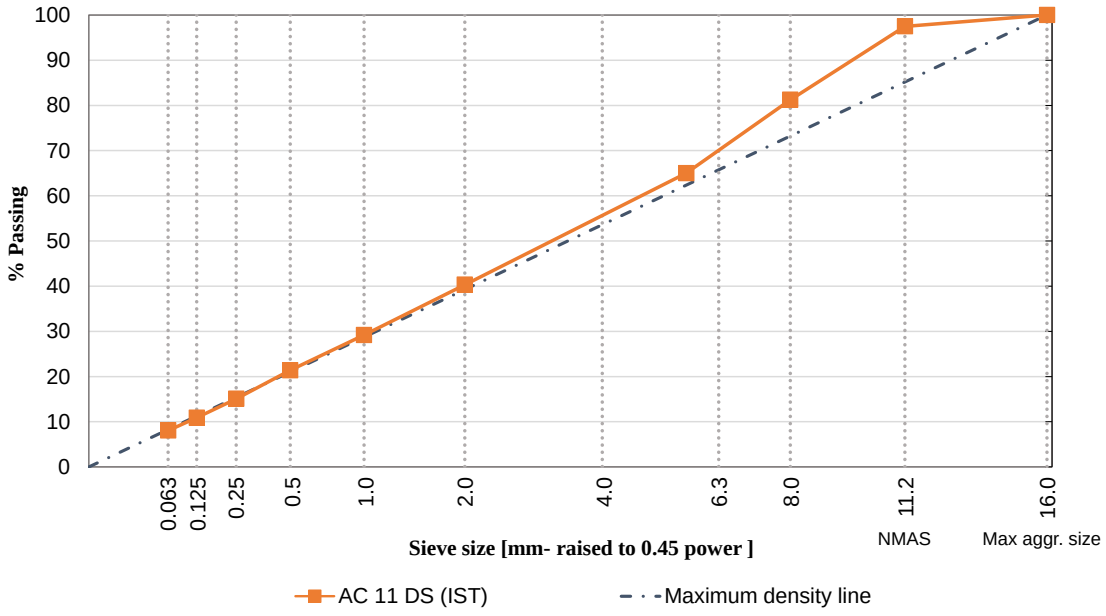

Fig. 13 *(a) Gradation curve and (b) 0.45 power gradation graph, with the corresponding maximum density line, of the asphalt mixtures.*

Table 3 *Aggregates and asphalt binder specific gravities.*

Apparent Specific Gravity of aggregates Gsa	**31.5-4 mm [UNI EN 1097-6 Chapter 8]**	2.867
	4-0.063 mm [UNI EN 1097-6 Chapter 9]	2.964
	Filler [UNI EN 1097-7]	2.748
Bulk Specific Gravity of aggregates Gsb	**31.5-4 mm [UNI EN 1097-6 Chapter 8]**	2.804
	4-0.063 mm [UNI EN 1097-6 Chapter 9]	2.464
	Filler [UNI EN 1097-7]	2.285
Effective Specific Gravity of aggregates Gse	**31.5-4 mm [UNI EN 1097-6 Chapter 8]**	2.826
	4-0.063 mm [UNI EN 1097-6 Chapter 9]	2.633
	Filler [UNI EN 1097-7]	2.441
Specific Gravity of asphalt binder Gb	1.023	

To produce the asphalt mixture samples, aggregates and binders were heated and mixed at 160°C. A segment steel roller compactor was used to produce four different slabs (one for each asphalt mixture) with dimensions of 320 x 200 x 50 mm^3 (Wistuba, 2016). From the asphalt mixture slabs, prismatic specimens were cut with the final dimensions of 40 x 40 x 160 mm^3.

The produced mixtures were subjected to control tests, such as the evaluation of G_{mb} (test specimens' bulk specific gravity) and G_{mm} (theoretical maximum specific gravity) to provide target values for the compaction of the asphalt mixtures, e.g. the air voids content (percent, %).

The geometrical and volumetric characteristics of the tested samples are given in Table 4.

Table 4 *Geometrical and volumetric composition of the tested samples.*

Samples ID	Gmb [g/cm^3]	Gmm [g/cm3]	Air Voids content [%]	B x h [mm x mm]	Height [mm]
Mix_111-5-1	2.485		3.938	40.81 x 41.54	162.50
Mix_111-6-3	2.477	2.587	4.245	39.57 x 40.75	162.70
Mix_111-4-2	2.486		3.898	38.96 x 41.19	163.18
Mix_211-4-5	2.488		4.155	39.81 x 41.76	162.04
Mix_211-5-1	2.484	2.595	4.287	40.96 x 40.81	162.40
Mix_211-6-5	2.490		4.065	40.79 x 41.11	163.08
Mix_321-4-3	2.483		3.795	39.69 x 41.43	162.10
Mix_321-5-2	2.482	2.580	3.823	40.31 x 41.57	161.46
Mix_321-6-3	2.484		3.745	40.03 x 41.28	161.40
Mix_421-5-3	2.485		3.778	40.03 x 40.97	160.66
Mix_421-5-5	2.485	2.583	3.794	40.29 x 41.14	160.58
Mix_421-6-4	2.486		3.769	40.11 x 41.04	160.46

The full mixture samples were tested in tension-compression mode in strain control, using a closed-loop servo-hydraulic testing machine associated with a thermal chamber for temperature control, to determine the asphalt mixture viscoelastic properties. Three replicates for each type of asphalt mixture were tested.

The prismatic samples were glued to steel end plates, then mounted on customized fixtures and tested using the tension-compression sinusoidal loading mode (DTC-CY- according to EN 12697-26- Annex D, 2018). Complex modulus tests were performed at five temperatures (-10, 0, 10, 15 and 20 °C) and six frequencies (10.0, 5.0, 3.0, 1.0, 0.3 and 0.1 Hz), with a 50 με imposed axial strain amplitude. The amplitude of 50 με was selected in order to remain in the LVE range and to avoid any damage in the samples.

Two LVDTs were placed on the samples and used to monitor the axial strain ε. Axial stress was calculated based on the force measured by a load cell positioned in the press. A surface temperature probe measured the temperature of the specimens' surface (Figure 14-a).

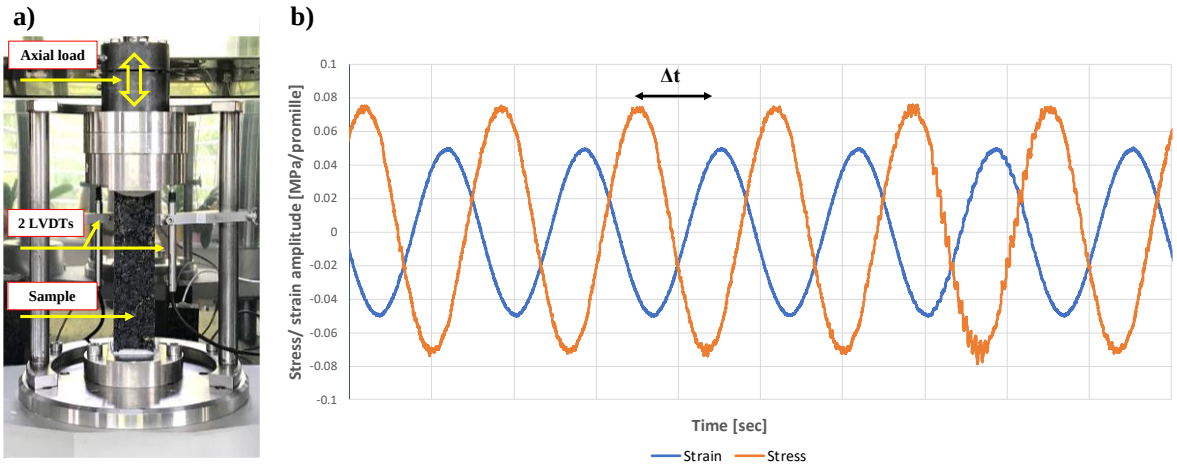

Fig. 14 *(a) Test setup of the tension-compression sinusoidal loading test and (b) an example of input and output signals of tension-compression sinusoidal loading mode.*

Expressions of axial strain ε and axial stress σ are presented in the following Equations. 16-17:

$$\varepsilon(t) = \varepsilon_0 \sin(\omega t) = Im[\varepsilon_0 e^{i(\omega t)}] \quad [16]$$

$$\sigma(t) = \sigma_0 \sin(\omega t + \varphi) = Im[\sigma_0 e^{i(\omega t+\varphi)}] \quad [17]$$

Where ε_0 is the axial strain amplitude, ω is the angular frequency ($\omega = 2\pi f$), i is the imaginary unit ($i^2 = -1$), σ_0 is the stress amplitude and φ is the phase shift between the axial stress and the axial strain (Figure 14-b).

The complex modulus E^* of asphalt mixture samples is defined as:

$$E^* = \frac{\sigma_0 e^{i(\omega t+\varphi)}}{\varepsilon_0 e^{i(\omega t)}} = |E^*| e^{i\varphi} \quad [18]$$

For each test temperature the specimens were kept for 5 hours at lower temperatures (-10 and 0°C) and for 4 hours at the other temperatures (10, 15 and 20°C) before testing.

The number of loading cycles for each frequency was limited to an appropriate number to effectively determine the complex modulus and the phase angle values. Balancing the need to reach steady-state loading and the desire to complete the test in as short of time as possible (Isailović & Wistuba, 2018).

3.2.2 Aggregates

The gradation curves of the different size of the Gabbro virgin aggregates and of the limestone filler , defined in accordance to the European standards (EN 933-1, 2012) (EN ISO 17892-4, 2016), are shown in Figure 15-(a). While, in Figure 15-(b) the 0.45 power gradation graph of the Gabbro virgin aggregates are reported.

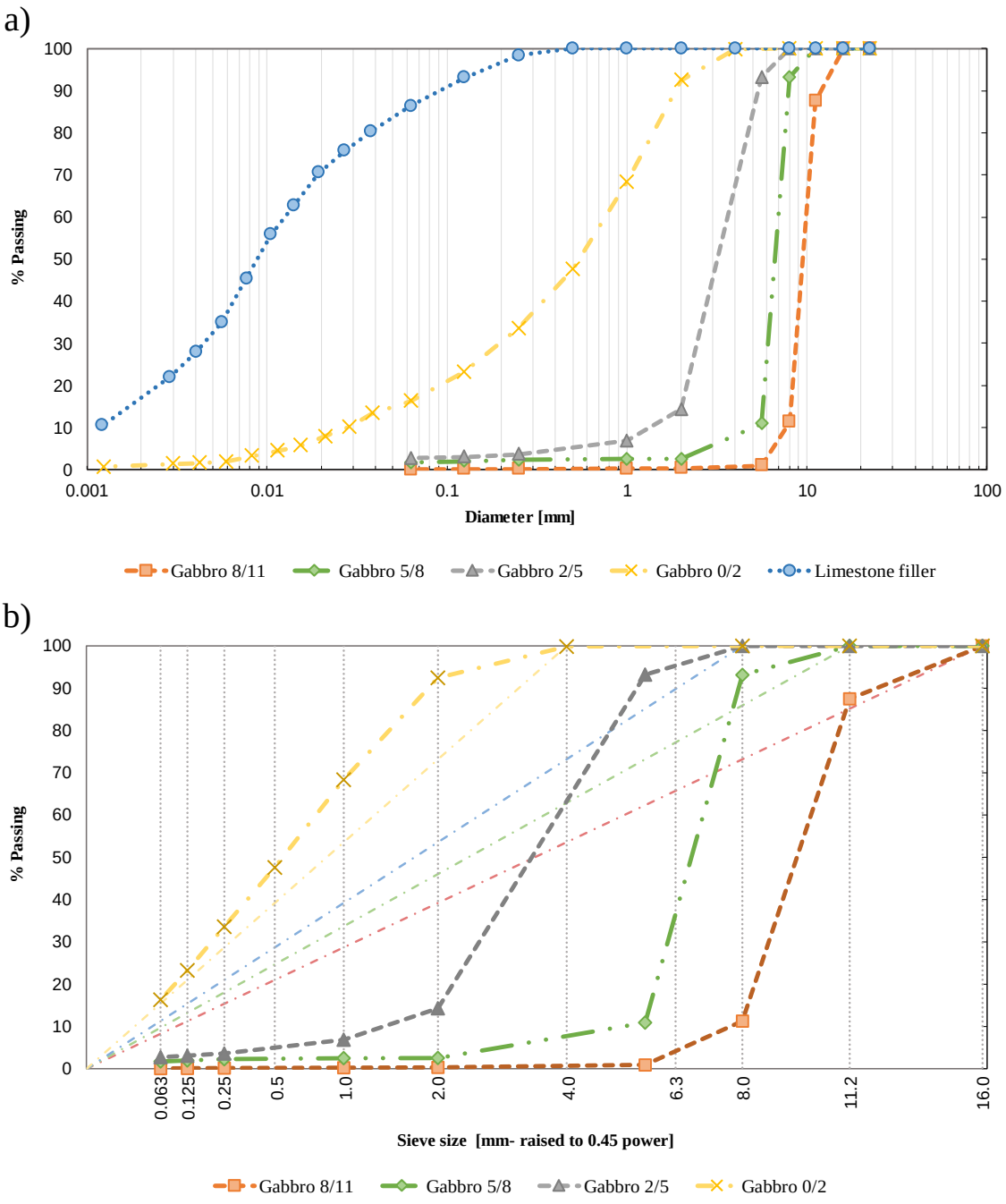

Fig. 15 *(a) Gradation curves and (b) 0.45 power gradation graph, with maximum density lines, of the virgin aggregates of the asphalt mixtures.*

Table 5 summarizes the particle density (the apparent specific density ρ_a, the bulk specific density determined on particles pre-dried in the oven ρ_{rd}, and the bulk saturated surface dry density ρ_{ssd}, and the water absorption W_{A24}), determined in accordance to EN 1097-6 (EN 1097-6, 2013).

Table 5 *Densities and water absorption of different aggregate size of asphalt mixtures- EN 1097-6.*

Material	ρ_a [g/cm3]	ρ_{rd} [g/cm3]	ρ_{ssd} [g/cm3]	W_{A24} [%]
31.5- 4 mm	2.859	2.796	2.818	0.79
4-0.063 mm	2.956	2.457	2.625	6.84

3.2.3 Asphalt binders

The four asphalt binders were identified as B_11, B_21, B_32 and B_42 respectively (acc. to VEGAS, FFG-Project Nr. 863063).

The B_11 and B_32 are unmodified binders, respectively a 50-70 and a 70-100 pen-grade, commonly used for base layer mixtures, according to the German technical specifications for roads construction (FGSV, 2013), while the B_21 and B_42 are polymer modified binders (PMBs) with thermoplastic elastomer Styrene Butadiene Styrene (SBS). Actually, B_21 is a low modified binder, while the B_42 is modified with a high content of SBS elastomer.

All binders were characterized using traditional semi-empirical tests, such as penetration (EN 1426, 2007) and softening point (EN 1427, 2007) tests, in agreement with the conventional European grading system. The Performance Grading (PG) (AASHTO M 320, 2016) was also evaluated to characterize the asphalt binders, according to AASHTO standards. In Table 6 the results of the conventional penetration and ring and ball tests performed on asphalt binders and their Performance Grading (PG) are presented.

Table 6 *Asphalt binders grading.*

Binder	B_11	B_21	B_32	B_42
Binder type	PEN 50-70	PMB 25/55-55A	PEN 70-100	PMB 45/80-65 A
Penetration @ 25 °C (dmm) [EN 1426]	64	46	85	58
Softening point R&B (°C) [EN 1427]	51.3	58.0	47.3	87.0
Performance Grading -PG [AASHTO M320]	70-22	76-22	64-22	82-22
High temperature Continuous PG [ASTM D7643]	73.27	81.12	64.04	84.59

Short-term aging procedure was performed with the standard Rolling Thin Film Oven Test (RTFO) at 163°C (EN 12607-1, 2014) for each asphalt binder prior to testing. The RTFO aged condition was used to simulate the aging that the binders suffer during the manufacture process of the FAM mixtures and of the asphalt mixtures.

Tests performed on RTFO aged binders included:

- Thermal Equibrium Tests to determine the conditioning time before testing, to guarantee that the samples had reached the thermal equilibrium (EN 14770 - Annex B, 2012) (AASHTO T315, 2012).

- Amplitude sweep stress/strain tests to define the optimal stress/strain levels to remain in the LVE range during the temperature-frequency sweep tests performed at different temperatures and for different testing geometries (EN 14770-Annex C, 2012) (AASHTO T315, 2012).

- Temperature-frequency (T-f) sweep tests to determine the rheological properties of binders in LVE range (complex shear modulus and phase angle mastercurves at the reference temperature, i.e. T_0=20°C) (EN 14770, 2012) (AASHTO T315, 2012).

The entire set of binders were tested using a Malvern Kinexus Pro Dynamic Shear Rheometer (DSR) device (Figure 16), with plate-plate geometry configuration and three different plate geometries (25 mm, 8 mm and 4 mm) to investigate their rheological properties in the LVE range.

Three different testing geometry dimensions of the plate were used, in order to enlarge the spectrum of the reduced frequency. The selected testing frequency ranged between 0.1 and 10 Hz and the temperature testing range was between -30 and 90°C, with a step of 10°C. Such wide range of testing temperatures was chosen to facilitate the fitting of the 2S2P1D model.

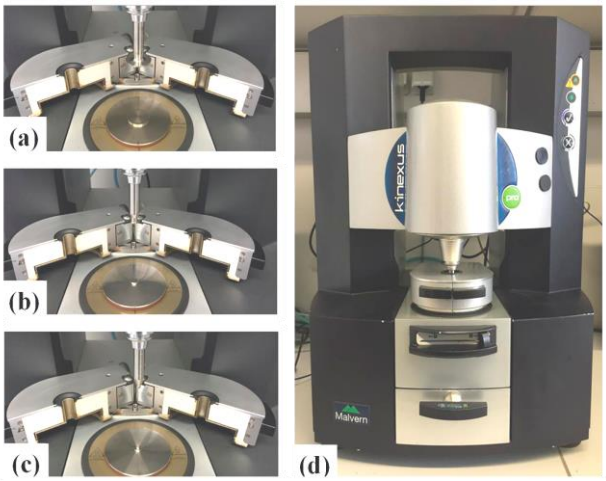

Fig. 16 *(a) 25 mm, (b) 8 mm and (c) 4 mm plate-plate geometries, (d) DSR Malvern Kinexus Pro device available at ISBS-TU Braunschweig.*

The strain-controlled mode was selected for high temperatures (25 mm), while for intermediate and low temperatures (8 mm and 4 mm) the stress-controlled mode was chosen. This is because the available DSR device provides a mixed controlled mode, which allows obtaining more reliable results in strain-controlled mode at high temperatures, while, the stress-controlled mode is more effective at intermediate and low temperatures (Bücher et al., 2019).

In order to remain in the Linear Viscoelastic (LVE) range, amplitude sweep stress/strain tests were performed preliminarly, in order to identify the optimal stress (for low temperatures) and strain (for high temperatures) levels to be used in the temperature-frequency sweep tests with different temperatures and different geometries. The LVE range was defined for the entire frequency and temperature domain of the temperature-frequency sweep tests. According to the standards the limit of the LVE range is defined

in correspondence of a drop of 5% in the initial value of the dynamic modulus over the increasing level of strains (EN 14770, 2012) (AASHTO T315, 2012).

The tests conditions for tests on asphalt binders are summarized in Table 7.

Table 7 *Stress and strain levels and characteristics for the different DSR testing geometries and temperatures used for the asphalt binders.*

Geometry diameter	Gap	Temperature range	Frequency range	Stress/Strain level
4 mm	1.75 mm	From -30°C to 0°C	From 0.1 to 10 Hz	$\tau = 1.5 \cdot 10^4$ Pa
8 mm	2.00 mm	From -10°C to 40°C	From 0.1 to 10 Hz	$\tau = 3 \cdot 10^3$ Pa
25 mm	1.00 mm	From 30°C to 50°C	From 0.1 to 10 Hz	$\gamma = 0.1$ %
		From 60°C to 90°C		$\gamma = 3.0$ %

3.2.4 Asphalt Mastics

Asphalt mastic sample were produced by adding the specific amount of filler (< 0.063 mm), pre-heated at 160°, to the designed amount of asphalt binder, RTFO-aged (EN 12607-1, 2014) and pre-heated at 160°C. The portion of filler was added gradually with a continuos stirring action, in order to prevent any formation of lumps and clusters, and to achieve a homogenous distribution of the filler particles in the binder. Mixing was performed for about 5-6 min, until the material was well blended and homogeneous in appearance.

The RTFO aged condition was used to simulate the aging that the mastics suffers during the manufacture process of the FAM mixtures and of the asphalt mixtures. When creating the mastic samples, the pre-aged asphalt binder was first heated to the mixing temperature and then combined with filler aggregates.

The composition of mastics is summarized in Table 8.

Table 8 *Composition of mastics.*

Mastic	Filler aggregate [M-%]	Binder RTFO aged [M-%]	Binder type	Ratio Filler-Binder
M_111	57.025	42.975	PEN 50-70	1.327
M_211			PMB 25-55-55A	
M_321			PEN 70-100	
M_421			PMB 45-80-65A	

Mastics were tested using the same DSR device used for binder testing before, with the plate-plate geometry configuration (Figure 16), performing temperature and frequency sweep tests in order to plot the mastercurves of the complex modulus and of the phase angle. The thermal equilibrium tests and amplitude sweep stress/strain tests were performed preliminarily to identify the conditioning time and the limits of the LVE range.

Tests performed on RTFO-aged mastics include:

- Thermal Equibrium Tests to determine the conditioning time before testing, to guarantee that the samples had the same temperature at all their coordinates.
- Amplitude sweep stress/strain test to define the optimal stress/strain levels to remain in the LVE range during the temperature-frequency sweep tests performed at different temperatures and for different testing geometries.
- Temperature-frequency (T-f) sweep test to determine the rheological properties of mastics in LVE range (complex shear modulus and phase angle mastercurves at the reference temperature, i.e. T_0=20°C).

Three different testing geometry dimensions of the plate were used, to enlarge the spectrum of the reduced frequency. The selected testing frequency ranged between 0.1 and 10 Hz and the temperature testing range was between -10 and 90°C, with a step of 5°C from -10 to 10°C and a step of 10°C for the other temperatures. Such wide range of testing temperatures was chosen to facilitate the fitting of the 2S2P1D model.
The strain-controlled mode was selected for high temperatures (25 mm geometry), while for intermediate and low temperatures (8 mm and 4 mm geometries), the stress-controlled mode was chosen (Bücher et al., 2019).

The tests conditions for tests on asphalt mastics are summarized in Table 9.

Table 9 *Stress and strain levels and characteristics for the different DSR testing geometries and temperatures used for the asphalt mastics.*

Geometry diameter	Gap	Temperature range	Frequency range	Stress/Strain level
4 mm	1.75 mm	From -10°C to 10°C	From 0.1 to 10 Hz	$\tau = 1 \cdot 10^3$ Pa
8 mm	2.00 mm	From -10°C to 10°C	From 0.1 to 10 Hz	$\tau = 3 \cdot 10^3$ Pa
		From 10°C to 40°C		$\tau = 1 \cdot 10^2$ Pa
25 mm	1.00 mm	From 30°C to 50°C	From 0.1 to 10 Hz	$\gamma = 0.03$ %
		From 60°C to 90°C		$\gamma = 0.1$ %

3.2.5 Fine Aggregate Matrix

In this study FAM specimens were produced in order to recreate this specific material phase as in the four asphalt mixtures tested in this research. The design of the FAM mixtures should be based on the gradation and composition of the full asphalt mixtures of which they represent a crucial part. Underwood et al. (Underwood & Kim, 2013b) demonstrated that FAM fabrication protocol should yield to a useful mixture-level insight to guarantee to the multiscale modelling efforts to be accurate.

Currently, there is no consensus among researchers about a proper design method of FAM phase that can be applied to most materials used to produce asphalt mixtures and that could replicate in the laboratory the FAM fraction within them. One on the main purposes of the present Thesis is to identify a procedure to accurately replicate the FAM phase.

An extensive literature review of the most common design methods for FAM samples was done. Several empirical (Countinho, 2012) (Sousa et al., 2013) and analytic methods (Castelo Branco, 2008) (Underwood and Kim, 2013) (Ng et al., 2018) have been proposed, as seen in Chapter 2 Paragraph 2.1.2. Concerning the aggregate gradation most of these methods define it by normalizing the gradation passing to the sieve of nominal size 1.19 mm (Sieve No. 16) (Mesh, US), chosen arbitrarily as the limit between the coarse and fine aggregates. The only method that suggests a delimitation between fine and coarse aggregates based on the corresponding asphalt mixture characteristics is the one proposed by Underwood and Kim. To define a standard protocol for FAM design methods in the present research were compared the analytic methods, trying to identify the most promising one, to ensure the best representativeness of the FAM phase in the asphalt mixture, between the methods proposed by Castelo Branco, Underwood and Kim and Ng et al..

To verify their reliability and to select the more suitable method, the analytically defined aggregate gradations and binder contents, were compared with the experimentally defined binder content and aggregate gradation post solvent extraction of the fine portion (passing the 1 mm sieve) of the loose mixture. The 1.00 mm sieve size was chosen for the experimental verification due to the huge efforts required by the sieving of the loose mixtures with a smaller diameter. The solvent extraction procedure was used in this study as an alternative to ignition oven testing for determining binder content of FAM samples

due to concern about losing part of the fine aggregate particles and filler amount during the ignition process.

Table 10 summarized the results of the comparison between the analytically defined mix design of FAM by means of different methods and the experimentally defined.

Table 10 *Results of the comparison between the analytically defined mix designs of FAM with different methods and the experimentally defined one.*

EXTRACTION WITH SOLVENT		**UNDERWOOD & KIM METHOD (2013)**		**CASTELO BRANCO (2008) AND NG et al. METHOD (2018)**	
Sieve size [mm]	**% Passing [M-%]**	**% Passing [M-%]**	**Δ**	**% Passing [M-%]**	**Δ**
1.0	100	100	0.00%	100	0.00%
0.5	69.25	69.00	-0.35%	75.82	9.50%
0.25	48.58	47.72	-1.77%	51.64	6.30%
0.125	35.79	34.54	-3.48%	37.30	4.24%
0.063	26.24	25.39	-3.25%	27.56	5.01%
Binder Content [M-%]	14.00 %	13.27 %	-5.2 %	5.92 % *[Ng et al. Method]*	-57.76%
				16.81 % *[Castelo Branco Method]*	20.06%

The gradation curves are also graphically reported in Figure 17, where the red curve describes the aggregate gradation experimentally obtained after the solvent extraction of the asphalt binder, while the green dotted line and the blue dotted line represent the analytically defined aggregate gradation with different methods.

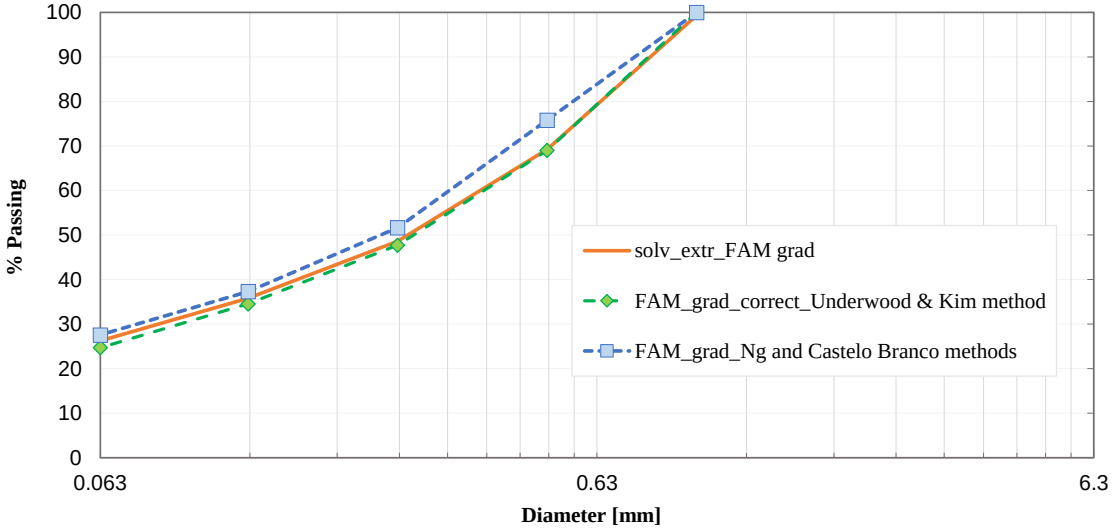

Fig. 17 *Comparison between the gradation curves of FAM.*

Considering the results obtained from these comparisons (Table 10 and Figure 17), the procedure of mix design definition proposed by Underwood and Kim (Underwood and Kim, 2013) seems the most promising and accurate in reproducing in the laboratory the FAM phase as it exists within the mixtures.

In this Thesis the aggregate gradation and binder content for FAM production was found by using the microstructural investigation procedure by Underwood and Kim, selected as the most promising method and verified through experimental solvent extraction procedures. The full analytical procedure is reported in the following paragraph.

3.2.5.1 FAM mix design

The aggregate size distribution of the fine particles and filler and the appropriate asphalt content in the FAM phase were defined according to the procedure proposed by Underwood and Kim in 2013. This procedure is based on the following fundamental assumptions:

- The first assumption is that FAM aggregate particles are uniformly coated by the mastic. The average mastic film thickness can be computed from the volume of the asphalt mastic within the asphalt mixture, from the volume of filler in the mastic and from the aggregate gradation parameters given from the job mix formula of asphalt mixtures.

- The second assumption is based on meso-gravimetric results: it is incorrect to include all of the filler-sized particles into the FAM's aggregate gradation, since some of these filler-sized particles coat together with the asphalt binder the coarse aggregate particles (Underwood and Kim, 2013), and therefore it is necessary to redefinite the aggregate gradation in the FAM.

The first task of the mix design definition was to determine the maximum aggregate size in the FAM. This maximum aggregate size in the FAM is defined in accordance to the packing principles (Vavrik et al., 2001) (Vavrik et al., 2002), and to the European specifications (EN 13043, 2013).

The full procedure for FAM mix design definition is defined as follows:

Step 1: Definition of the maximum aggregate size in the FAM is equal to the Fine Aggregate Initial Break sieve (D_{FAIB}), as function of the NMAS of the asphalt mixture. It is defined, by means of Equation [1] (Chapter 2), according to the packing principles introduced in the Bailey method of mix design (Vavrik et al., 2001) (Vavrik et al., 2002). In Figure 18 is illustrated the schematic demonstration of D_{FAIB} definition according to Bailey method and the rationale for 0.22 factor.

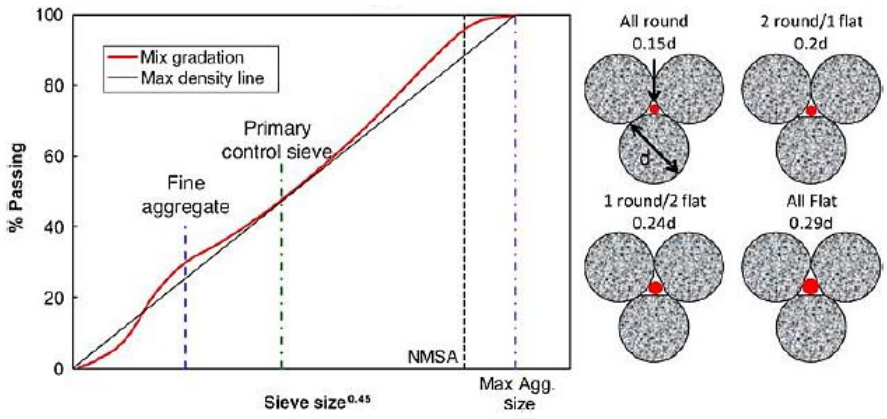

Fig. 18 *Schematic demonstration of D_{FAIB} definition and rationale for 0.22 factor* (Underwood & Kim, 2013b).

Step 2: Estimation of the initial gradation of the FAM, keeping the proportion of the fine aggregates that comprise the FAM, and normalization of the gradation particles smaller than the D_{FAIB}, as given in Equation [19].

$$\hat{P}_i = \frac{P_i}{P_{DFAIB}} x100 \qquad [19]$$

Where $\hat{P}_i$ is the initial percentage passing sieve size i within the FAM, P_i is the percentage passing sieve size i from the mix formula (in the total mix gradation) and P_{DFAIB} is the percentage passing the break sieve $\mathrm{D_{FAIB}}$ from the mix formula.

Step 3: Determination of the mass of each stockpile, M_i, in the FAM, except for the filler, using Equation [20]:

$$M_i = \frac{(\hat{P}_{i+1} - \hat{P}_i)}{(G_{sb,i} \cdot \rho_{water})} \quad [20]$$

Where $G_{sb,i}$ is the bulk specific gravity of aggregate size i (EN 1097-6, 2013) (EN 1097-7, 2008) and ρ_{water} is the density of water at 25°C (0.997 g/cm^3).

Step 4: Estimation of the number of particles of each size, using Equation [21]:

$$N_i = \frac{M_i}{(\pi/6)((d_{i+1} + d_i)/2)^3} \quad [21]$$

Step 5: Computation of the volume of mastic that coats the FAM aggregates using Equations [22] and [23]:

$$V_{mastic,i} = \frac{\pi}{6}\left[\left(\frac{d_{i+1} + d_i}{2} + 2t\right)^3 - \left(\frac{d_{i+1} + d_i}{2}\right)^3\right] \quad [22]$$

$$V_{mastic,calc} = \sum_{i=1}^{J}\left[N_i \cdot V_{mastic,i}\right] \quad [23]$$

Where $V_{mastic,i}$ is the volume of mastic that coats a single particle of size i and t is the thickness of the mastic film in cm. Underwood and Kim (Underwood and Kim, 2013) proposed the following particle-size-dependent Equation [24] for the calculation of the film thickness:

$$t_i = 0.033\left(\frac{d_{i+1} + d_i}{2}\right)^{0.32} \quad [24]$$

However, due to the lack of physical justification for such particle-size-dependent film thickness formula, it is assumed that the mastic uniformly coats all aggregate particles is adopted. In this case, the average mastic thickness t is found according to Equation [25]:

$$V_{mastic,calc,mix} = V_{mastic,JMF,mix} = V_{063} + V_{be} \quad [25]$$

Where V_{063} is the volume of the filler-sized particles (<0.063 mm) in cm^3 and V_{be} is the effective asphalt binder volume in cm^3.

Step 6: Calculation of the amount of asphalt binder absorbed by the FAM particles from Equation [26]:

$$M_{ba} = \sum_{i=1}^{N} M_{ba,i} = \sum_{i=1}^{N} \left[(P_{i+1} - P_i) \left[\frac{1}{G_{sb,i}} - \frac{1}{G_{se,i}} \right] G_b \right] \quad [26]$$

Where M_{ba} is the total mass of absorbed asphalt binder in the asphalt mixture (g), $M_{ba,i}$ is the mass of absorbed asphalt binder for aggregate retained on sieve i (g) and $G_{sb,i}$, $G_{se,i}$ and G_b are the bulk specific gravity of aggregate size i, the effective specific gravity of aggregate size i (EN 1097-6, 2013) (EN 1097-7, 2008) and the specific gravity of asphalt binder respectively.

Step 7: Calculation of the total mass of filler and asphalt binder in the FAM using the volume of mastic, the volumetrically averaged concentration (VC%, Equation [27]), the absorbed mass of asphalt binder and the specific gravities of the filler and mastic, $G_{sb,063}$ and G_b, as given in Equations [28] and [29]:

$$VC\% = \frac{V_{063}}{V_{063} + V_{be}} x100 \quad [27]$$

$$M_{063} = \frac{VC\%}{100} x\, V_{mastic,calc} \left(G_{sb,063} \cdot \rho_{water} \right) \quad [28]$$

$$M_b = \left[1 - \frac{VC\%}{100} \right] x\, V_{mastic,calc} \left(G_b \cdot \rho_{water} \right) + M_{ba} \quad [29]$$

Step 8: Redefinition of the aggregate gradation based on the masses of each stockpile in the FAM, M_i, derived at Step 3, and the filler mass, derived at Step 7.

Step 9: Calculation of the total asphalt binder content.

For FAM mix design procedure (Steps 3 and 6) the bulk and the effective specific gravity of aggregates of size smaller than the break sieve D_{FAIB} from the job mix formula was defined according to the standards:

- UNI EN 1907-6 for aggregates of sizes between the break sieve D_{FAIB} size and retained to 0.063 mm sieve;

- UNI EN 1097-7 for aggregates of sizes smaller than 0.063 mm (filler).

The averaged results between three determinations are reported in Table 11.

Table 11 *Density and water absorption of different aggregate sizes for FAM mix design- EN 1097-7 and EN 1097-6.*

Material	ρ_{rd} [g/cm^3]	ρ_a [g/cm^3]	ρ_{ssd} [g/cm^3]	W_{A24} [%]	Porosity [%]
Aggregate size [0.5-0.125 mm]	2.835	2.883	2.829	0.582	1.68
Filler [< 0.063 mm]	2.433	2.740	2.277	-	-

In Table 12 the aggregate gradation and the characteristics of FAM mix design are summarized.

Table 12 *Characteristics of FAM mix design.*

FAM	FAM_ 111	FAM_ 211	FAM_321	FAM_421
Binder type	PEN 50/70	PMB 25-55-55A	PEN 70/100	PMB 45-80-65A
D_{FAIB} [mm]	0.5			
FAM gradation	**Sieve size [mm]**	**% Passing**		
	0.5	100		
	0.25	65.55		
	0.125	45.12		
	0.063	31.23		
Mastic volumetric concentration [%]	40.36			
Thickness of mastic film [µm]	23.68			
Binder content [%]	16.22			

The gradation curves of the full graded asphalt mixture and of the corresponding FAM are shown in Figure 19. The dotted blue line represents the FAM aggregate gradation after the initial normalization of the gradation particles smaller than D_{FAIB}, while the gradation curve of the FAM after the correction (Step 8) is reported with a grey line.

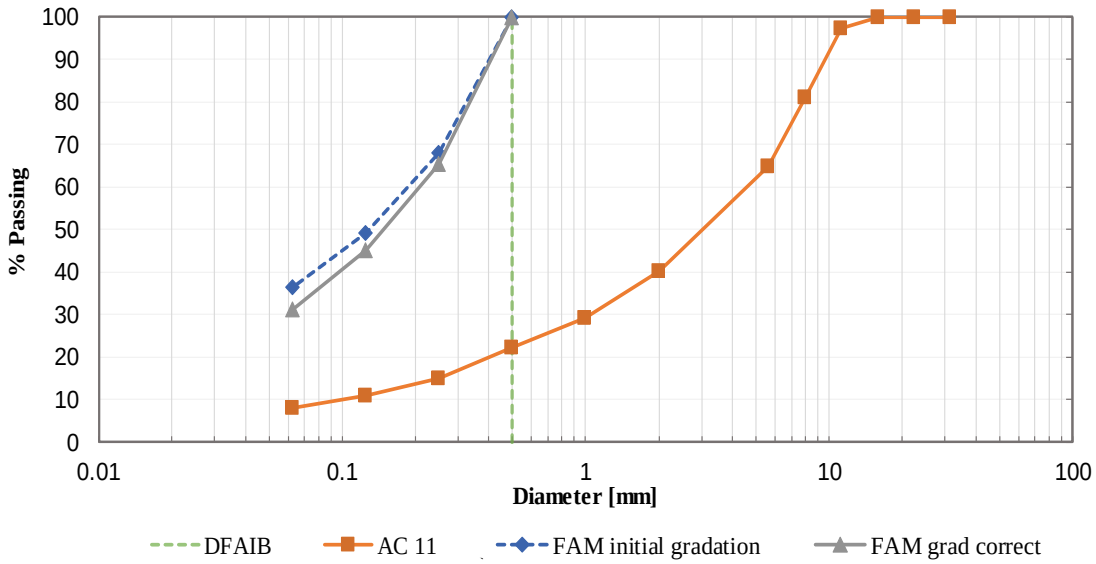

Fig. 19 *Gradation curve of the asphalt mixture and of the corresponding FAM.*

3.2.5.2 FAM compaction and specimen fabrication

Besides mix design definition, sample compaction plays a fundamental role in determining the significance of FAM-based experimental results. Previous researches demonstrated that samples fabricated by means of Gyratory compaction, with a procedure analogous to the one used to prepare asphalt mixture specimens, show a better resemblance to FAM phase within an asphalt mixture (Izadi et al., 2011) (Underwood and Kim, 2013), in comparison to the FAM samples fabricated with cylindrical molds.

In this Thesis, mixing and compaction temperatures are defined according to AASHTO TP 4 (AASHTO TP 4, 2000) and EN 12697-31 (EN 12697-31, 2007). The fine aggregates, with the correct aggregate gradation, and the binder were preheated to the mixing temperature of 160°C, and then mixed, while taking care at not to lose the finest portion of the material. FAM samples of 150 mm in diameter and of 130 mm in height were compacted in the Superpave Gyratory Compactor (SGC), with a pressure of 600 ± 18 kPa and a gyration angle of 1.25 ± 0.02°. The design height of 130 mm for the compacted FAM was selected in order to maximize the number of FAM specimens that can be cored from the compacted samples and to achieve a uniform air voids distribution along the FAM sample height (Gudipudi & Underwood, 2015) (Gudipudi & Underwood, 2017a) (Gudipudi & Underwood, 2017b). The criterion to stop the compaction was defined when the height variation between one gyration and the other was negligible (maximum compaction).

Both ends of the compacted samples were sawed in order to guarantee smooth surfaces and to obtain homogeneous air voids distribution along the samples. From the Gyratory compacted samples, small cylinders with a diameter of 14 mm and a height of about 50 mm were drilled using a water-cooled coring machine. About 35 FAM specimens were cored from each slice of the compacted samples (h= 50 mm and d=150 mm).

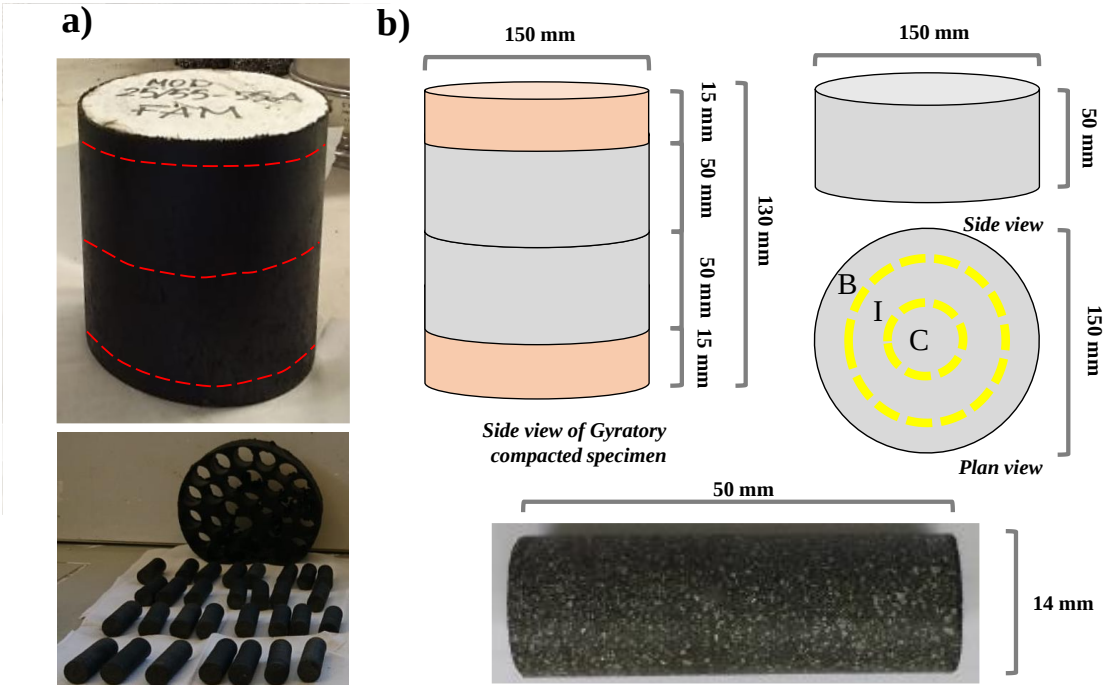

Fig. 20 *Pictures (a) and schemes (b) of Gyratory compacted samples and their cutting procedure and dimensions of FAM specimens.*

According to the recommendations provided by the literature and previous experiences (Castelo Branco, 2008) (Gudipudi & Underwood, 2017a), the FAM specimens were separated into three groups:

- Labelled with the letter "C", the FAM specimens cored from the inner concentric zone (center);
- Labelled with the letter "I", the FAM specimens cored in the intermediate region;
- Labelled with the letter "B", the FAM specimens cored from the border.

One of the main concerns about the repeatability of test results using FAM specimens is the range of air voids of the samples cored from different zones of the SGC samples. For this reason, an analysis of the air voids distribution was performed.

The air voids content was measured for each SGC sample and for each cored FAM specimen, to ensure consistency in test specimens and conformity with the target

equivalent mixture air voids content. The FAM specimens should contain between 50 and 75% of the total air voids of the asphalt mixture (Underwood & Kim, 2013). Taking into account asphalt mixtures with an air voids content of 3.5%, the FAM air voids content should range from 1.8 to 2.6%. The FAM specimens with air voids content differing from these reference values were discarded and not used for the following tests.

The density and the air voids content of each FAM specimen were measured, using the procedure outlined in AASHTO T 166 and UNI EN 12697-6; with a balance of 0.01 g of accuracy. First the surface-dry specific gravity G_{mb} was determined (AASHTO T 166, 2016) (EN 12697-6, 2008), and then the air voids content was calculated considering the previously measured theoretical specific gravity G_{mm} of the uncompacted FAM mixes, according to AASHTO T 209 (AASHTO T 209, 2019), Equation 30.

$$Air\ Voids\ content\ (\%) = \left(\frac{G_{mm}-G_{mb}}{G_{mm}}\right) \cdot 100 \quad [30]$$

Table 13 *G_{mm} and air voids content of FAM specimens.*

FAM	FAM_ 111	FAM_ 211	FAM_321	FAM_421
Theoretical maximum specific gravity of FAM specimen - G_{mm} [g/cm^3]	2.231	2.227	2.230	2.221
Average air voids content [%] AASHTO T166	2.51±0.42	2.61±0.45	2.45±0.32	2.92±0.29

Figure 21 shows the air voids contents measured for the FAM specimens.

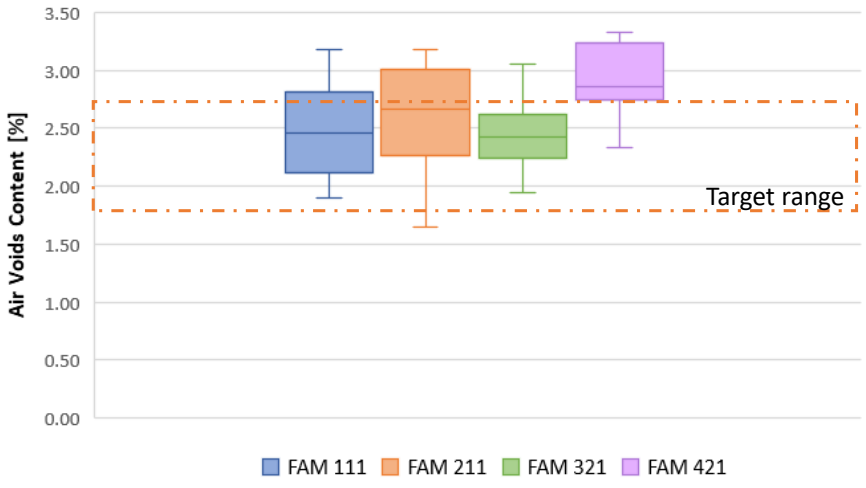

Fig. 21 *FAM samples air-void contents for the four FAM mixes.*

The air voids content of FAM specimens ranged between 1.7 and 3.3 %. Considering the previously mentioned target range (highlighted by the red dotted line in Figure 21), some FAM specimens show higher values of air voids content. In particular, the highest values were identified for the FAM 421 specimens.

Because of considering different zones when coring, the FAM specimens from SGC samples it was possible to investigate the air voids distribution in relation to the zone within the SGC samples. The air voids contents of FAM specimens cored from three different zones were averaged in order to investigate their differences and possible significant deviations. In Figure 22 the results of the distribution of air voids content in the three different coring zones are summarized.

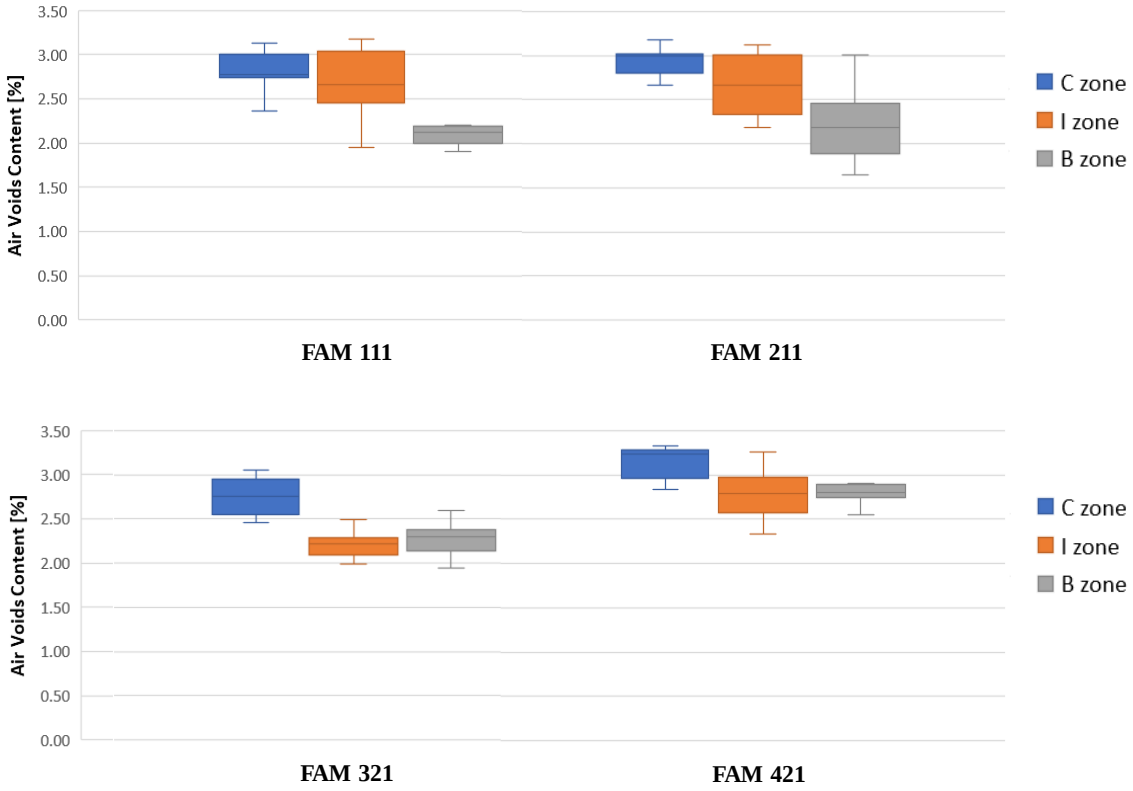

Fig. 22 *Air voids content distributions of the FAM specimens extracted from different zones of the SGC samples.*

From this analysis a decreasing trend from the central zone -C to the outer zone- B was observed. This difference is remarkable in particular for FAM 321 and 421 specimens. Zone C is always characterized by the highest values of air voids content. This phenomenon is assumed to be related to the criterion used to stop the compaction process. Recently, other researchers suggested to keep the same number of gyrations used to

compact the asphalt mixtures (Ng et al., 2018). For following experimentations on FAM mixes is advisable to use such criterion. While, for the present Thesis was avoided the use for tests of FAM specimens cored from the central zone- C. In Figure 23 the air voids contents of FAM specimens cored exclusively in the zones B and I. The air voids contents of the FAM specimens cored from these zones are almost completely included in the target range.

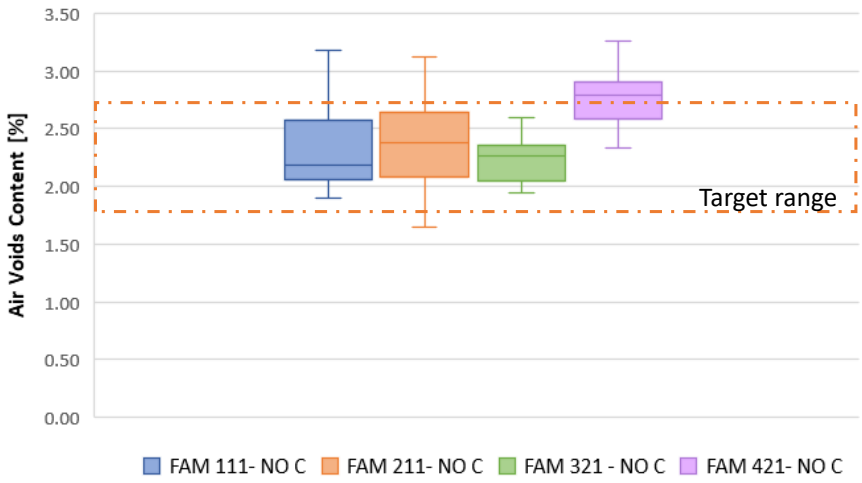

Fig. 23 *Air voids contents of FAM specimens cored exclusively from zones B and I of SGC samples.*

3.2.5.3 FAM test setup

The cylindrical FAM specimens, of 14 mm in diameter and of about 50 mm in height, were tested using a torsion bar fixture in a Dynamic Shear Rheometer (DSR), also known as a Dynamic Mechanical Analyzer (DMA) test setup (Caro et al., 2015) (Gudipudi & Underwood, 2015) (Sousa, 2010). For cylindrical asphalt specimens undergoing torsional deformation, previous researchers demonstrated that geometry and clamping barely affect the shear moduli, and the torsion bar measurements essentially coincide with those obtained using parallel plates (Dessi et al., 2016). However, more research may be needed to investigate possible differences more clearly.

FAM specimens were tested using a solid torsion bar fixture in an Anton Paar MCR301 DSR (available at the department of Civil and Environmental Engineering of the University of Pisa, Italy). In Figure 24 are reported pictures and schemes of the test setup. The FAM specimens were clamped between the movable and the stationary fixture and then enclosed in a thermal chamber. When performing the test, special attention was given

to ensure that the specimen was correctly aligned and clamped in the DSR. Each specimen has been carefully inspected and checked to assure that it is undamaged in the clamping zone and there were no localized weak areas that could influence the results.

Currently, despite the growing interest and the great potentialities of FAM testing in the prediction of mixture performance, there are no specific standards for FAM testing procedures. One of the main objectives of the present research is to define testing protocols guidelines for the determination of the FAM mastercurves in LVE range.
In this study, testing of the FAM specimens focused on strain-controlled amplitude sweep tests, in order to identify the thresholds of the linear viscoelastic (LVE) range, and on temperature-frequency sweep tests, in order to assess full rheological behavior in the LVE range of the FAM. The temperature-frequency sweep tests were conducted at the small strain values within the LVE region identified with the amplitude sweep strain tests.

The experimental plan included:

- Thermal Equilibrium tests, in order to identify the conditioning time required to the FAM specimen to reach the thermal equilibrium at any specific each test temperature (EN 14770- Annex B, 2012) (AASHTO T315, 2012).

- Strain-controlled amplitude sweep (A-sweep) tests, to determine the thresholds of the linear viscoelastic (LVE) range. In the LVE range, the obtained shear stiffness of any FAM specimen can be considered independent from the shear strain. The limits between the linear and the non-linear viscoelastic range were defined (according to the standard definition for asphalt binder), as the strain rate where the shear modulus |G*| decreases to 95% of its initial value (EN 14770- Annex C, 2012) (AASHTO T315, 2012).

- Temperature-frequency sweep (T-f sweep) tests, were conducted to obtain mastercurves, in analogy to test standard prescriptions for asphalt mixtures (EN 12697-26, 2018). The response functions of primary interest are the complex shear modulus |G*| and phase angle δ mastercurves, and the Cole-Cole diagrams.

The geometrical and volumetric characteristics of the FAM specimens are summarized in Table 14.

Table 14 *Geometrical and volumetric characteristics of tested FAM specimens.*

Tests	Number of samples	Sample ID	Air voids content [%]	Diameter [mm]	Height [mm]
Thermal Equilibrium and A-sweep Tests	2	FAM_111-28 B	2.09	13.92	43.98
		FAM_111- 21 B	2.17	13.99	44.00
Thermal Equilibrium and T-f sweep tests	5	FAM_111-9 B	2.21	13.94	45.36
		FAM_111- 26 B	1.92	13.91	45.38
		FAM_111- 14 B	2.02	13.42	45.51
		FAM_111 -1 B	1.90	13.89	44.67
		FAM_111 -23 B	2.49	13.94	44.56
Thermal Equilibrium and A-sweep Tests	2	FAM_211-26 B	1.41	13.93	47.86
		FAM_211- 21 B	2.43	13.92	48.31
Thermal Equilibrium and T-f sweep tests	5	FAM_211-20 B	2.05	13.86	48.38
		FAM_211-23 B	1.50	13.90	48.00
		FAM_211-5 B	2.60	13.74	48.59
		FAM_211-27 B	1.65	13.91	47.16
		FAM_211-25 B	2.18	13.88	47.92
Thermal Equilibrium and A-sweep Tests	2	FAM_321-29 B	1.60	13.76	54.37
		FAM_321-28 B	2.22	13.76	54.26
Thermal Equilibrium and T-f sweep tests	5	FAM_321-37 I	1.99	13.66	53.16
		FAM_321-41 I	2.01	13.78	53.66
		FAM_321-39 I	1.60	13.76	53.66
		FAM_321-32 B	1.95	13.74	53.94
		FAM_321-31 B	2.29	13.72	53.98
Thermal Equilibrium and A-sweep Tests	2	FAM_421-37 B	2.55	13.72	55.00
		FAM_421- 46 I	2.86	13.86	54.42
Thermal Equilibrium and T-f sweep tests	5	FAM_421-36 B	2.75	13.88	56.40
		FAM_421-50 B	2.86	13.83	56.26
		FAM_421-48 I	2.55	13.87	54.44
		FAM_421-47 I	2.59	13.88	54.15
		FAM_421-43 I	2.33	13.88	55.76

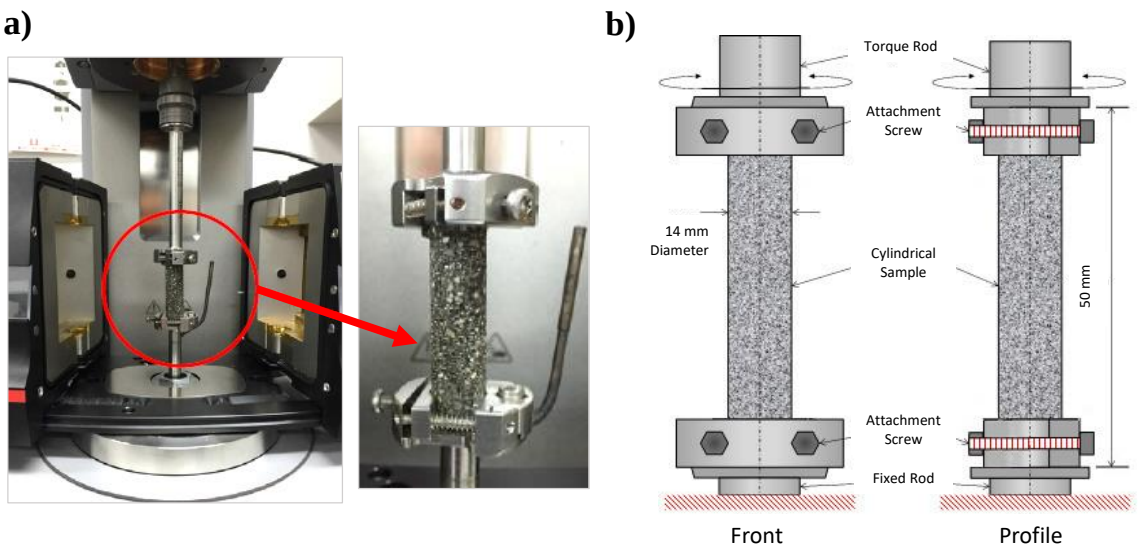

Fig. 24 *Picture (a) and scheme (b) of setup for testing FAM specimens using a torsion bar fixture.*

For full characterization of the rheological properties within the LVE range, temperature and frequency (T-f) sweep tests in strain-controlled mode were conducted.

Before starting a test, the FAM specimen was conditioned to the test temperature in an environmental chamber, in order to guarantee the same temperature within the entire specimen.

3.2.5.4 Thermal Equilibrium Tests

Before performing tests on FAM specimens, they must be conditioned to the test temperature. It takes some time to reach the thermal equilibrium. Therefore, each FAM specimen was stored for at least 2 hours at lower temperatures (-10, 0 and 10°C), and for at least 1 hour at the other temperatures (20, 30 and 40°C), in a thermal chamber before testing.

However, fixing the FAM specimens in the testing machine requires some time, at which specimen temperature may change. For this reason, before testing, the Thermal Equilibrium Test must be performed.

The equilibrium time can be determined by monitoring the complex shear modulus |G*| variations with time, while the phase angle is less sensitive to temperature changes and may therefore not be used for this purpose. According to Annex B of EN 14770 (EN

14770, 2012) the equilibrium is reached when the complex shear modulus |G*| equals a constant value during temperature conditioning.

The Thermal Equilibrium Test is run at a given frequency of 1.00 Hz with a shear strain of 0.0001%, such conditions were chosen to test the specimens within the LVE range. The complex shear modulus is recorded every 5 minutes, until the difference between two records is less than 0.5% and the shear modulus can be considered constant. Then the temperature within the specimen is considered to be steady, and the amplitude sweep, and frequency sweep tests can be started.

In Figure 25 is shown an example of a Thermal Equilibrium Test results.

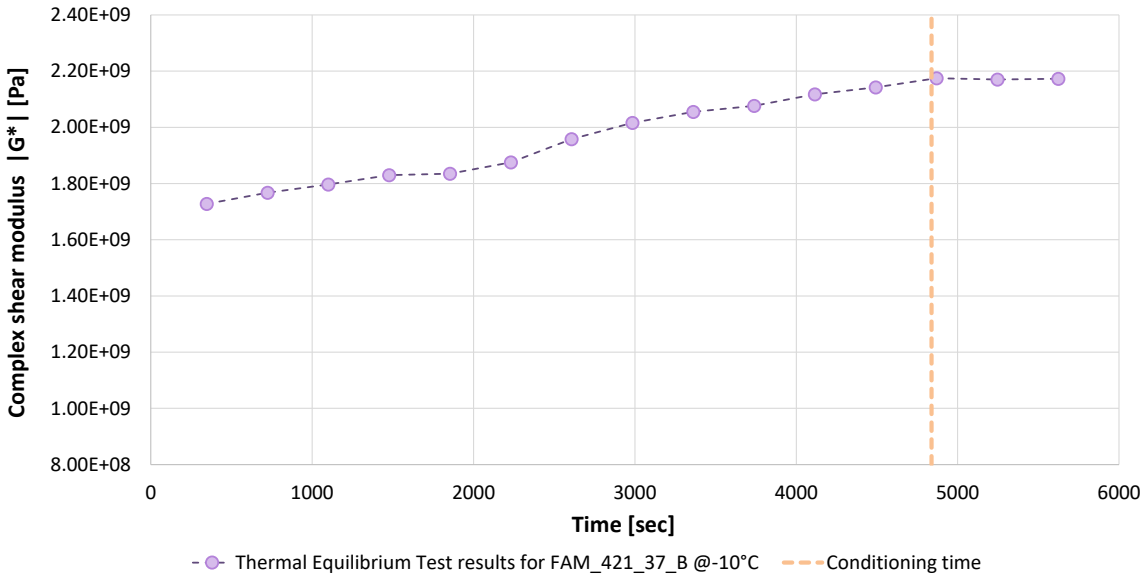

Fig. 25 *Example of a Thermal Equilibrium Test, obtained for FAM_421-37 B at a temperature of -10°C, by checking the development of the complex shear modulus every 5 minutes.*

3.2.5.5 Amplitude Sweep Tests

The strain limits for the LVE range were determined from the results of the amplitude sweep tests. The strain sweep tests were performed at different frequency-temperature combinations by increasing the strain level logarithmically. For temperatures from -10°C to 10°C the strain was stepwise increased from 0.00001 to 0.001 %, and for temperatures from 10°C to 40°C from 0.0001 to 0.01 %.

The limits of the LVE range were defined in accordance to the standards for asphalt binders, which claim that the LVE range is limited by a drop by 5% of the initial value of

the complex shear modulus |G*| over the increasing level of strains, in accordance to the indications provide by the Annex C of EN 14770 and by AASHTO T315.(EN 14770, 2012) (AASHTO T315, 2012).

The results of the torsional shear sweep strain tests are shown in Figure 26. The geometrical and volumetric characteristic of the tested specimens are listed in Table 14.

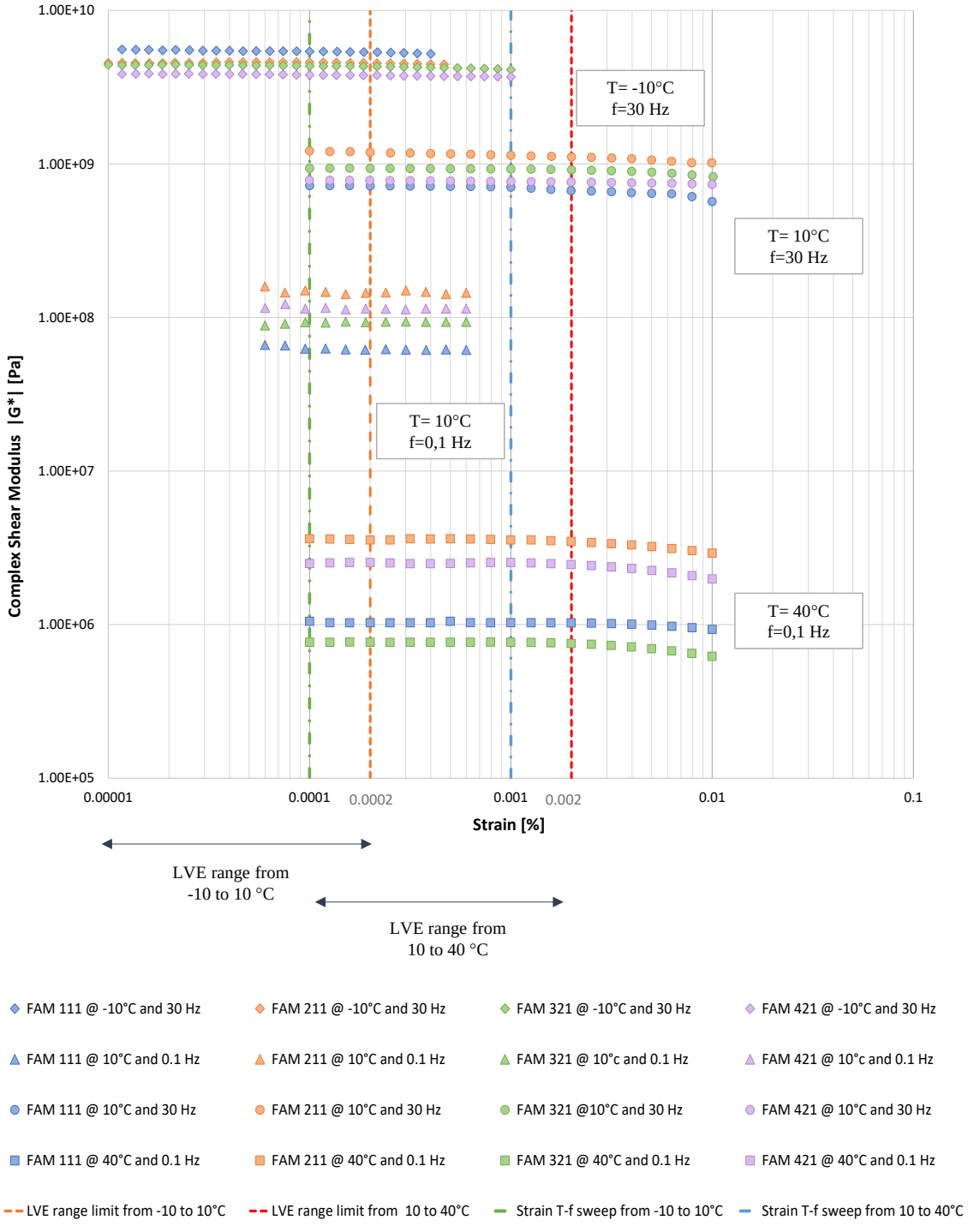

Fig. 26 *Results from strain-controlled torsion bar shear tests for different temperature-frequency combinations.*

The the red and the orange dotted lines in Figure 26 highlight the limits of the LVE range for the two temperature ranges; from -10 to 10 °C it held until around 0.0002% strain= 2 με, while from 10 to 40 °C until around 0.002% strain= 20 με. The green and the blue dotted line depict the strain levels used to perform T-f sweep tests on FAM specimens within the LVE range (Paragraph 3.2.5.6) respectively for the two temperature ranges.

3.2.5.6 Temperature and Frequency sweep tests

Temperature-frequency (T-f) sweep tests were perfomed to determine the rheological properties of FAM in LVE range. These tests were performed by applying oscillatory torsional deformation in strain-controlled mode on the FAM specimens at different loading frequencies and temperatures. Testing frequencies ranged from 0.1 to 30 Hz, while temperatures ranged between -10 and 40 °C, with a step of 10°C between the temperatures. The range of testing temperatures was chosen to facilitate the fitting of the 2S2P1D model of FAM data. The strain amplitudes used to perform T-f tests, selected based on the results of the amplitude sweep tests (Figure 26), are summarized in Table 15:

Table 15 *Strain levels used to test FAM specimens in the torsion bar configuration.*

Temperature range	Frequency range	Strain level
From -10°C to 10°C	From 0.1 to 30 Hz	0.0001% = 1.00 με
From 10°C to 40°C	From 0.1 to 30 Hz	0.001% = 10.00 με

Tests performed on FAM specimens showed a good repeatability (consistent results on multiple specimens by the same operator) and a low variability in general, with an average coefficient of variation of 3.26%. The number of test replicates was fixed to n=5, according to Miranda-Arguello et al. (Miranda-Arguello et al., 2014). Such sample size should be the optimal one to ensure the best repeatability in test results.

3.3 Tests results, data elaboration and modelling

The data obtained from T-f sweep tests of the four material scales (binders, mastics, FAM and mixtures) were used to develop mastercurves. The mastercurves provide a simple visual understanding of the response of viscoelastic materials and allow estimating the rheological properties over a wide range of temperatures and frequencies.

3.3.1 Asphalt mixtures mastercurves development

Complex modulus |E*| and corresponding phase angles δ were computed from the test results, and the mastercurves of the different mixtures were plotted considering the Christensen Andersen Maresteanu (CAM) model, reported in Equation 12 (Chapter 2), also used for binders, mastics and FAM, and the sigmoidal model, reported in Equation 15 (Chapter 2), also used for FAM results. The measured data are modelled based on the assumption that the effects of loading time and temperature can be expressed through one joint parameter, the time-temperature shift factor a_T, expressed using the Williams-Landel-Ferry (WLF) equation (Equation 6) for bituminous materials at a specific reference temperature T_0 (in this research T_0=20°C).

The two asphalt mixtures made with modified binders (MIX_211 and MIX_421) showed a thermorheologically complex behavior and did not conform to the Time-Temperature Superposition Principle (TTSP). However, in first approximation, the complex modulus mastercurves were plotted at the reference temperature, using the "Partial Time-Temperature Superposition Principle" (PTTSP) shifting procedure proposed by Olard in 2003 (Olard et al., 2003a) (Olard et al., 2003b). This procedure allows the definition of a unique and continuous mastercurve for the complex modulus of asphalt mixtures.

In order to plot the mastercurves of the asphalt mixtures, the average value of the complex moduli and of the phase angles of the three samples tested for each type of mixtures was used. The repeatability was high, with an average coefficient of variation of about 4%.

For both the models, used to plot the mastercurves of the asphalt mixtures, the Root Mean Squared Error in percentage (RMSP) and the coefficient of determination (R^2) were calculated to evaluate their capability predicting the measured data. Both models were satisfactory in predicting the experimental values. Here after, are reported the mastercurves fitting parameters of the CAM model (Table 16) and of the sigmoidal model (Table 17) for all the tested asphalt mixtures.

The mastercurves obtained from these fitting processes are reported in Figures 27 and 28.

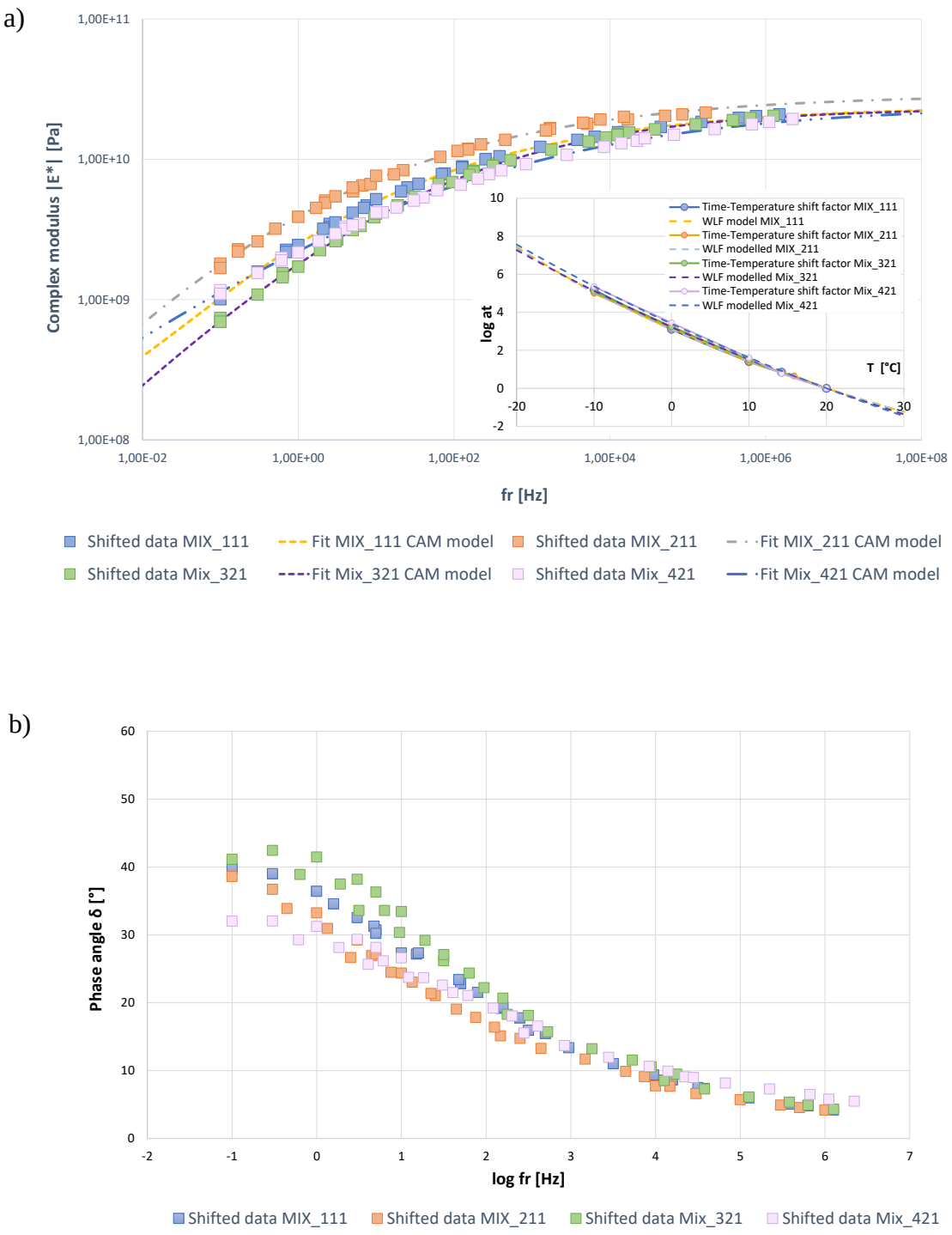

Fig. 27 *Mastercurves of the asphalt mixtures at the reference temperature of 20°C using the CAM model: (a) Complex modulus |E*| and (b) phase angle δ.*

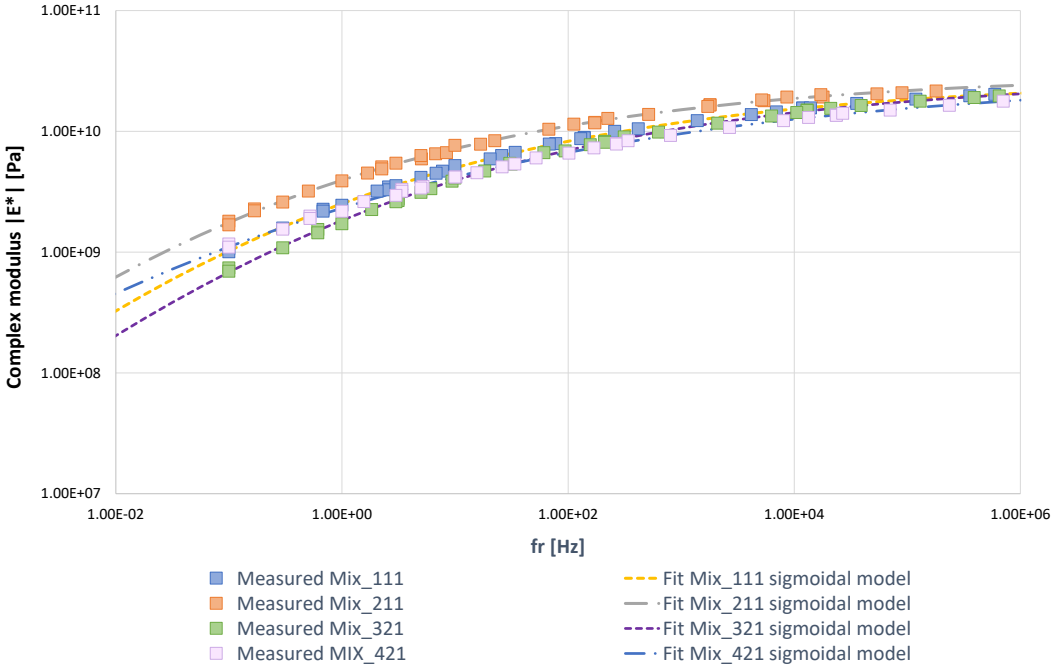

Fig. 28 *Mastercurves of asphalt mixtures at the reference temperature of 20°C using the sigmoidal model*.

Table 16 *Fitting parameters of complex modulus mastercurves at the reference temperature of 20°C of asphalt mixtures.*

Asphalt Mixture	*Complex modulus mastercurve parameters at T_0=20°C*						
	E_e*	E_g*	f_c	k	m_e	R^2	RMSP
	[Pa]	[GPa]	[Hz]	[-]	[-]	[-]	[%]
MIX_111	$1.20 \cdot 10^8$	24.11	0.090	0.198	0.948	0.999	1.76
MIX_211	$1.11 \cdot 18^8$	29.10	0.136	0.193	0.750	0.997	2.85
MIX_321	$4.50 \cdot 10^7$	23.28	16.296	0.239	0.568	0.999	2.20
MIX_421	$1.25 \cdot 10^8$	24.15	37.584	0.191	0.416	0.999	1.79

Table 17 *Mastercurves fitting parameters of sigmoidal model at the reference temperature of 20°C for asphalt mixtures.*

Asphalt Mixture	*Mastercurve parameters at T_0=20°C*					
	δ	α	β	γ	R^2	RMSP
	[Pa]					[%]
MIX_111	3.01	7.42	-1.825	-0.386	1.000	1.76
MIX_211	3.03	7.45	-2.009	-0.392	0.998	2.82
MIX_321	3.36	7.09	-1.602	-0.383	0.999	2.78
MIX_421	3.35	7.10	-1.715	-0.314	1.000	2.37

3.3.2 Binders and mastercurves development

Complex shear modulus $|G^*|$ and phase angle δ mastercurves of the different asphalt binders were plotted considering the Christensen Anderson Maresteanu (CAM) model and the Time-Temperature Superposition Principle (TTSP).

The two unmodified binders (50-70 and 70-100, respectively, B_11 and B_32) respected rather well the Time-Temperature Superposition Principle (TTSP), while the two SBS modified binders did not confirm the Time-Temperature Superposition Principle, as their Black diagram curves (phase angle vs complex shear modulus) were not unique. Nevertheless, the complex shear modulus mastercurves were plotted at the reference temperature, using the PTTSP shifting procedure. This procedure (Olard et al., 2003a) (Olard et al., 2003b) allows the definition of a unique and continuous mastercurve for the complex shear modulus of binders.

To plot the mastercurves, the average values of the complex shear moduli $|G^*|$ and phase angles δ of at least three samples tested for each type of binder were used.

In the present research before the binder data fitting, the raw data measured at low temperature were elaborated. Indeed, to investigate the low-temperature rheological properties of bituminous binders was used the method proposed in the recent past by the Western Research Institute (WRI) and based on the DSR tests with 4 mm parallel plates and 1.75 mm gap, combined with the systematic correction of radial instrument compliance (Sui et al., 2010).

In Figure 29 is reported the schematic representation of binders' data elaboration:

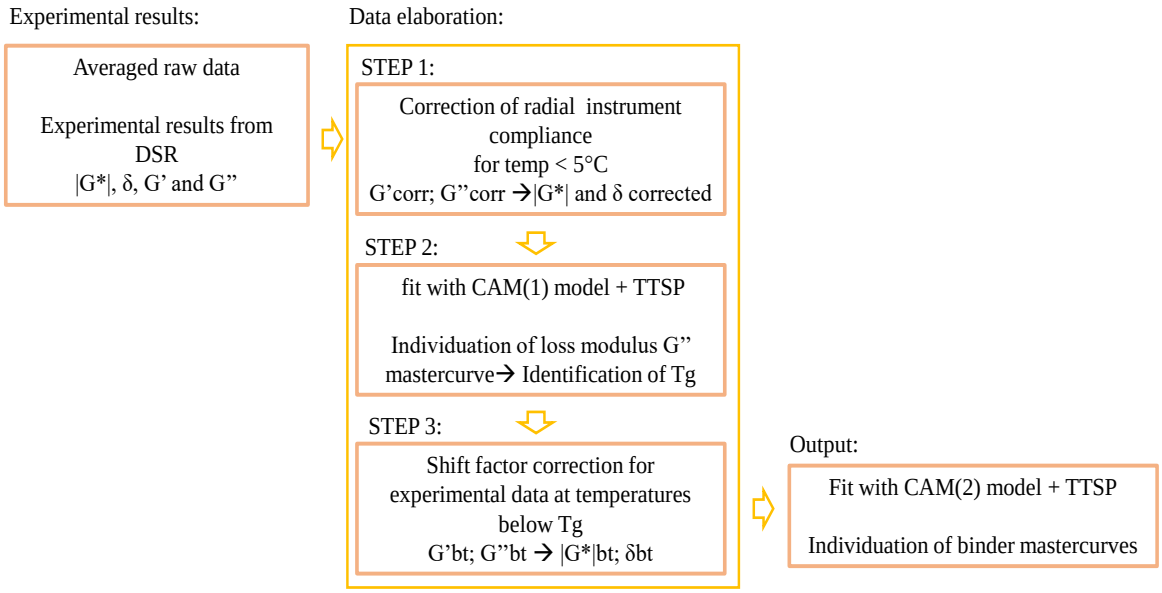

Fig. 29 *Schematic representation of binders' data elaboration for binders' mastercurves definition.*

3.3.2.1 Radial Instrument Compliance J correction

In a draft standard (AASHTO XXX-12,2012) the 4 mm parallel-plate with a gap of 1.75 mm geometry was identified as the most convenient testing geometry to reduce the effect of instrument compliance (Gottlieb & Macosko, 1982) (Lu et al., 2016), while avoiding the use of sample molds. Several researchers succeeded in implementing this testing procedure in the measurement of low temperature properties of various types of asphalt binders (unaged, aged, neat and modified etc.) (Sui et al., 2010) (Sui et al., 2011) (Farrar et al., 2015) (Bücher et al., 2019).

However, even using the 4 mm parallel plate geometry the high stiffness of asphalt binders in the low temperature range requires considering the instrument compliance, which significantly influenced the rheological parameters. Indeed, according to previous studies (Farrar et al., 2015) (Riccardi et al., 2017), the DSR measurements at temperatures lower than 5°C are significantly affected by errors associated with the instrument compliance. Hence, the radial instrument compliance must be evaluated and systematically corrected (Schröter et al., 2006).

To measure the instrument compliance *J* for the DSR used in this Thesis, the procedure developed by the Western Research Institute was used (Farrar et al., 2015).

Figure 30 shows the exponential function of the DSR compliance with respect to frequency *f*, developed as part of a previous research (Wang, Cannone Falchetto, Alisov, Schrader, & Riccardi, 2019) (Wang, Cannone Falchetto, & Riccardi, 2019).

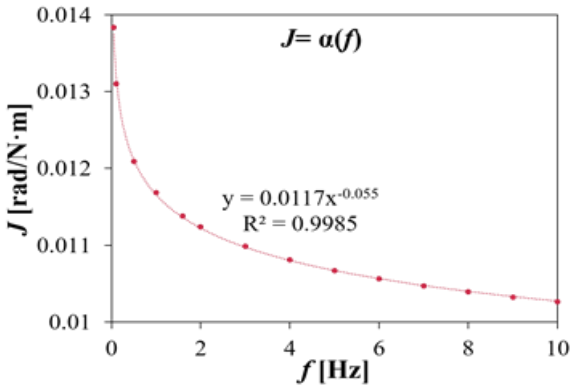

Fig. 30 *Exponential function of the DSR compliance J with respect to frequency f* (Wang et al., 2019a) (Wang et al., 2019b).

Both storage modulus *G'* and loss modulus *G''* data, obtained at temperatures below 5°C from the 8 mm and 4 mm geometries, were corrected considering the instrument compliance *J* as reported in the following equations:

$$G'_s = \frac{G'_m\left(1-\frac{J}{K_g}G'_m\right)-\frac{J}{K_g}G''^2_m}{\left(1-\frac{J}{K_g}G'_m\right)^2+\left(\frac{J}{K_g}G''_m\right)^2} \quad [31]$$

$$G''_s = \frac{G''_m}{\left(1-\frac{J}{K_g}G'_m\right)^2+\left(\frac{J}{K_g}G''_m\right)^2} \quad [32]$$

Where G_s is the modulus after machine compliance correction and G_m is the measured modulus, J is the DSR compliance in function of the testing frequency, and K_g is the geometry conversion factor in function of the geometry gap and of the radius of the sample.

In Figure 31 the original Cole-Cole diagram and the plot after the correction of theDSR compliance are illustrated, exemplarily for asphalt binder B_11. Similar results were obtained for all other binders.

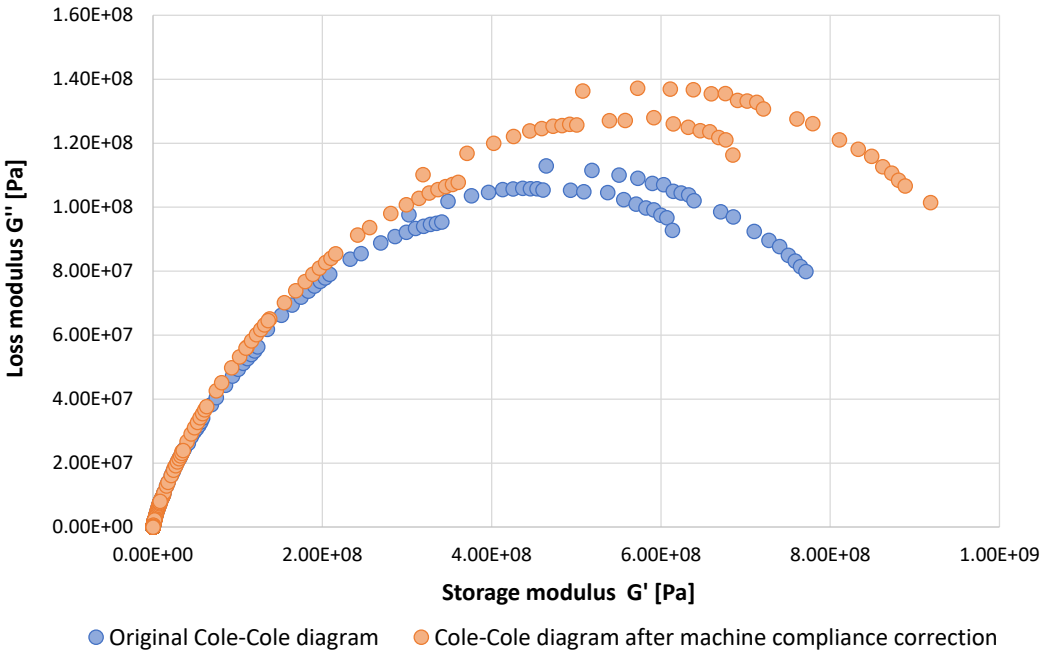

Fig. 31 *Cole-Cole plot before and after compliance correction, exemplarily shown for Binder B_11.*

3.3.2.2 Glass Transition Temperature *Tg* definition and shift factor correction of Cole-Cole diagram

A second important aspect have been considered in this research for low-temperature rheological investigations on asphalt binders: the glass transition temperature *Tg*.

The glass transition temperature *Tg* is the characteristic temperature at which asphalt binder changes from the viscoelastic state to the glassy one and it plays an important role in the low-temperature behavior of asphalt binders. Recent studies demonstrated that physical and steric hardening occur near the glass transition temperature *Tg* (Tabatabaee et al., 2012).

Some researchers focused on *Tg* identification methods (Laukkanen, 2015) and more recently Wang et al. (Wang et al., 2019b) proposed the application of a normal shift factor correction, *bt*, at low temperature behavior, to take into account the deviation due to the glass transition phenomena of asphalt binders at low temperature and to produce smooth mastercurves. This shift factor must be applied to data collected below *Tg*.

In the present Thesis, the *Tg* was identified in correspondence with the maximum peak of the loss modulus *G''* mastercurve.

In accordance with the CAM model and the Time-Temperature Superposition Principle, the loss modulus *G''* mastercurve can be derived. This mastercurve is used to calculate the glass transition temperature *Tg* for each asphalt binder, which is the temperature backcalculated from the *Log* f_{red} in correspondence with the maximum value of the loss modulus *G''*, assuming a reference frequency of 1.59 Hz.

In the previous literature there are several arguments in favor of defining the glass transition temperature in terms of the maximum loss modulus G''_{max} (Rieger, 2001) (Laukkanen, 2015). In Figure 32 is shown the calculation method for *Tg* identification. In Table 18 are reported the glass transition temperature *Tg* and the corresponding reduced frequency for each asphalt binder.

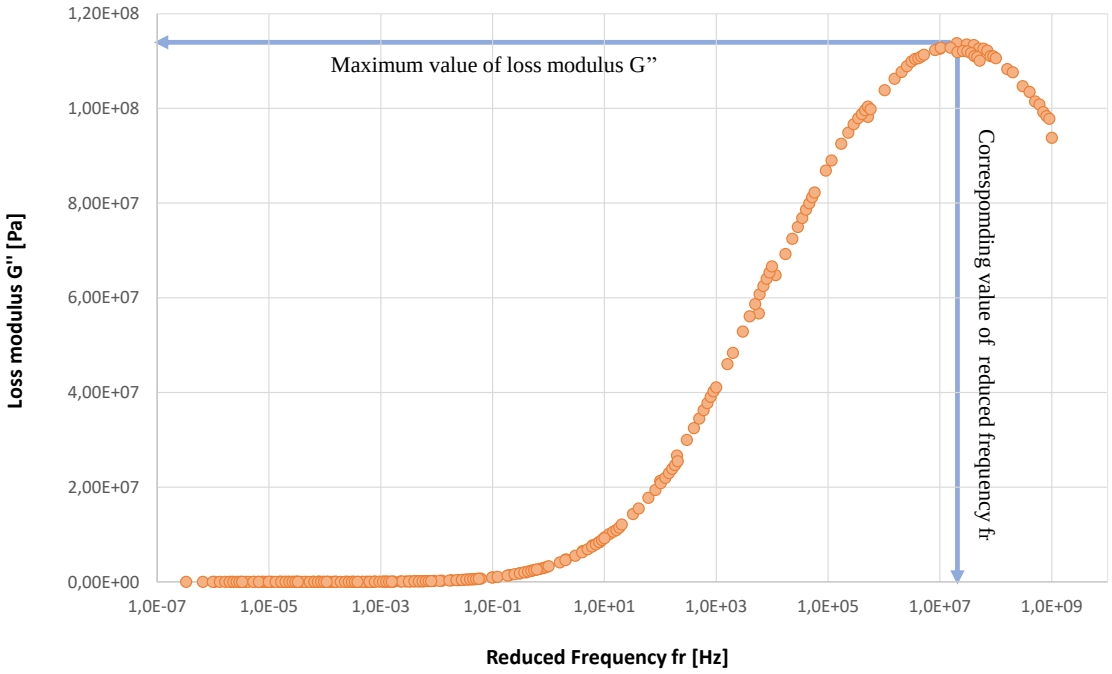

Fig. 32 *Calculation of Tg by means of loss modulus mastercurve, exemplary for asphalt binder B_21.*

Table 18 *Glass transition temperature and corresponding reduced frequency of asphalt binders.*

Binder	*Tg* [°C]	*Log* f_{red} [Hz]
B_11	-14.52	6.04
B_21	-15.73	5.71
B_32	-14.00	5.83
B_42	-15.08	5.40

A shift factor *bt* was applied for experimental data determined at temperatures below the glass transition temperature Tg obtaining a smooth Cole-Cole diagram. The shift factor bt was determined visually by means of the Cole-Cole diagram and applied to both storage modulus *G'* and loss modulus *G''* (Wang et al., 2019b). This factor mitigates the significant negative effects on asphalt binders' rheological behavior that occur at low testing temperatures. Figure 33 shown the Cole-Cole diagram before and after the application of shift factors for data corresponding to temperatures below the glass transition temperature *Tg*.

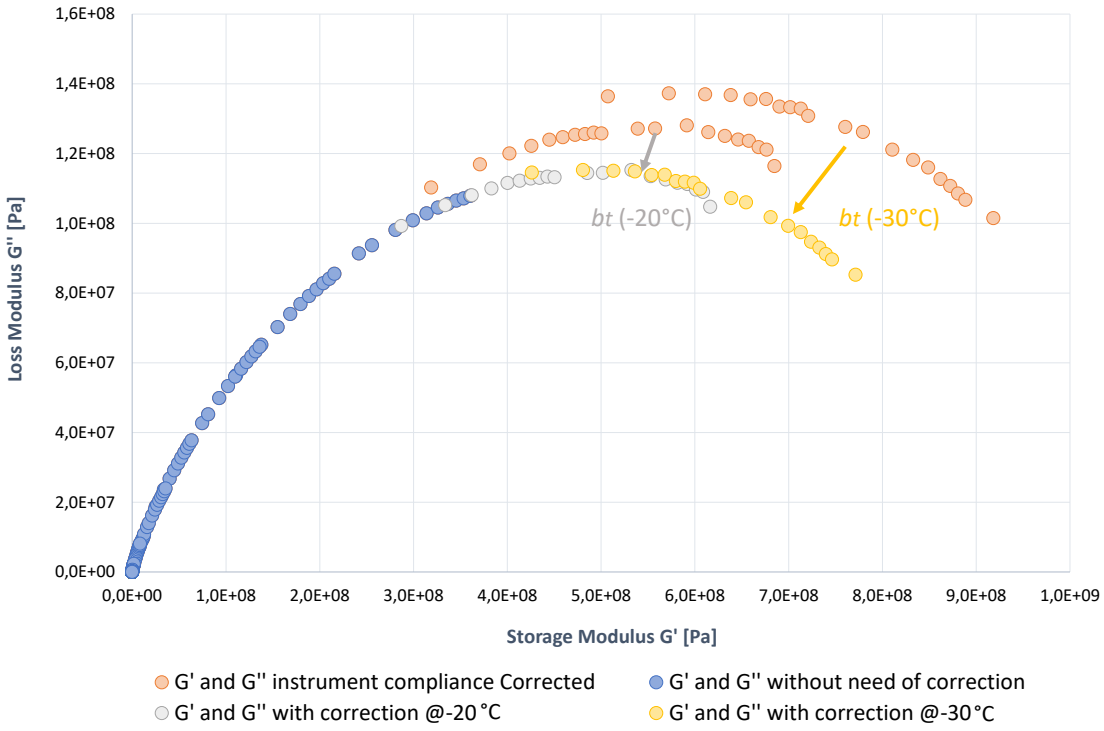

Fig. 33 *Cole-Cole diagram of asphalt binder B_11 before and after shift correction for temperatures below glass transition temperature Tg.*

In Figure 34 the original Cole-Cole diagram and the Cole-Cole diagram after both corrections are shown. Table 19 summarizes the shift factors *bt* applied for each asphalt binder at temperatures below the glass transition temperature *Tg*.

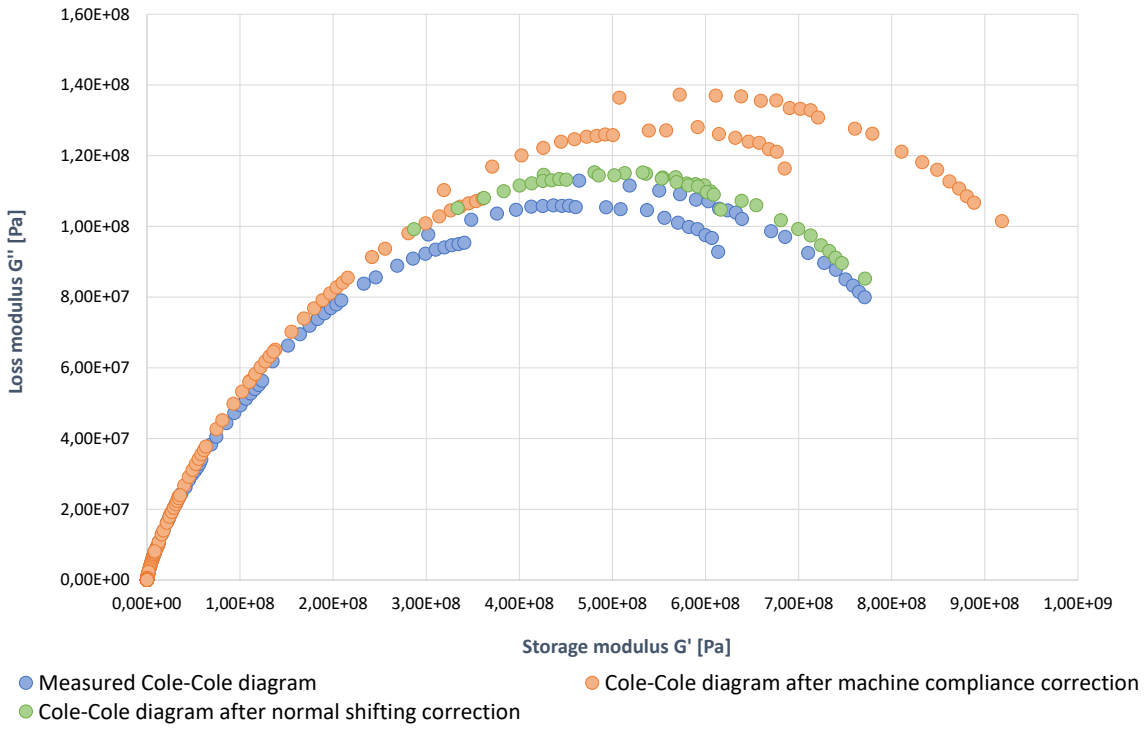

Fig. 34 *Original Cole-Cole diagram from experimental data and the Cole-Cole diagram after both corrections, i.e. machine compliance and normal shift factor.*

Table 19 *Shift factors bt for each asphalt binder at temperatures below Tg.*

Binder	*bt* @ -20°C	*bt* @ -30°C
B_11	0.90	0.84
B_21	0.94	0.88
B_32	0.91	0.81
B_42	0.98	0.94

The corrected complex shear modulus $|G^*|$ and the phase angle δ were used together with the experimentally obtained values for modelling the rheological properties. The isothermal mastercurves at the reference temperature T_0= 20°C of the norm of the complex shear modulus $|G^*|$ and phase angle δ were built using the CAM model (Equation 12) in combination with the WLF model (Equation 6), by minimizing the sum of the squared errors between the measured complex shear modulus and phase angle at each temperature/frequency combination and the calculated values.

The Time-Temperature Superposition Principle (TTSP) and the Partial Time-Temperature Superposition Principle (PTTSP), were applied, respectively for unmodified

and modified binders, to obtain the temperature shift factor a_T, which were modelled with the Williams-Landel-Ferry (WLF) equation.

In Figure 35, the mastercurves of binders after data correction are reported, while the mastercurves fitting parameters and the regression coefficients R^2 are summarized in Tables 20 and 21. To evaluate the accuracy of the CAM model the Root Mean Squared Percentage (RMSP) Error was calculated for each binder. The average RMSP of 3.53% indicates that the CAM model is able to model satisfactorily the measured value.

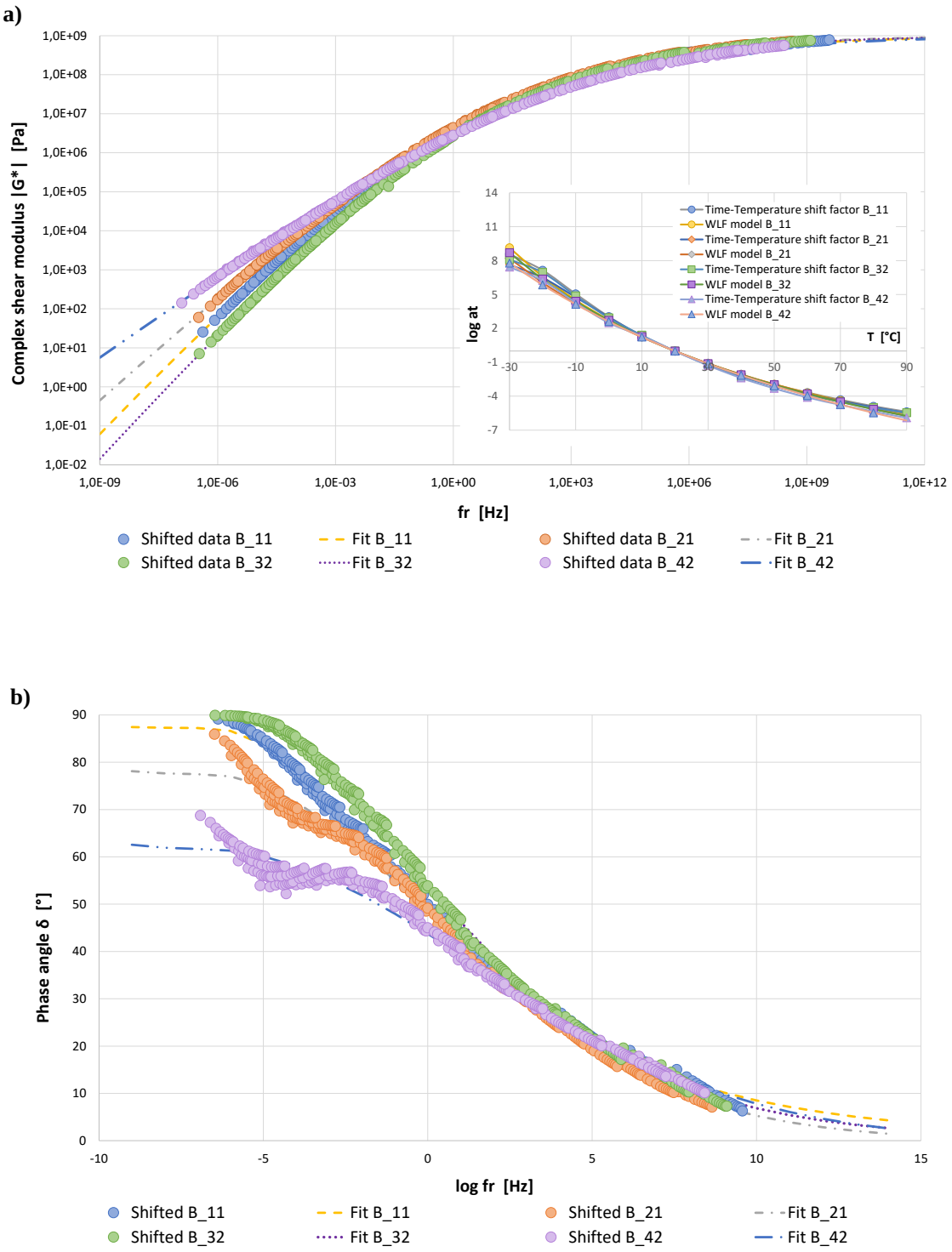

Fig. 35 *Mastercurves of the asphalt binders at the reference temperature of 20°C using the CAM model: (a) Complex shear modulus |G*| and (b) Phase angle δ.*

Table 20 *Fitting parameters of complex shear modulus mastercurves of asphalt binders at the reference temperature of 20°C.*

Binder	*Complex shear modulus mastercurve parameters at T_0=20°C*						
	G_e*	G_g*	f_c	k	m_e	R^2	RMSP
	[Pa]	[Pa]	[Hz]	[-]	[-]	[-]	[%]
B_11	*0*	$1.045 \cdot 10^9$	*1.778*	*0.141*	*1.087*	*0.998*	*4.08*
B_21	*0*	$1.002 \cdot 10^9$	*14.478*	*0.154*	*0.913*	*0.998*	*3.21*
B_32	*0*	$1.070 \cdot 10^9$	*4.062*	*0.152*	*1.118*	*0.999*	*3.71*
B_42	*0*	$1.001 \cdot 10^9$	*292.402*	*0.144*	*0.716*	*0.998*	*3.13*

Table 21 *Fitting parameters of phase angle mastercurves of asphalt binders at the reference temperature of 20°C.*

Binder	*Phase angle mastercurve parameters at T_0=20°C*				
	δ_m	f_d	R_d	m_d	R^2
	[°]	[Hz]	[-]	[-]	[-]
B_11	*87.22*	$2.00 \cdot 10^{-7}$	*12.83*	*4.69*	*0.995*
B_21	*77.45*	$1.81 \cdot 10^{-7}$	*37.69*	*29.88*	*0.994*
B_32	*92.13*	$2.02 \cdot 10^{-7}$	*18.97*	*9.05*	*0.995*
B_42	*61.67*	$1.30 \cdot 10^{-7}$	*840.70*	*1024.24*	*0.984*

3.3.3 Mastics data elaboration and mastercurves development

The complex shear modulus |*G**| and the phase angle δ data of asphalt mastics, obtained after the machine compliance and the normal shifting correction for low-temperatures (with a raw data elaboration procedure similar to the one used for binders), were modelled with the CAM model. The isothermal (at the reference temperature T_0= 20°C) mastercurves of norm of the complex shear modulus |*G**| and phase angle δ of mastics were developed by minimizing the sum of the squared errors between the measured output values and the calculated ones at each temperature/frequency combination.

The *Tg* has been identified in correspondence of the maximum peak of the loss modulus *G''* mastercurve of mastics, using the same criterion of binders' *Tg* definition. Hence the mastics data obtained at temperature below *Tg* were adjusted before modelling.

In Table 22 are reported the determined the glass transition temperature *Tg* for each mastic.

Table 22 *Glass transition temperature and corresponding reduced frequency of asphalt mastics.*

Mastic	*Tg* [°C]	*Log* f_{red} [Hz]
M_111	-9.30	4.62
M_211	-13.36	5.74
M_321	-9.45	4.49
M_421	-16.05	4.75

In Figure 36 the mastercurves of mastics after data correction are reported, while the mastercurves fitting parameters and the regression coefficients R^2 of the modelling for the complex shear modulus and the phase angle are summarized in Table 23 and Table 24. The Root Mean Squared Error in Percentage (RMSP) was calculated to estimate the accuracy of the CAM model to approximate the experimental data. The average RMSP for the mastics results equal to 2.54%, therefore the CAM model seems to fit satisfactory the measured data.

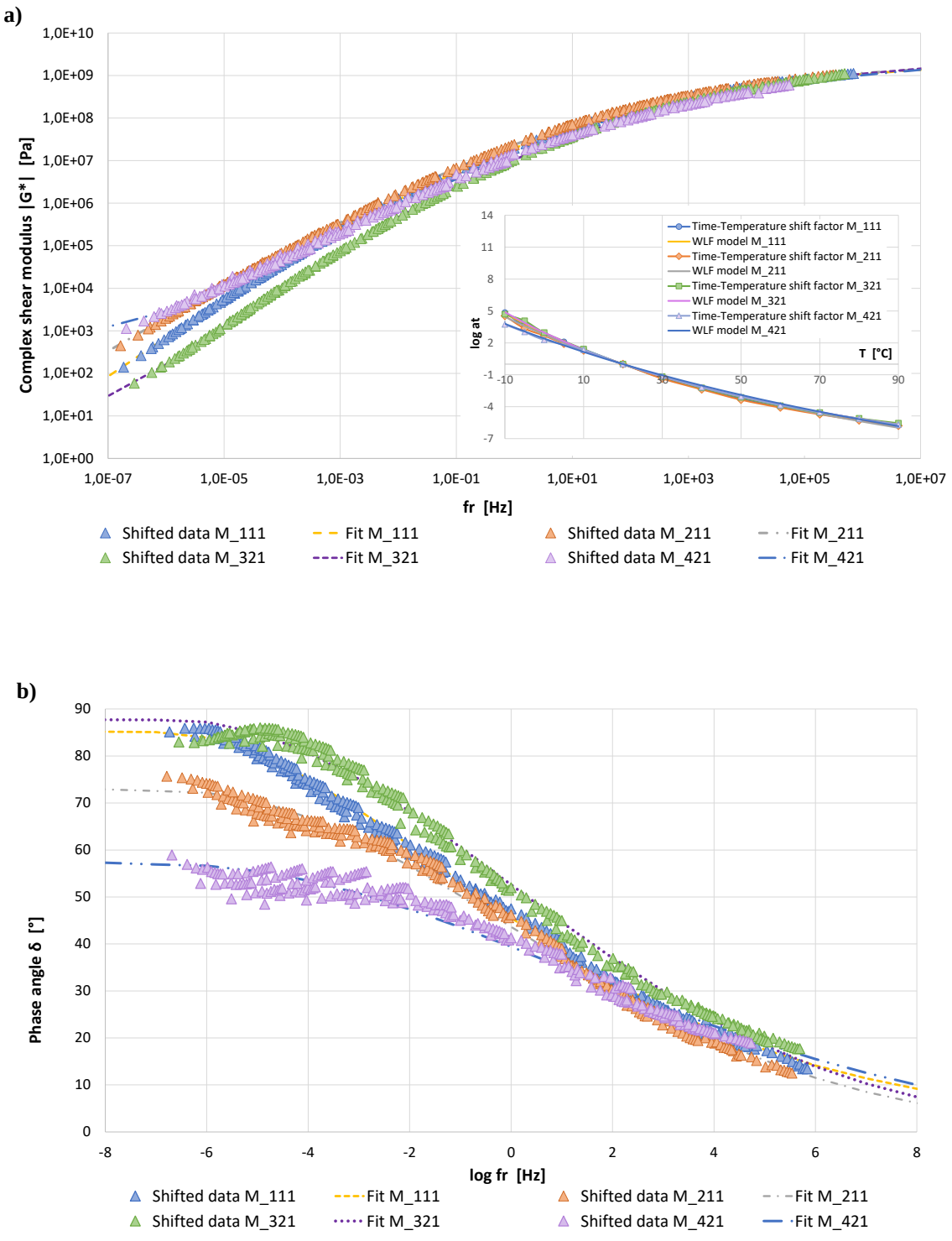

Fig. 36 *Mastercurves of the asphalt mastics at the reference temperature of 20°C using the CAM model: (a) Complex shear modulus |G*| and (b) Phase angle δ.*

Table 23 *Fitting parameters of complex shear modulus mastercurves of asphalt mastics at the reference temperature of 20°C.*

Mastic	*Complex shear modulus mastercurve parameters at T_0=20°C*						
	G_e*	G_g*	f_c	k	m_e	R^2	RMSP
	[Pa]	[Pa]	[Hz]	[-]	[-]	[-]	[%]
M_111	*11.231*	*$2.396 \cdot 10^9$*	*1.925*	*0.154*	*0.995*	*0.997*	*2.79*
M_211	*4.394*	*$2.101 \cdot 10^9$*	*12.873*	*0.174*	*0.830*	*0.999*	*2.03*
M_321	*13.411*	*$2.815 \cdot 10^9$*	*5.943*	*0.157*	*1.039*	*0.997*	*2.83*
M_421	*19.416*	*$2.875 \cdot 10^9$*	*515.73*	*0.1478*	*0.619*	*0.999*	*2.51*

Table 24 *Fitting parameters of phase angle mastercurves of asphalt mastics at the reference temperature of 20°C.*

Mastic	*Phase angle mastercurve parameters at T_0=20°C*				
	δ_m	f_d	R_d	m_d	R^2
	[°]	[Hz]	[-]	[-]	[-]
M_111	*85.094*	*$1.01 \cdot 10^{-7}$*	*15.539*	*6.768*	*0.997*
M_211	*72.491*	*$2.29 \cdot 10^{-7}$*	*479.483*	*5269.438*	*0.994*
M_321	*87.585*	*$2.10 \cdot 10^{-7}$*	*481.305*	*5299.272*	*0.995*
M_421	*55.426*	*$1.58 \cdot 10^{-7}$*	*594.848*	*5293.642*	*0.985*

3.3.4 FAM mastercurves development

The data obtained from temperature and frequency T-f sweep tests for the different FAM were used to develop the FAM mastercurves considering both the Christensen Andersen Maresteanu (CAM) model, as reported in Equation 12 (Chapter 2), and the sigmoidal model, as reported in Equation 15 (Chapter 2).

The measured data were analysed based on the assumption of thermorheological simplicity. Hence, the mastercurves were constructed by shifting the data horizontally at a target reference temperature T_0 of 20°C, in accordance with the TTSP. To plot the mastercurves five replicates for each type of FAM were tested, and the average values of the complex modulus and of the phase angle at each testing temperature were calculated. The mastercurves obtained from these fitting processes are reported in Figures 37 and 38, while Tables 25-26 and 27 summarize the fitting parameters of the CAM model, of the WLF model and of the sigmoidal model for all the tested FAM mixes. The Root Mean

Squared Percent (RMSP) Error and the coefficient of determination (R^2) were calculated to validate prediction quality.

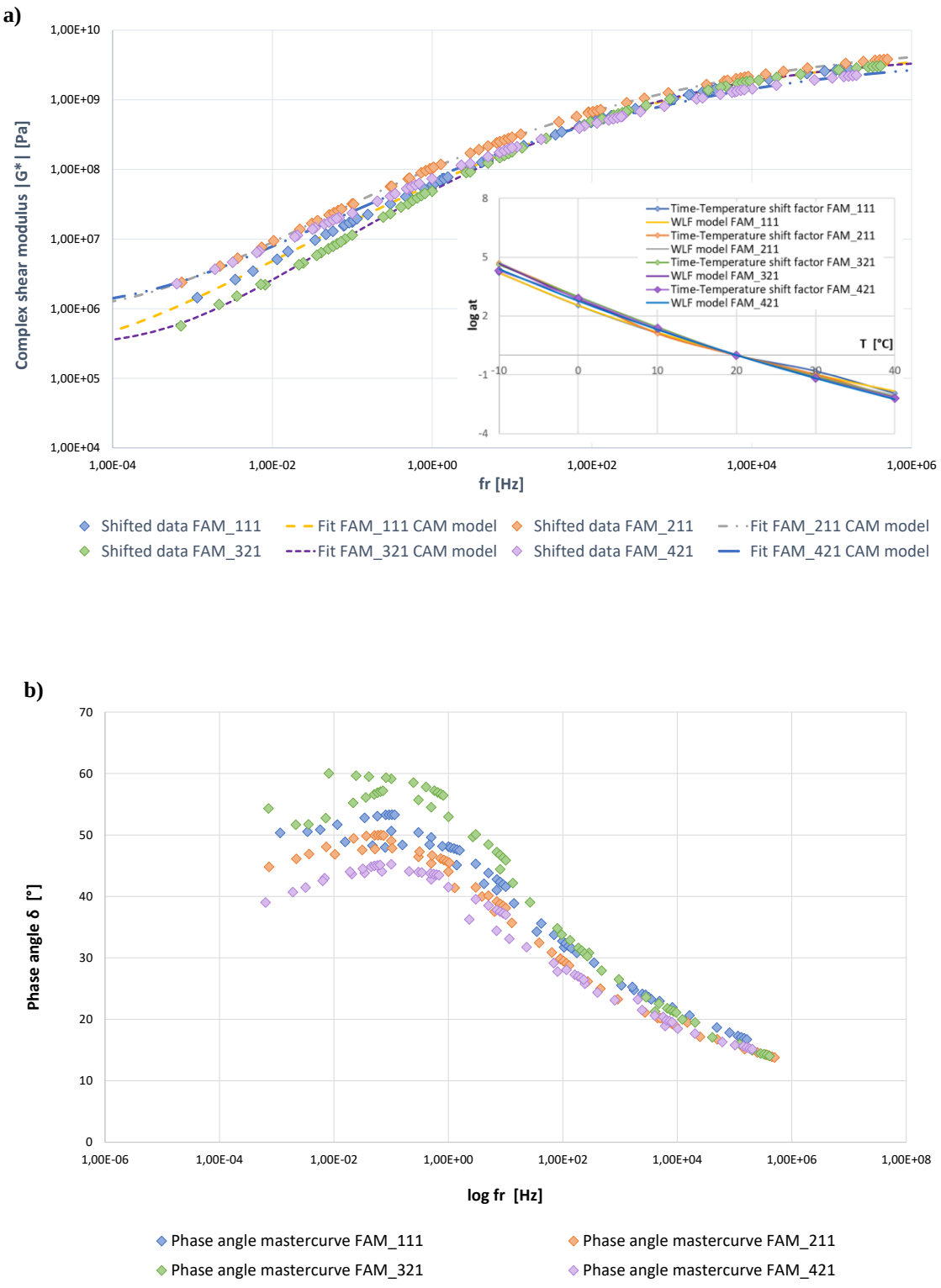

Fig. 37 *Mastercurves of the FAM at the reference temperature of 20°C using the CAM model: (a) Complex shear modulus |G*| and (b) phase angle δ.*

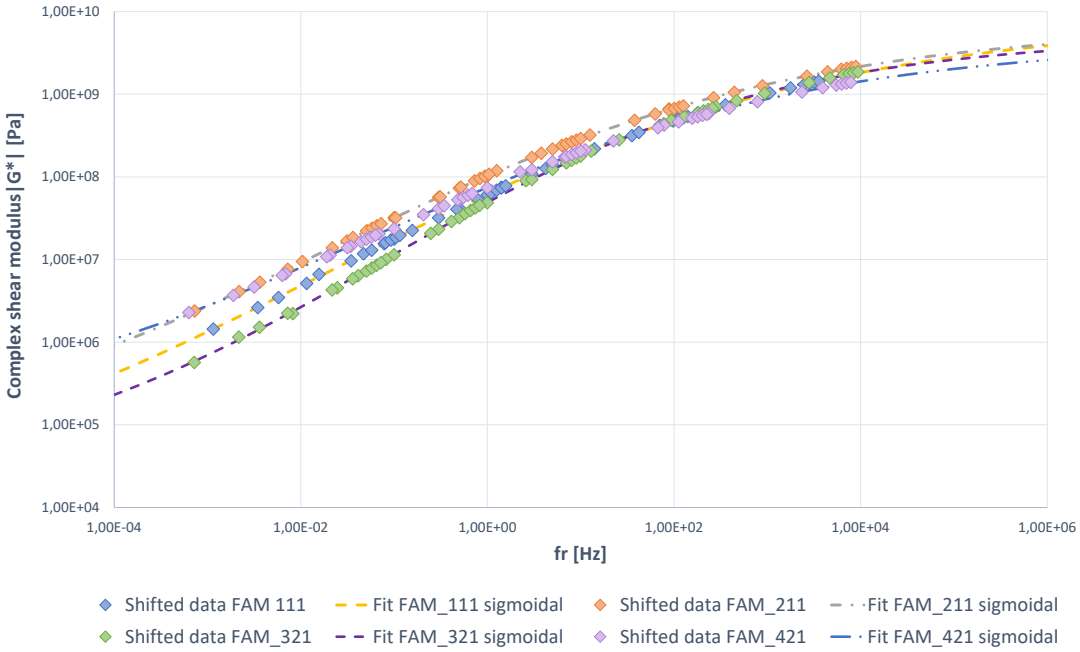

Fig. 38 *Mastercurves of FAM at the reference temperature of 20°C using the sigmoidal model*.

Table 25 *Mastercurves parameter of CAM model of complex shear modulus of FAM.*

FAM	Complex modulus mastercurve parameters @ T_0=20°C						
	G_e*	G_g*	f_c	k	m_e	R^2	RMSP
	[Pa]	[MPa]	[Hz]	[-]	[-]	[-]	[%]
FAM_111	$2.06 \cdot 10^5$	$5.17 \cdot 10^3$	326.373	0.231	0.652	1.000	1.56
FAM_211	$8.62 \cdot 10^5$	$7.16 \cdot 10^3$	24.661	0.183	0.754	1.000	1.05
FAM_321	$2.83 \cdot 10^5$	$4.63 \cdot 10^3$	87.238	0.240	0.798	0.999	2.29
FAM_421	$9.59 \cdot 10^5$	$7.45 \cdot 10^3$	74.143	0.192	0.662	1.000	1.93

Table 26 *WLF parameters C1 and C2 for FAM.*

FAM	C1 [-]	C2 [°C]
FAM_111	13.7	127.55
FAM_211	14.9	124.96
FAM_321	18.1	146.45
FAM_421	24.3	196.51

Table 27 *Mastercurves parameters of sigmoidal model for FAM.*

FAM	Mastercurve parameters at T_0=20°C					
	δ	**α**	**β**	**γ**	**R^2**	**RMSP [%]**
FAM_111	*3.80*	*6.12*	*-0.630*	*-0.373*	*1.000*	*1.54*
FAM_211	*4.41*	*5.43*	*-0.675*	*-0.399*	*1.000*	*1.20*
FAM_321	*4.24*	*5.46*	*-0.539*	*-0.473*	*0.999*	*2.77*
FAM_421	*4.86*	*4.78*	*-0.533*	*-0.413*	*0.999*	*1.89*

3.4 Comparison of mechanical properties

The temperature-frequency T-f sweep tests were used to assess the LVE properties of binders, mastics, FAM and asphalt mixtures. The results of the T-f sweep tests for all the characteristic phases, modelled with the CAM model, and reported as complex shear modulus |*G**| and phase angle δ mastercurves at the reference temperature of 20°C, in order to provide a simple visual understanding of the viscoelastic properties of the material phases and allow the comparison of their mechanical properties over a wide range of temperatures and frequencies.

Hereinafter, in Figure 39, the results are summarized in terms of complex shear modulus |*G**| and phase angle δ exemplary for asphalt mixture MIX_111 and for the corresponding characteriphases (B_11, M_111 and FAM_111). The corresponding complex shear moduli |*G**| for asphalt mixtures were calculated from the measured complex moduli |*E**| by assuming an arbitrary Poisson's ratio equal to 0.5 ($|G^*| = 1/3\,|E^*|$), which means that incompressibility and isotropy are supposed, but it allows to plot all results as function of complex shear modulus |G*| only. Such assumption was done in accordance to the literature (Olard et al., 2003) (Mangiafico et al., 2013) (Riccardi, 2017).
The mastercurves of the other analyzed asphalt mixtures and their corresponding characteristic phases are reported in Annex A.

Lastly, some observation on mastercurves trends and materials properties are reported.

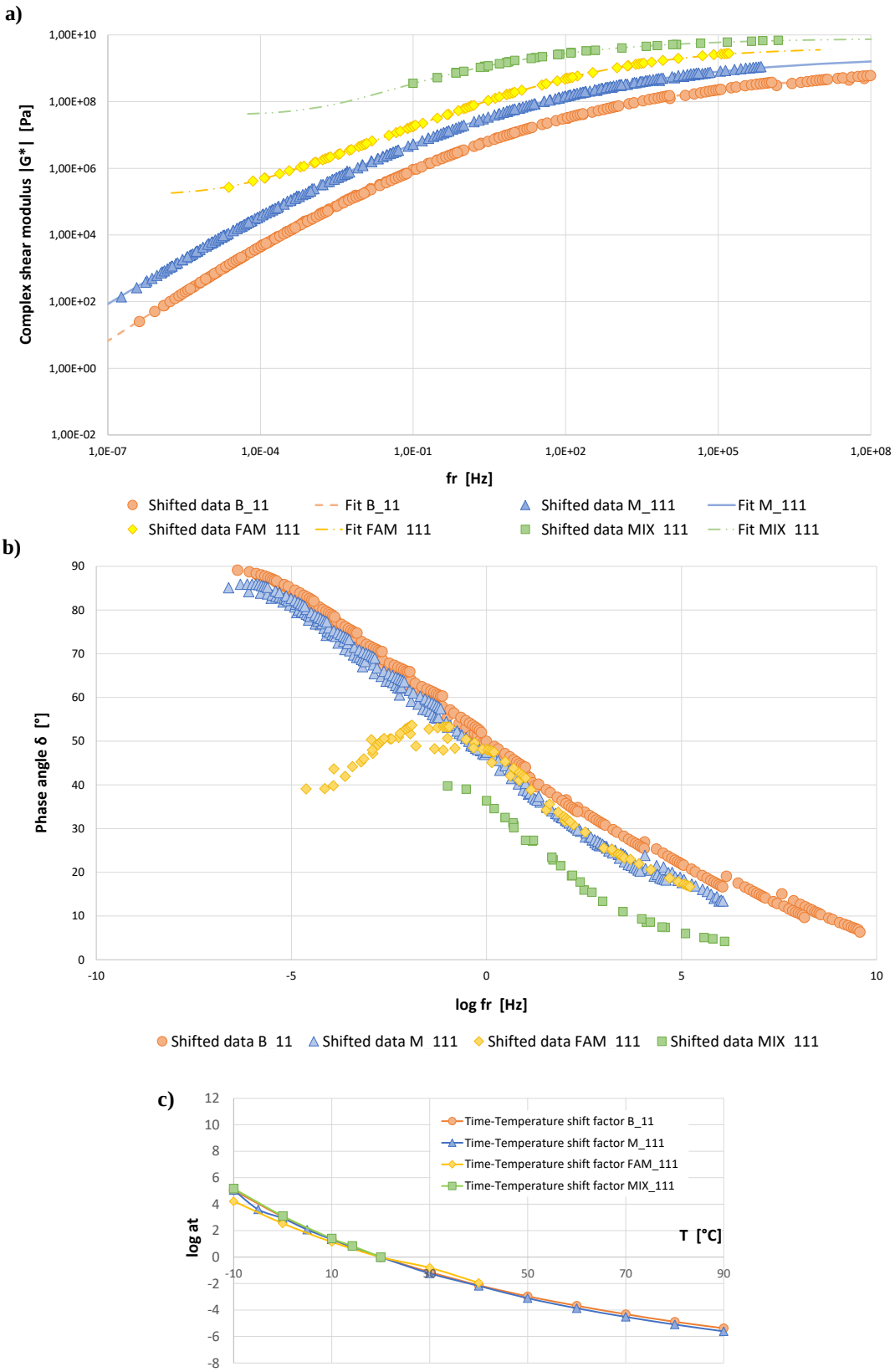

Fig. 39 *LVE characteristics of each characteristic phase in an asphalt mixture: (a) complex modulus |G*| and (b) phase angle δ mastercurves in logarithmic space and (c) t-T shift factor, exemplary for binder B_11, mastic M_111, FAM_111 and asphalt mixture MIX_111.*

From the LVE characterization curves is possible to observe that FAM have the same overall characteristics of the corresponding full-graded asphalt mixture, such as:

- the complex shear modulus |*G**| mastercurve S-shaped trend,
- the increasing then decreasing phase angle δ mastercurve,
- similar t-T shift factor function.

For low frequencies the FAM mixtures behavior seems to be influenced by the aggregate skeleton (constituted by fine particles and filler), while for the high frequencies the material behavior is mostly influenced by the asphalt binder's characteristics. Analyzing the *me* and *k* shape parameters of the CAM model, the shape index *R* was calculated. It is obtained by multiplying the ratio of *me* to *k* by log2. The *R* index is an indicator of the width of the relaxation spectrum. The FAM shows lower value of *R* index than mastic and binder, which indicates a sharper transition from the elastic behaviour to viscous behaviour. It also indicates more sensitivity of the FAM to frequency changes.

Figure 39- (a) shows that the modulus increases as the material length scale increases. FAM has a higher modulus than mastic, and a lower modulus in comparison to asphalt mixture. However, the internal structure of the characteristic phases, responsible for the change in modulus, is a complex phenomenon, which appears to be related not only to aggregate gradation and volumetric composition of particles, and therefore it requires further investigations. Hence, despite the only structural difference between asphalt mixture and the corresponding FAM phase consists of the coarse aggregate particles, internal structural and microstructural investigations must be considered to better understand the rheological behavior of this phase.

Comparing these results with the literature ones (Underwood et al., 2013), where the complex modulus trend of FAM and of the corresponding mixture were almost vertically parallel to one another, it is important to take into account the significant difference in volumetric concentration of the two different mixtures (VC%, Equation [27]). Figure 40 shows the differences between the two research works, in terms of aggregate gradations of both asphalt mixture and FAM and mastic volumetric concentrations.

Considering that the mastic volumetric concentration is depending on asphalt mixture design, further investigations are needed using different mixture designs, and

consequently different volumetric characteristics of binders, mastics and fillers, to better understand the influence of these parameters on the LVE characteristics of FAM.

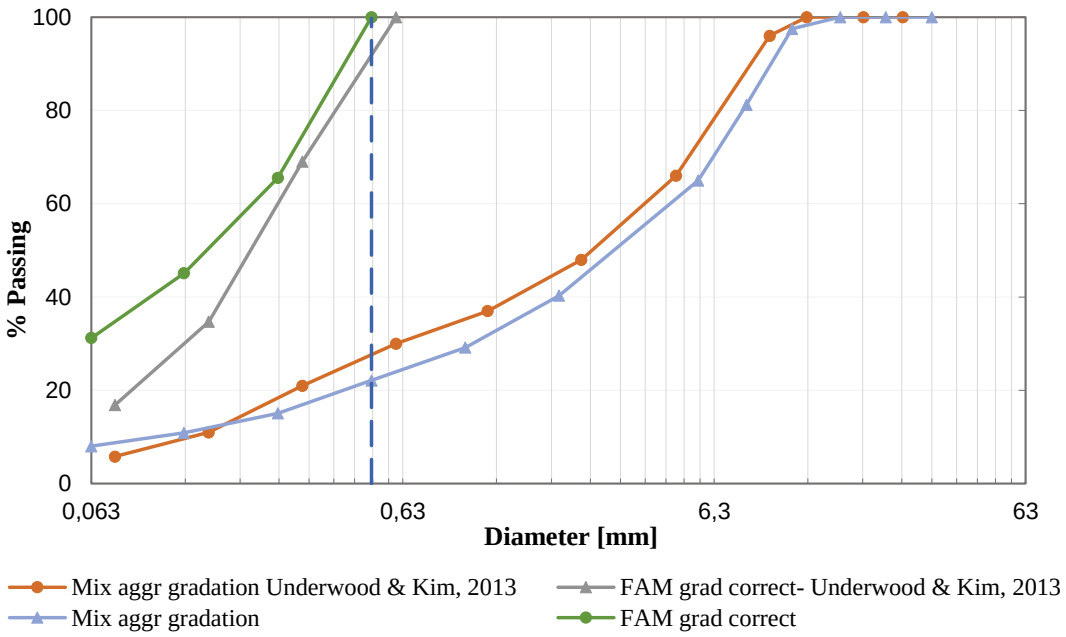

MASTIC VOLUMETRIC CONCENTRATION VC % [UNDERWOOD and KIM, 2013]	MASTIC VOLUMETRIC CONCENTRATION VC % [THIS RESEARCH]
25,48	40,36

Fig. 40 *Comparison of asphalt mixtures and FAM mix designs in terms of aggregate gradations and mastic volumetric concentrations VC%, between Underwood and Kim, 2013 and the present research.*

CHAPTER 4

4 IMPLEMENTATION OF 2S2P1D MODEL FOR FAM IN THE MULTISCALE TRANSITION FROM BINDER TO ASPHALT MIXTURE-*Model calibration and the relationships between different material phases*

In this Chapter the 2S2P1D model is used to link the FAM rheological properties both backward to its sub-phases, binder and mastic, and forward, to the asphalt mixture. The relationship that links the characteristic time of FAM with the binder, mastic and the corresponding asphalt mixture is investigated. In particular, the relationship between mixture and FAM is used to backcalculate the complex modulus of the asphalt mixture after testing the corresponding FAM specimens, as graphically summarized in Figure 41.

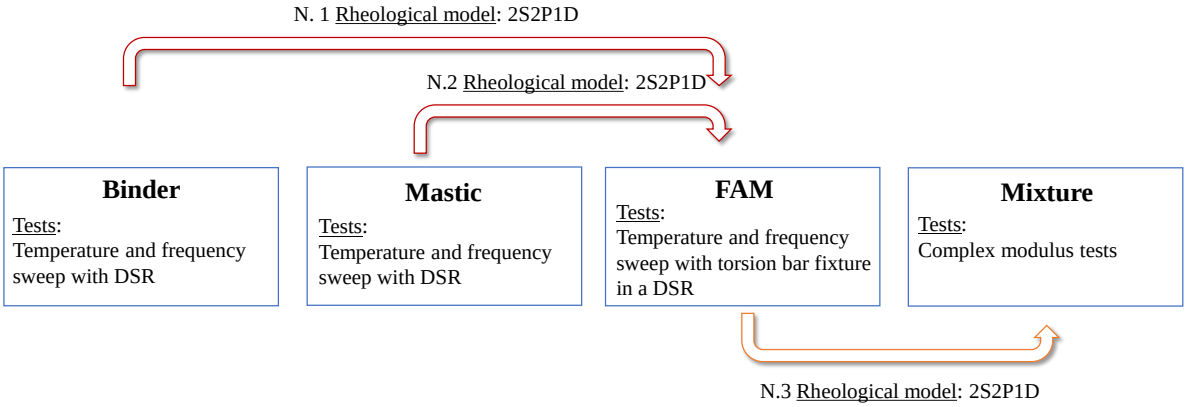

Fig. 41 *Implementation of the 2S2P1D model to link different phases of asphalt materials.*

Firstly, it is verified if the 2S2P1D model successfully fits the experimental data of complex modulus of the FAM in the LVE range, as it does for the other asphaltic materials.

Then, three new relationships are proposed, which respectively link the characteristic times of binder, mastic and asphalt mixture to the corresponding FAM phase. These relationships between the characteristic times allow the prediction of the rheological properties in LVE range of the asphalt mixtures in a wide range of temperatures and frequencies, starting from tests on FAM or the prediction of the rheological behavior of FAM from binder and mastic tests. The SHStS transformation (Chapter 2, Paragraph 2.2.1), which depends upon the definition of the transformation parameter α, is used to link the characteristic time of the FAM with the other material scales (binder, mastic and asphalt mixture).

Hence, the SHStS transformation and these new relationships between the characteristic times of the different asphalt mixture scales allow the back-calculation of FAM complex modulus from the complex modulus of binder or mastic and the back-calculation of asphalt mixture modulus starting from the complex modulus of FAM.

The tested materials (the asphalt mixtures and the corresponding FAM) have been already introduced in Chapter 3, as well as the testing procedures. The results of 2S2P1D fitting for three of the investigated mixtures (MIX_211, MIX_321 and MIX_421) and their sub-phases are used to interrelate the characteristic times of the different material phases (binder-FAM, mastic-FAM and FAM-MIX). To verify the accurateness of such interrelations and their effectiveness in predicting the LVE behavior from another material phase, the complex modulus of FAM_111 and MIX_111 are backcalculated from binder and mastic and from the FAM respectively, and measured data are compared to modelled data.

Using the relationship between FAM and asphalt mixture, the complex modulus of the mixture can be back calculated starting from tests on binder and FAM (Chapter 4) or starting directly from tests on FAM (Chapter 5). The results of these two modelling approaches will be investigated and compared.

4.1 2S2P1D model fitting and determination of the α parameter using parameters from binder

The experimental results of asphalt binders' complex shear moduli and phase angles were fitted by 2S2P1D model. Thus, the values of the seven model parameters were computed by minimizing the sum of the square of the distances between the experimental complex shear modulus and the predicted one obtained from the model.

To calibrate the parameters of each characteristic phase (i.e. binder, mastics, FAM and asphalt mixtures) and to establish a relationship between their characteristic times τ_0, the constants δ, k, h and β were fixed.

Actually the 2S2P1D model (Equation 3, Chapter 2) requires seven constants to completely define the LVE behaviour of a specific material, however, according to the literature, the constants δ, k, h and β are assumed the same for binder and the corresponding upscaling phases, owing to their dependence only on binder source (Olard & Di Benedetto, 2003) (Di Benedetto et al., 2004) (Delaporte et al., 2009).

This feature, combined with the relationship between the characteristic time parameter of each phase allows the definition of the so-called SHStS transformation (Equation 10, Chapter 2), which enables the prediction of the LVE behaviour of the specific asphaltic material at a given temperature.

In Table 28 the entire set of 2S2P1D model parameters for all the material phases are summarized.

Table 28 *Parameters of the 2S2P1D model for all material phases.*

Material	Δ	k	h	E_0 (Pa)	E_∞ (Pa)	β	$\log(\tau_0)$ at 20°C (s)	R^2
B_11	5.06	0.27	0.60	0	$3.121 \cdot 10^9$	801	-4.77	1.000
M_111	5.06	0.27	0.60	27.04	$7.188 \cdot 10^9$	801	-4.02	0.999
FAM_111	5.06	0.27	0.60	$1.54 \cdot 10^6$	$2.22 \cdot 10^{10}$	801	-4.04	0.998
MIX_111	5.06	0.27	0.60	$9.50 \cdot 10^7$	$2.41 \cdot 10^{10}$	801	-1.37	0.991
B_21	8.48	0.27	0.70	0	$3.002 \cdot 10^9$	1750	-4.11	0.999
M_211	8.48	0.27	0.70	343.72	$6.304 \cdot 10^9$	1750	-3.21	0.999
FAM_211	8.48	0.27	0.70	$4.81 \cdot 10^6$	$2.37 \cdot 10^{10}$	1750	-3.12	0.999
MIX_211	8.48	0.27	0.70	$1.10 \cdot 10^8$	$2.96 \cdot 10^{10}$	1750	-0.33	0.997
B_32	3.41	0.26	0.55	0	$3.211 \cdot 10^9$	950	-5.37	1.000
M_321	3.41	0.26	0.55	48.62	$8.446 \cdot 10^9$	950	-4.62	0.999
FAM_321	3.41	0.26	0.55	$6.17 \cdot 10^5$	$2.11 \cdot 10^{10}$	950	-4.61	0.998
MIX_321	3.41	0.26	0.55	$1.16 \cdot 10^7$	$2.43 \cdot 10^{10}$	950	-2.03	0.992
B_42	7.35	0.25	0.59	0	$3.001 \cdot 10^9$	4245	-5.00	1.000
M_421	7.35	0.25	0.59	574.40	$8.624 \cdot 10^9$	4245	-4.08	0.998
FAM_421	7.35	0.25	0.59	$2.79 \cdot 10^6$	$2.37 \cdot 10^{10}$	4245	-3.87	0.999
MIX_421	7.35	0.25	0.59	$1.65 \cdot 10^7$	$2.42 \cdot 10^{10}$	4245	-1.21	0.995

Figure 42 exemplary compares the measured and the predicted values with the 2S2P1D model in the Cole-Cole diagram, for each analysed phase (from binder to the corresponding asphalt mixture). As can be seen in the plot, the model fits reasonably well the experimental data. Similar trends were observed for the remaining asphalt binders, mastics, FAM and asphalt mixtures.

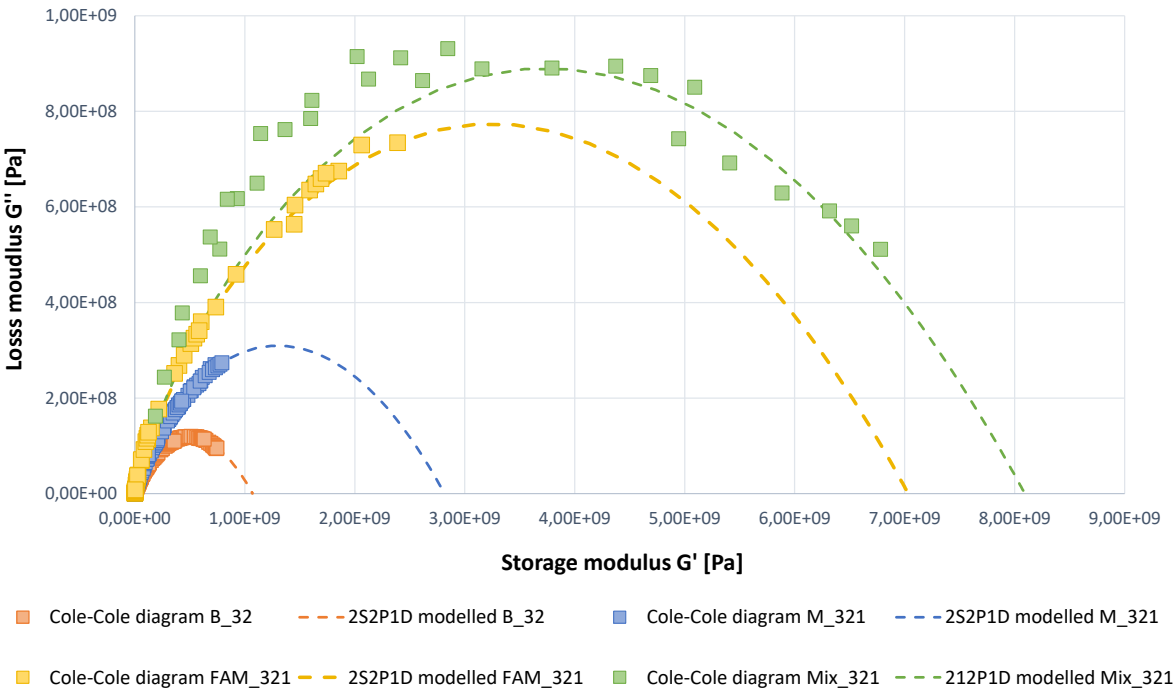

Fig. 42 *Comparison of experimentally obtained Cole-Cole diagram and 2S2P1D model predictions for binder B_32, mastic M_321, FAM_ 321 and asphalt mixture MIX_321.*

To confirm the assumption that the time-temperature dependency of the different characteristic phases originates from the binder behaviour, regardless the aggregate skeleton structure, and that is possible to predict the LVE behaviour of a phase from the LVE properties of another corresponding phase, is introduced the so-called normalized modulus:

$$G^*_{norm} = \frac{G^* - G_0}{G_\infty - G_0} \qquad [33]$$

Plotting in the Cole-Cole plot the normalized moduli of the different material's phases, it can be seen that the binder, mastic, FAM and asphalt mixture curves reasonably superimpose with each other, as exemplary shown in Figure 43. Similar results were obtained for all the tested materials (see Annex C).

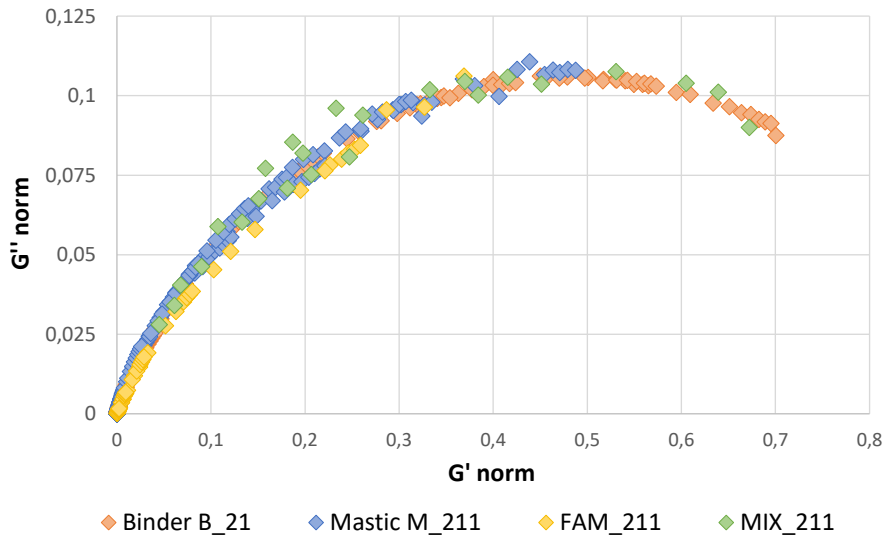

Fig. 43 *Example of the normalized Cole-Cole plots of binder B_21 and of the corresponding mastic M_211, FAM FAM_211 and asphalt mixture MIX_211.*

In conclusion, by means of Equation 33, it is possible, starting from the normalized moduli values (storage modulus and loss modulus) of one characteristic phase of the asphalt mixture (binder, mastic or FAM), knowing the glassy and the static moduli of the corresponding asphalt mixture, is possible to back-calculate the storage modulus and loss modulus of the mixture.

4.1.1 Relationships between the characteristic times of binder, mastic and FAM

When plotting the characteristic times of the FAM mixes versus the characteristic times of the corresponding sub-phases, respectively binders and mastics, linear trends in the log-log scale are found, as reported in Figures 44 and 45. The intercepts of the linear relationships, obtained by fitting the experimental results, correspond to the SHStS transformation parameters α between the asphaltic phases, which link the characteristic times of the different material phases.

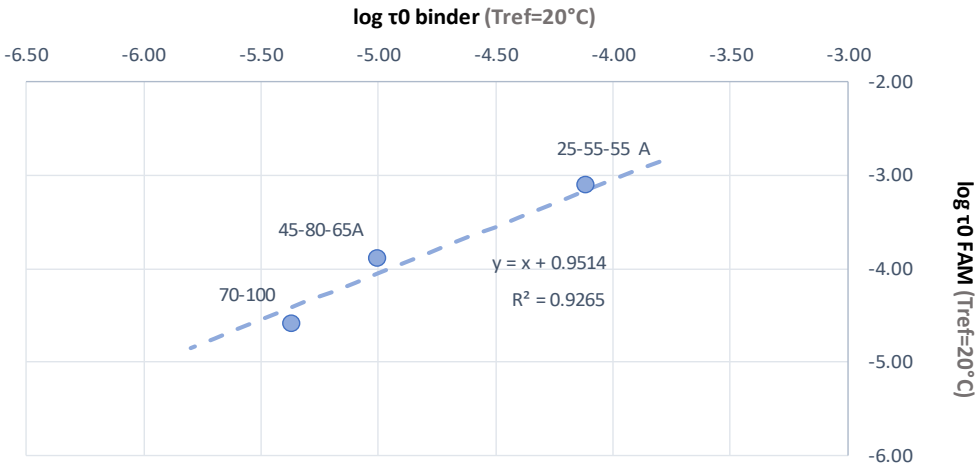

Fig. 44 *Relationship between the characteristic times of binder and FAM, determined at the reference temperature Tref=20°C.*

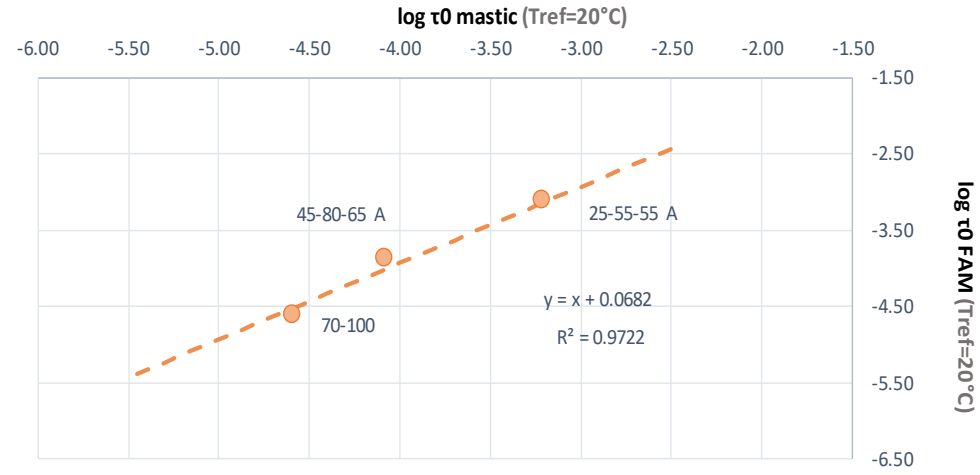

Fig. 45 *Relationship between the characteristic times of mastic and FAM, determined at the reference temperature Tref=20°C.*

Therefore, thanks to the definition of these linear relationships it is possible, starting from the characteristic time of the binder or of the mastic, to calculate the characteristic time of the FAM:

$$\tau_{FAM} = 10^{\alpha}\tau_{binder/mastic} \qquad [34]$$

For known $|G_0|$and $|G_\infty|$ of the FAM, the complex shear modulus $|G^*|$ can be backcalculated for any different mixture by means of the SHStS transformation (Equation 10) in the complete range of the frequency domain.

4.1.1.1 Validation of the binder-FAM interrelation

Using the relationship described in the previous paragraph, the complex shear modulus of the FAM_111 was predicted from the complex shear modulus of the corresponding binder B_11 and then compared with the experimentally obtained values from FAM testing.

Since the time-temperature shift factors as well as the δ, k, h and β parameters of the 2S2P1D model are the same for binders and the corresponding FAM, and taking into account the linear link defined in Equation 34 the following relationship between the FAM complex shear modulus and the binder complex shear modulus can be obtained:

$$G^*_{FAM}(\omega,T) = G_{0_{FAM}} + (G^*_{binder}(10^{\alpha}\omega,T) - G_{0_{binder}})\frac{G_{\infty_{FAM}} - G_{0_{FAM}}}{G_{\infty_{binder}} - G_{0_{binder}}} \quad [35]$$

Equation 35 provides the mathematical expression of the SHStS transformation in the frequency domain and allows to predict the complex shear modulus of the FAM G^*_{FAM} at a given temperature, if the binder complex shear modulus G^*_{binder} at the same temperature and the constants $G_{0_{FAM}}$ and $G_{\infty_{FAM}}$ are known.

In Figure 46 the experimental and the predicted data of the complex shear modulus mastercurves of FAM_111 are shown. The Mean Squared Error in Percentage (RMSP) of this prediction equals to 19.43%. While in Figure 47 the predicted versus measured FAM complex modulus values are reported. The model overestimates the measured complex shear modulus of the corresponding FAM, with an error of 6.8%.

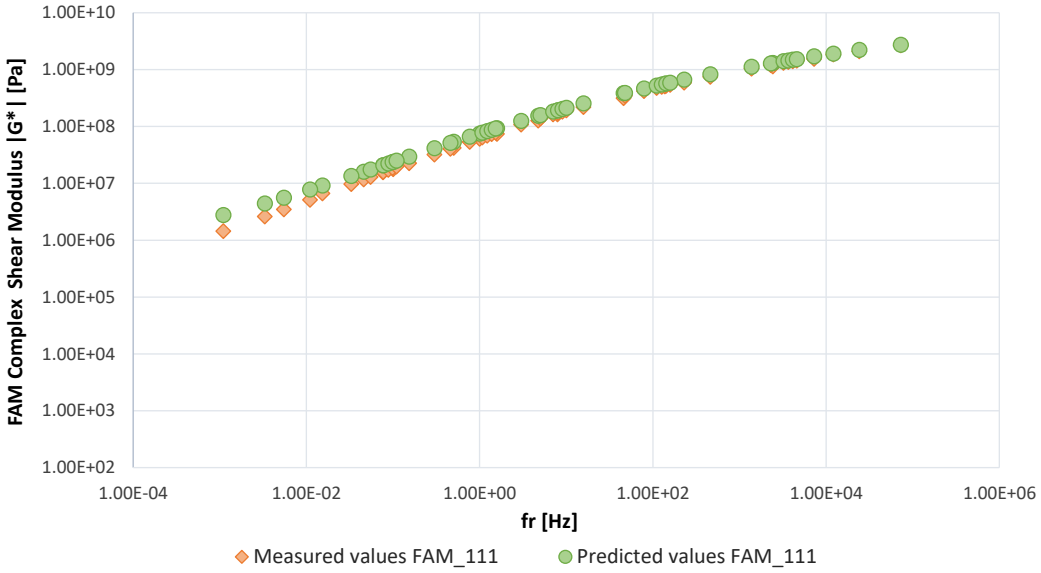

Fig. 46 *Comparison between the experimental and the modelled data for the complex shear modulus of FAM_111.*

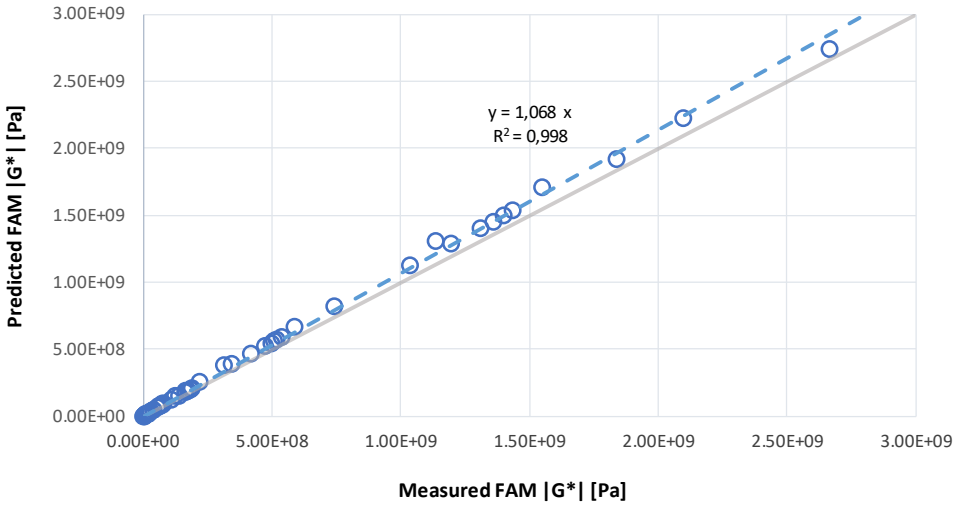

Fig. 47 *Predicted versus measured complex shear modulus |G*| values for FAM_111.*

4.1.1.2 Validation of the mastic-FAM interrelation

In analogy, the linear link between the characteristic times of the mastic and of the FAM, in logarithmic scale, can be used similarly to estimate the complex shear modulus of the FAM from the corresponding mastic, by means of the following equation:

$$G^*_{FAM}(\omega,T) = G_{0_{FAM}} + (G^*_{mastic}(10^{\alpha}\omega,T) - G_{0_{mastic}})\frac{G_{\infty_{FAM}} - G_{0_{FAM}}}{G_{\infty_{mastic}} - G_{0_{mastic}}} \quad [36]$$

To validate this interrelation between mastic and FAM, in Figure 48 the experimental complex shear modulus mastercurve of FAM_111 is compared to the predicted complex shear modulus values obtained from Equation 36. The RMSP of the prediction equals to 13.92%.

The predicted versus modelled diagram is reported in Figure 49. The model over-estimates the measured complex shear modulus of the corresponding FAM, with an error of 2.2%.

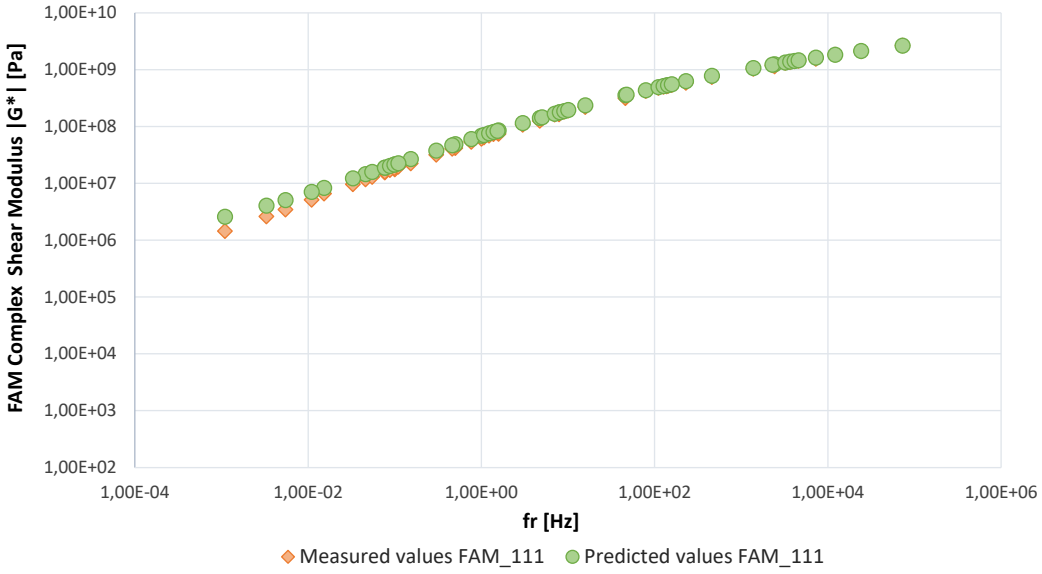

Fig. 48 *Comparison between the experimental and the modelled data for FAM_111.*

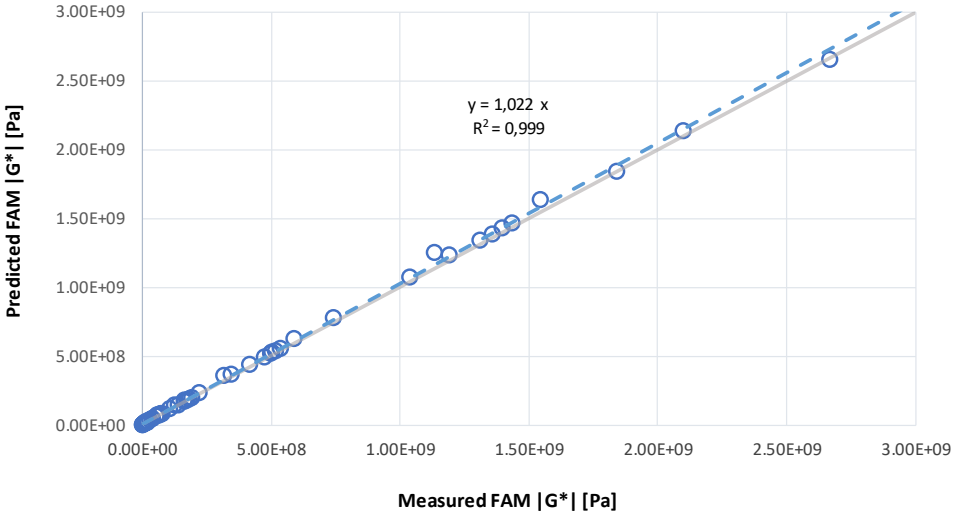

Fig. 49 *Predicted versus measured complex shear modulus |G*| values for FAM_111.*

4.1.2 *Relationship between the characteristic times of FAM and asphalt mixtures*

Similarly to what was done in the previous paragraphs to relate FAM to the corresponding binder and mastic phase, the characteristic times of the asphalt mixtures and of the corresponding FAM were plotted at the reference temperature of 20°C and a linear trend in the log-log scale was found. In Figure 50, the relationship between characteristic times of asphalt mixtures and of the corresponding FAM is reported in logarithmic scale.

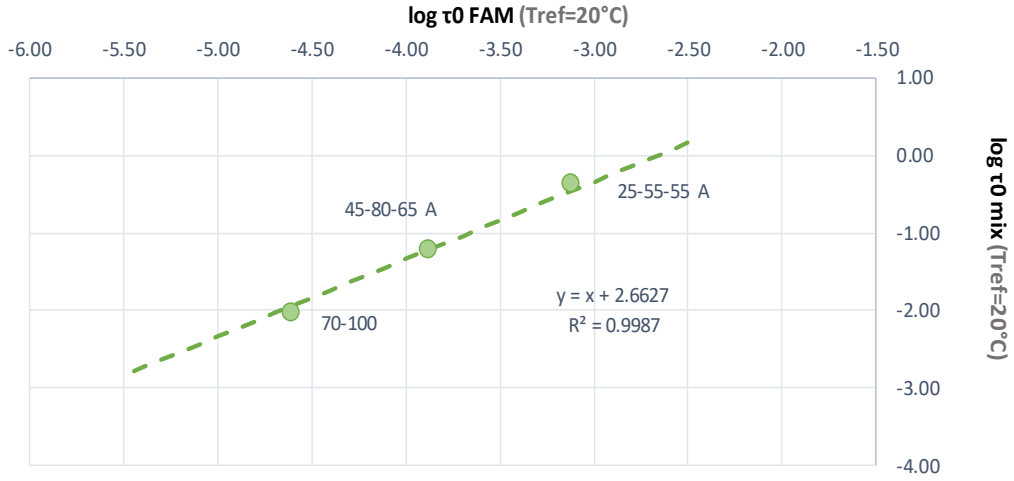

Fig. 50 *Relationship between the characteristic times of FAM and asphalt mixture determined at the reference temperature Tref=20°C.*

Combining the relationship in Figure 50 between the characteristic time of FAM and asphalt mixture with the Equation 3 of the 2S2P1D model for both material scales, is possible, knowing the $|E_0|$ and the $|E_\infty|$ of the mixture, to backcalculate the complex modulus $|E^*|$ of mixtures by means of the SHStS transformation (Equation 37).

Such relationship links FAM and mixtures in the complete range of the frequency domain.

$$G^*_{Mix}(\omega,T) = G_{0_{Mix}} + (G^*_{FAM}(10^{\alpha}\omega,T) - G_{0_{FAM}})\frac{G_{\infty_{Mix}} - G_{0_{Mix}}}{G_{\infty_{FAM}} - G_{0_{FAM}}} \quad [37]$$

4.1.2.1 Validation of FAM-asphalt mixture interrelation

Using the relationship between characteristic times of FAM and asphalt mixture, the complex modulus $|E^*|$ of asphalt mixture Mix_111 was predicted from the complex shear modulus of the corresponding FAM FAM_111, in order to validate that linear relationship. The results were then compared with the experimental measured data.

The complex modulus $|E^*|$ of FAM was calculated from the measured complex shear modulus $|G^*|$ considering a Poisson's ratio of 0.5 ($|E^*| = 3|G^*|$) (Olard et al., 2003) (Mangiafico et al., 2013) (Riccardi, 2017). The Poisson's ratio of FAM was not measured, in this research was assumed that $|\nu^*|_{FAM} = |\nu^*|_{MIX}$ for all temperatures and frequencies. This assumption seems reasonable, given the qualitative and quantitative similarities between the moduli of asphalt mixtures and FAM.

Since the time-temperature shift factors obtained from the WLF equation (Equation 6) are the same for the FAM and asphalt mixtures, as well as the δ, k, h and β parameters of the 2S2P1D model (Equation 3, Chapter 2), and since the characteristic times of FAM and asphalt mixture are linked (Figure 50), the relationship between the asphalt mixture and FAM complex modulus can be described by Equation 37. Such formula provides the mathematical expression of the SHStS transformation, linking FAM and the corresponding asphalt mixture. Hence, if the FAM complex shear modulus $|G^*|$ is known at a given temperature and frequency combination, Equation 37 allows the computation of the complex modulus of the asphalt mixture at the same temperature and frequency, assuming that static and glassy modulus are known.

Must be observed that only the transformation parameter α appears in the SHStS transformation Equation 37. The relation between the complex moduli of the asphalt mixture and the corresponding FAM seems to be independent from the specific model used to derive it. On the contrary, the transformation parameter α provides the direct link between the FAM and the mixture properties and must be further investigated and well understood. This finding seems to extend the observations of previous studies on other phases to the FAM one.

Figure 51 compares the complex modulus of asphalt mixture predicted and measured. The Root Mean Squared Error in Percentage (RMSP) equals to 6.3% and confirms that the model predictions are satisfactory.

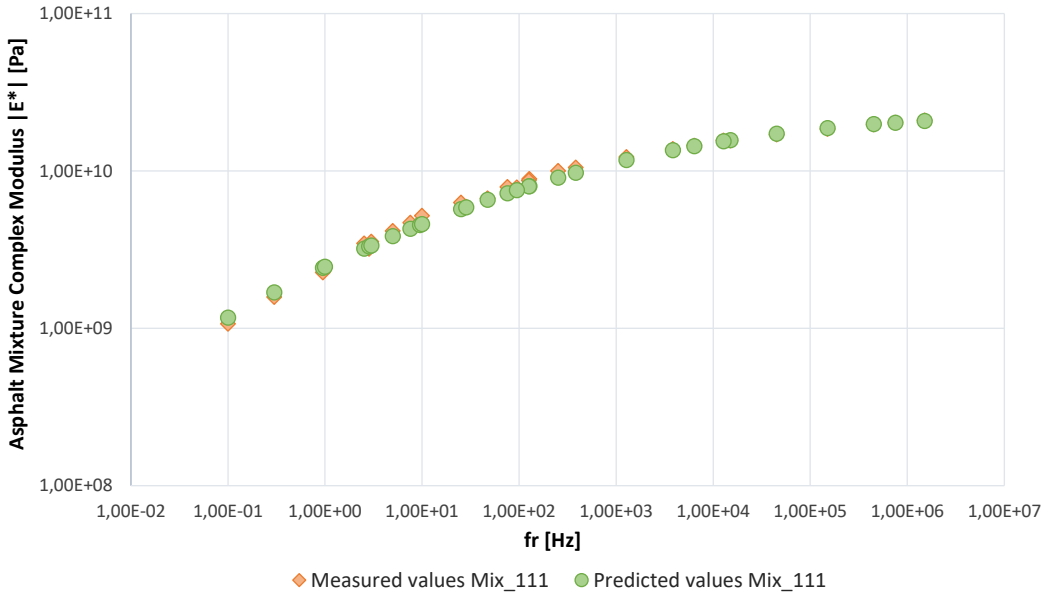

Fig. 51 *Comparison of the mixture mastercurves obtained by the experimental and predicted data.*

Finally, Figure 52 shows a comparison between the predicted and measured data, with the correspondent correlation coefficient R^2, which gives a measure of their correlation, and therefore determines the accuracy of the fitting model. The model slightly underestimates the measured complex modulus of the corresponding mixture, with an error of 1.42%. A R^2 close to 1 and the proximity to the Line of Equality (LOE) shows the accuracy of the linear relationship between the two phases.

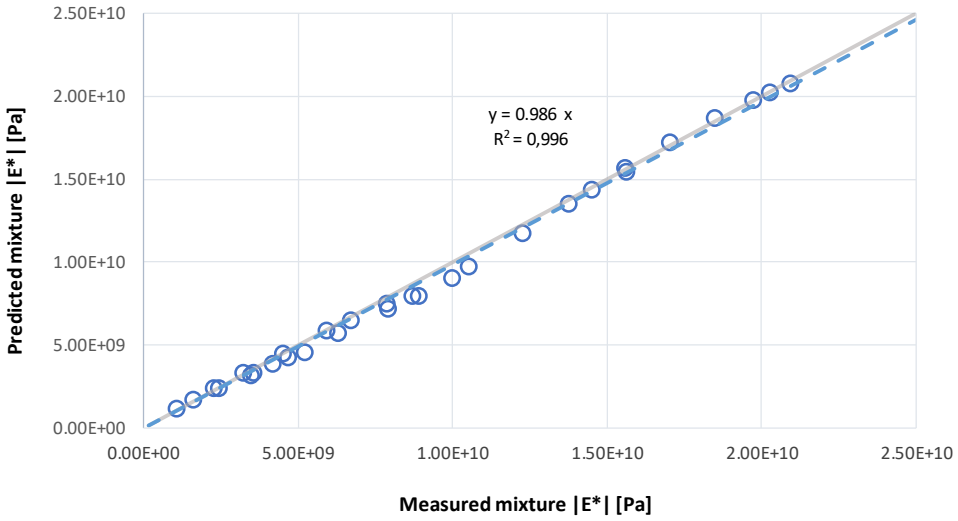

Fig. 52 *Predicted versus measured complex modulus |E*| values for asphalt mixture MIX_111.*

4.2 Summary of Chapter 4

In the present Chapter was investigated the possibility to implement the 2S2P1D model in the multiscale transition between four different material scales (binder, mastic, FAM and asphalt mixture). The analogical 2S2P1D model was used to link the four material phases. After verifying that the model satisfactorily fits the experimental data of FAM (as it does for the others bituminous materials) three relationships linking the characteristic times of the different phases were proposed.

Indeed, the parameter that governs the SHStS transformation between the different materials' phases is the so-called transformation parameter, α, which allows to link the characteristic times of different phases. The transformation parameter corresponds to the intercept of the linear relationship in log-log scale obtained by plotting the characteristic times of a material scale versus the characteristic times of another one.

Therefore, combining such relationships with the 2S2P1D model formulations, the resulting equations define the SHStS transformation between the phases. Hence, the 2S2P1D model can describe and relate all the different material phases analyzed, which result clearly interconnected to one each other. The validations of such interconnections, thanks to the comparison of measured and modelled data, underlined that the model predictions are satisfactory.

Despite that the 2S2P1D model seems to provide good estimates of the FAM properties within the LVE range, as well as for the binders, mastics and mixtures, focusing on SHStS transformation parameter α of FAM phase and mastic one (Figure 45), it can be seen that it is close to zero. According to the literature, the transformation parameter is deeply related to the mix design and to the microstructure of the phase. The physical meaning of the transformation parameter was firstly investigated by Di Benedetto et al. (Di Benedetto et al., 2004) using a simple microstructural model, considering two elements of the mixture: the aggregate (elastic contribution) and the binder (linear viscoelastic contribution). However, more recently Cannone Falchetto et al. (Cannone Falchetto, Montepara, Tebaldi, & Marasteanu, 2012) (Cannone Falchetto, Montepara, Tebaldi, & Marasteanu, 2013) (Cannone Falchetto & Moon, 2015) proposed a micromechanical-analogical material model based on microstructural and volumetric information to obtain an explicit mathematical expression for the SHStS transformation parameter and to gain a more deeply understanding of the meaning of this parameter. In particular, the results

obtained by Cannone Falchetto and Moon shown that the transformation parameter α calculated with their mathematical expression is highly sensitive to the volume fraction of the mastic phase, which represents the most critical material phase within the mixture. Riccardi (Riccardi, 2017) found that the SHStS transformation parameter between binder and asphalt mixture depends on the binder content and on the fractal dimensions of the mixture.

For this reason, further investigations on different mixtures with different aggregate gradations and volumetric characteristics are required to better understand these parameters. Particular attention must be given to the volume fraction of the mastic phase within the FAM phase and its interrelation with the transformation parameter.

Concluding, performing an experimental multiscale investigation from binders to asphalt mixtures, and a following rheological modelling in the LVE domain of the measured data was possible to identify three forward multiscale interrelations (from binder to FAM-N.1, from mastic to FAM-N.2 and from FAM to asphalt mixture- N.3) which allow reliable back-calculations of the complex modulus of a phase starting from test results of another.

However, the transformation parameters α, that links the FAM phase to the binder, mastic and asphalt mixture properties, must be further investigated to gain a more deeply understanding of them. Future research on the multiscale transition must include other volumetric compositions of the mixture and the FAM phase. According to the existing literature the transformation parameter is function of the volumetric composition of the phase and highly influenced to the volume fraction of the mastic phase. To reach such objective the accurate mix design of the FAM phase, extensively and carefully studied in the present Thesis, is definitively crucial.

CHAPTER 5

5 IMPLEMENTATION OF 2S2P1D MODEL FOR MULTISCALE MODELLING FROM FAM TO ASPHALT MIXTURE

In this Chapter the relationship between the characteristic times of the FAM and the asphalt mixture is defined starting from the fitting of the FAM phase with the 2S2P1D model. The link between the characteristic times of the two phases allows the backcalculation of the complex modulus $|E^*|$ of the mixture from FAM measured data.
The tested materials (the asphalt mixtures and the corresponding FAM) have been already introduced in Chapter 3, as well as the testing procedures. As already mentioned in the previous Chapters, to allow the fitting of the 2S2P1D model for FAM samples a wide range of testing temperatures was investigated.

Figure 53 shows the research approach. First, FAM and asphalt mixtures specimens are tested in torsion and tension-compression mode respectively, to measure complex moduli and phase angles within the LVE range. Then, a relationship linking the characteristic times of the FAM and of corresponding asphalt mixtures was proposed. The δ, k, h and β parameters of the 2S2P1D model are defined from FAM experimental data fitting and are then kept constant for the modelling of asphalt mixture data.

The interrelation between the characteristic times of the FAM and asphalt mixtures, allows the back-calculation of the complex modulus of the mixture using the 2S2P1D model, starting directly from the FAM test data. After the validation of this relationship, the predictions of the asphalt mixture complex modulus are compared with the ones obtained from asphalt mixture testing. This allows to test directly FAM specimens to predict the rheological behaviour of full-graded asphalt mixture, avoiding any other test procedure. Therefore, costly and time-consuming tests on mixtures can be significantly reduced.

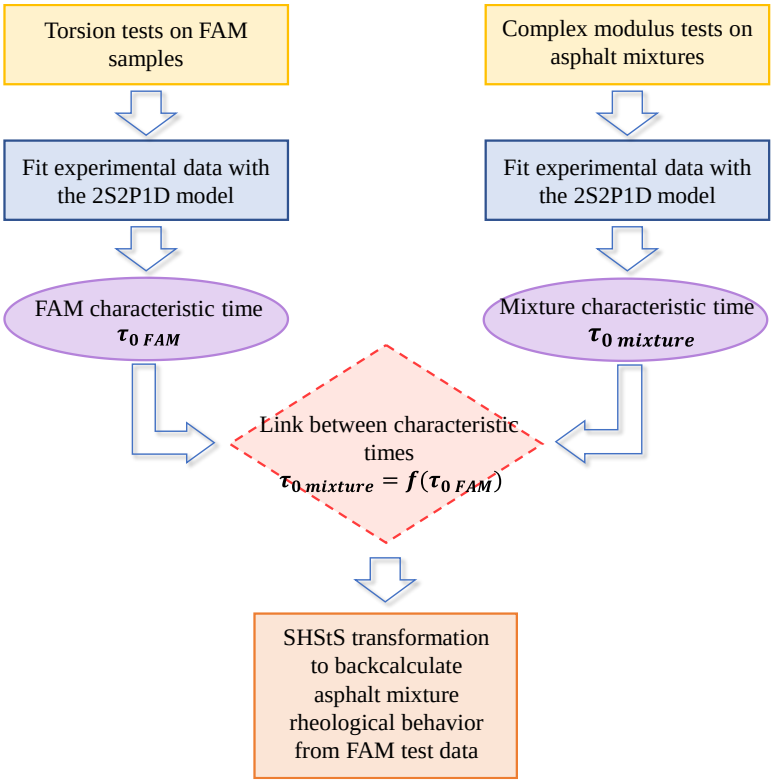

Fig. 53 *Research approach of Chapter 5*

5.1 2S2P1D model fitting

The 2S2P1D model was fitted by minimizing the sum of the square of the distance between the measured and the modelled values. This fitting procedure leads to the calibration of the parameters of the model. For FAM, all the seven parameters of the 2S2P1D model were calibrated, while, for the asphalt mixtures the δ, k, h and β parameters were kept constant from the corresponding FAM phase. The complex moduli $|E^*|$ of the FAM were calculated from the measured complex shear moduli $|G^*|$ by applying a Poisson's ratio of 0.5 ($|E^*| = 3|G^*|$) (Olard et al., 2003) (Mangiafico et al., 2013) (Riccardi, 2017). The seven parameters of the 2S2P1D model of the two material phases (FAM and mixtures) are summarized in Table 29.

Table 29 *Parameters of the 2S2P1D model for FAM and the corresponding asphalt mixtures.*

Material	δ	k	h	E_0 (Pa)	E_∞ (Pa)	β	$\log(\tau_0)$ at 20°C (s)	R^2
FAM_111	*4.60*	*0.271*	*0.610*	$1.38 \cdot 10^6$	$2.23 \cdot 10^{10}$	*450.221*	*-3.77*	*0.999*
MIX_111	*4.60*	*0.271*	*0.610*	$9.50 \cdot 10^7$	$2.52 \cdot 10^{10}$	*450.221*	*-1.32*	*0.997*
FAM_211	*4.81*	*0.262*	*0.601*	$4.08 \cdot 10^6$	$2.37 \cdot 10^{10}$	*506.41*	*-3.64*	*1.000*
MIX_211	*4.81*	*0.262*	*0.601*	$1.10 \cdot 10^7$	$3.05 \cdot 10^{10}$	*506.41*	*-1.06*	*0.997*
FAM_321	*5.44*	*0.282*	*0.697*	$6.17 \cdot 10^5$	$2.11 \cdot 10^{10}$	*141.07*	*-3.99*	*1.000*
MIX_321	*5.44*	*0.282*	*0.697*	$1.16 \cdot 10^7$	$2.37 \cdot 10^{10}$	*141.07*	*-1.50*	*0.992*
FAM_421	*5.92*	*0.237*	*0.571*	$2.53 \cdot 10^6$	$2.37 \cdot 10^{10}$	*4141.88*	*-4.05*	*0.996*
MIX_421	*5.92*	*0.237*	*0.571*	$1.25 \cdot 10^7$	$2.46 \cdot 10^{10}$	*4141.88*	*-1.35*	*0.998*

Figure 54 exemplary compares the measured and the predicted values with the 2S2P1D model in the Cole-Cole diagram, for FAM_321 and the corresponding asphalt mixture Mix_321. As can be seen in the plot, the model fits reasonably well the experimental data. Similar trends were observed for the remaining asphalt binders, mastics, FAM and asphalt mixtures.

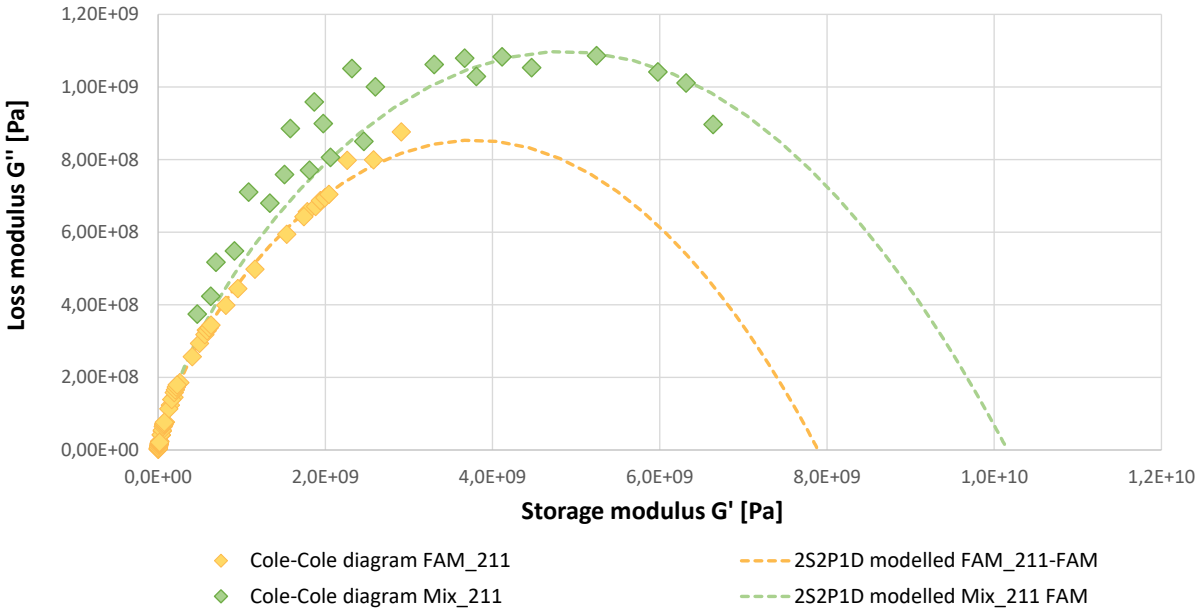

Fig. 54 *2S2P1D model fitting experimentally obtained Cole-Cole diagrams of FAM_211 and MIX_211*

When plotting the normalized moduli of FAM and the corresponding asphalt mixtures in the Cole-Cole plot, by means of Equation 33 (Paragraph 4.1) the curves superimpose with

each other, as exemplary shown in Figure 55. Similar results were obtained for all the tested mixtures (see Annex D).

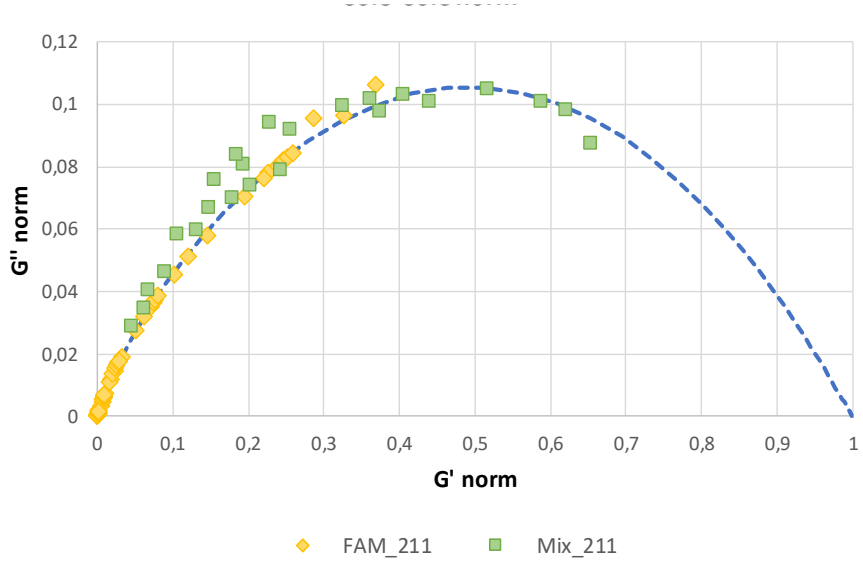

Fig. 55 *Example of the normalized Cole-Cole plot of FAM_211 and MIX_211.*

By means of Equation 33, starting from the normalized moduli values (storage modulus and loss one) of FAM, and knowing the glassy and the static moduli of the corresponding asphalt mixture, it is possible to back-calculate the storage and loss moduli of the asphalt mixture.

In the following paragraphs the characteristic times obtained from the 2S2P1D model by fitting three FAM (FAM_211, FAM_321 and FAM_421) and the corresponding asphalt mixtures are plotted in log-log scale, to identify the transformation parameter α. This parameter allows to directly link the FAM to the corresponding properties of asphalt mixture. To verify the goodness of such interrelation and the goodness of the transformation in predicting the complex modulus of the mixture, the complex modulus of the Mix_111 was computed and compared to the experimental data.

5.2 Relationship between the characteristic times of FAM and asphalt mixture

By plotting the characteristic times of the asphalt mixtures and of FAM in log-log scale, the linear relationship shown in Figure 56 is found.

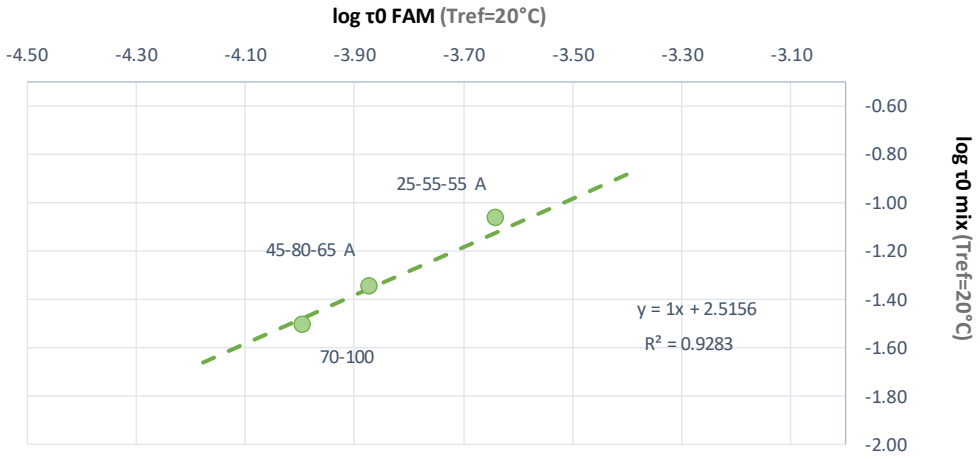

Fig. 56 *Relationship between the characteristic times of FAM and asphalt mixture determined at the reference temperature Tref=20°C.*

The linear relationship given in Figure 56, can be used to calculate the characteristic time of the asphalt mixture from the characteristic time of the corresponding FAM. In addition, knowing the static $|E_0|$ and the glassy $|E_\infty|$ asymptotic moduli of the asphalt mixtures, the complex modulus of the different asphalt mixtures can be backcalculated. However, the range of variation of the results is very limited and more analysis are required to further confirm this interrelationship between FAM and mixtures. Other FAM samples with different binder source will be investigated in future developments of the research.

5.3 Validation and goodness of the fit

To validate the relationship between characteristic times of FAM and asphalt mixture defined in the previous paragraph, the complex modulus $|E^*|$ of an asphalt mixture was predicted from the complex shear modulus of the corresponding FAM. Then the results were compared with the measured values for the asphalt mixtures. In Figure 57 the experimental and the modelled complex modulus mastercurve of asphalt mixture MIX_111 are reported. The Root Mean Squared Error in Percentage (RMSP) equals to 5.41% and confirms that the model predictions are satisfactory.

While, Figure 58 shows a comparison between the predicted and measured data, with the correspondent correlation coefficient R^2. The R^2 close to 1 and the proximity to the Line of Equality LOE validate the goodness of the linear relationship between the two phases. The model slightly overstimates the measured complex modulus of the corresponding mixture, with an error of 0.41%.

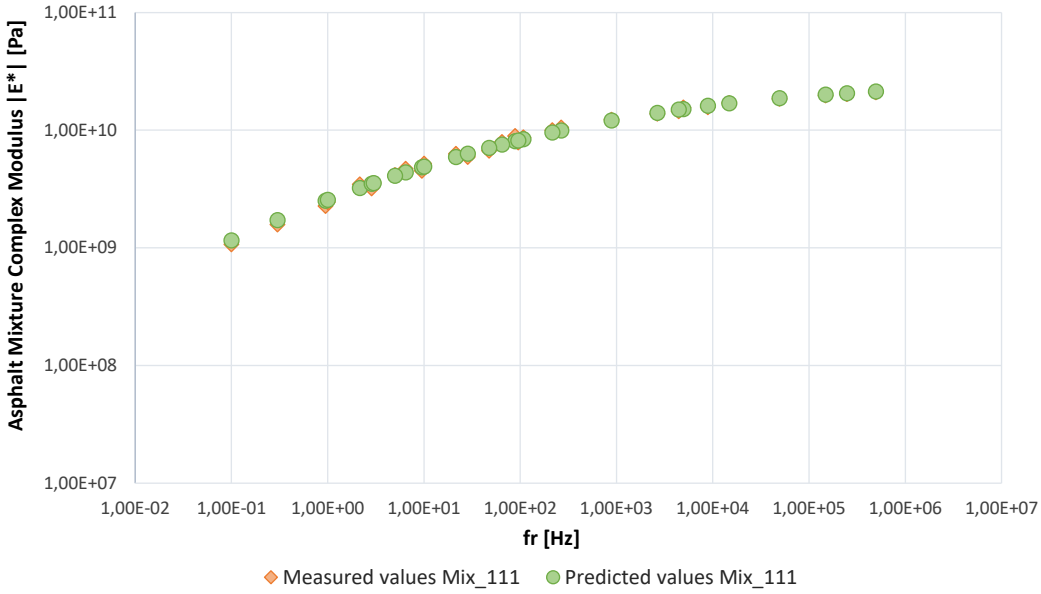

Fig. 57 *Comparison between the measured and the modelled complex modulus mastercurves of asphalt mixture MIX_111.*

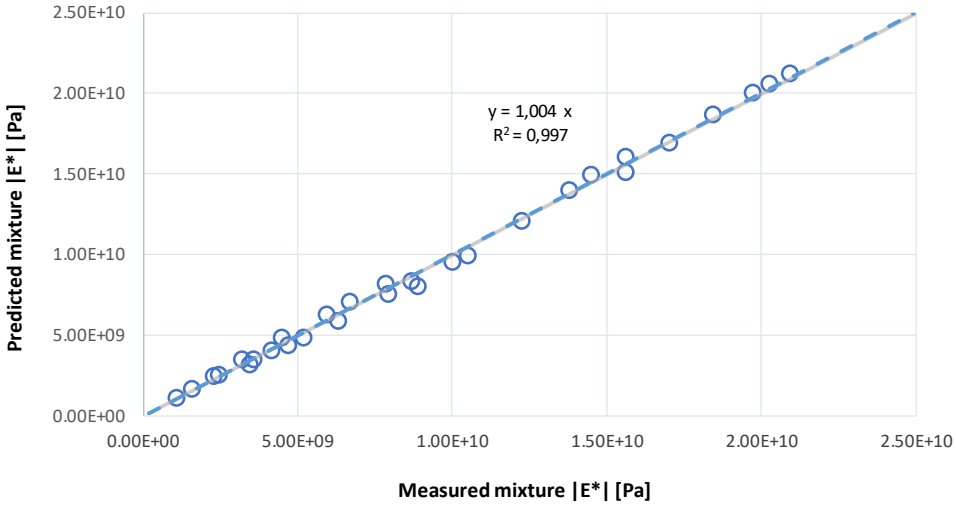

Fig. 58 *Predicted versus measured complex modulus |E*| values for MIX_111.*

5.4 Summary of Chapter 5

In this chapther the transformation parameter α, which relates the FAM phase to the corresponding asphalt mixture, was obtained by fitting both FAM and asphalt mixture experimental data with the 2S2P1D model, without keeping the δ, k, h and β parameters fixed from the binder phase. The resulting transformation parameter α, which corresponds to the intercept of the linear relationship between the FAM and the asphalt mixture characteristic times, is very close to the one obtained in the previous chapter by fixing the parameters δ, k, h and β investigating the binder preliminarly. The range of variation of

the characteristic times of the FAM phase obtained with this procedure is very limited and despite the verification of this interrelation suggests that the model provides satisfactory estimates of the complex modulus of the corresponding asphalt mixture, avoiding time-consuming test procedures on binders, the results seem to confirm the dependence of the transformation parameter on the mix design and microstructure of the mixes. For this reason, a better understanding of the transformation parameter α, that links the properties of the FAM phase to the corresponding properties of the asphalt mixture, is required.

Indeed, considering that SHStS transformation expression is independent of the rheological model used to derive the α parameter, other modelling approach could be investigated in the future to compute the transformation parameter α in the multiscale transition between the FAM and the asphalt mixture, gaining, for example, a better understanding of the influence of the volumetric and microstructural characteristics of the mixes.

CHAPTER 6

6 CONCLUSIONS AND FUTURE DEVELOPMENTS

The present Thesis focuses on the experimental investigation and the following rheological modelling in LVE range of the Fine Aggregate Matrix (FAM). In particular, this phase was introduced in the forward multiscale interrelations (from binder to FAM, from mastic to FAM and from FAM to asphalt mixture) between asphalt mixtures components, with the aim of making reliable forecasts of asphalt mixture performance properties starting from its more representative sub-phase.
This objective was achieved through the experimental investigation of the rheological properties of binders, mastics, FAM and their corresponding asphalt mixtures and by the analytical modelling of the interrelation between these material phases.

6.1 Summary and conclusions

In the first Chapter were listed all the primary objectives considered and investigated to achieve the main goal of this Thesis. At the end of the Thesis the following conclusions could be drawn:

- The mix design of the Fine Aggregate Matrix mixes is bindigly related to the corresponding asphalt mixture. In particular, to replicate FAM phase as it exists within the full graded asphalt mixture, the mix design of the asphalt mixture itself (aggregate gradation, binder content and air voids content) and the characteristics of the aggregates (fine and coarse ones) must be investigated and considered.

- An analytical method has been identified as the more solid and accurate in the representation of the FAM fraction and its reliability was empirically verified by means of solvent extraction of the sieved loose asphalt mixture.

- To achieve the better resemblance to the FAM phase within the mixture the samples were fabricated by means of Gyratory compaction, avoiding the compaction of samples with cylindrical molds, and the air voids distribution of each specimens was investigated, discarding from the tests the specimens with an air voids content outside the target range suggested by the literature.

- A testing protocol for evaluating the LVE rheological properties and performance of FAM specimens was proposed, with analogies to both binders and asphalt mixtures tests standards.

- The 2S2P1D model was extended for modelling the experimental behavior of FAM in LVE range. This model successfully fitted the experimental data of FAM, both with modified and unmodified asphalt binder.

- A multi-scale approach based on the rheological 2S2P1D model was implemented in order to interrelate four material scales (binders, mastics, FAM and asphalt mixtures). Thanks to the definition of the linear interrelationships in the log-log scales between the characteristic time of the FAM and of the others bituminous materials was possible to relate it, backward, to binder and mastic and, forward, to the corresponding asphalt mixture. The intercepts of such linear trends correspond to the SHStS transformation parameters α, which could be used to backcalculate the complex shear modulus of FAM from the experimental binder or mastic data or to predict, with reasonably good results, the rheological behavior of asphalt mixture based on the complex shear modulus data of FAM. All these inter-phases links were found by defining four of the 2S2P1D parameters in the binder phase and by keeping them constant for all the other corresponding phases, since, according to literature, these parameters depend only on binder source.

- Moreover, the relationship between the characteristic time of the asphalt mixtures and the characteristic time of the corresponding FAM was found. This relationship allows the computation of the characteristic time of the asphalt mixture knowing the characteristic time of the FAM and the identification of the moduli of the asphalt mixture from the FAM measured data using the 2S2P1D model.

- Despite that the 2S2P1D model seems to provide good estimates of FAM properties within the LVE range, as well as for binders, mastics and asphalt mixtures, in this research the model parameters were obtained by fitting the experimental data and they have not been linked to the mixture constituents. Indeed, the α parameter, that corresponds to the intercept of a linear function in the logarithmic scale of the characteristic time of the different phases, and that, according to the SHStS transformation, directly links the properties of a sub-phase to the upper phase one (forward) and vice-versa (inverse), seems to be deeply

related to volumetric and microstructural composition of the material. This further confirms the findings of several previous studies (Di Benedetto et al., 2004) (Cannone Falchetto et al., 2012) (Cannone Falchetto et al., 2013) (Cannone Falchetto & Moon, 2015), and underlines the importance to investigate and relate to the transformation parameter α the contribution of all the different material phases: air voids, mastic and aggregates.

- If careful attention is given to FAM samples fabrication, there is a potential use of FAM scale tests for materials characterization and ranking of mixtures. FAM scale tests seem a good alternative for predicting asphalt mixtures behavior and performance, which may bring significant savings in experimental tests and costs. However, further investigations are needed concerning the interrelation between phases and the influence of volumetric and microstructural factors.

6.2 Future developments

This research constitutes a first part of a broader work on FAM testing. The linkages between the phases using a multiscale approach were pointed out and the potentialities of such approach were observed. Although more studies and investigations with many other cases need to be considered and carried out to reach any definitive conclusion.

Hereinafter, are listed some proposals and outlooks for the future developments of the research on FAM scale tests:

- Future experimental investigations into the multiscale behavior of asphalt mixtures must include other volumetric compositions of asphalt mixtures and of FAM, consequently. This will allow to further investigate the results and the conclusions of the present research. Moreover, the relationship between the SHStS transformation parameters and the volumetric compositions (binder content, aggregate gradation, mastic volumetric concentration etc) of the different material scales should be inquired, using the Moon Cannone Falchetto (MCF) model (Cannone Falchetto & Moon, 2015) for example.

- Other FAM testings could be further carried out to study the internal mechanisms in mixtures, including the investigations on the performance of various sustainable materials, such as Warm Mix Asphalts (WMA), asphalt mixtures containing Recycled Asphalt Pavements (RAP) and crumb rubber. The testing

protocols to investigate other mechanical and fatigue properties of FAM must be as well defined in detail.

- FAM scale tests could have interesting applications to test and investigate the performance of blended binders in asphalt mixtures containing high quantities of Recycled Asphalt Pavements (RAP) materials. Indeed, it could be considered an alternative method to blended binders testing, which required extraction and recovery procedures (that could alter the chemical and rheological properties of the material) and to asphalt mixtures tests, which are very expensive and time consuming. To test FAM with RAP content (FAM-RAP) an extensive work must be done to identify an appropriate procedure for their proper mix design, in order to ensure a suitable representativeness.

- The 2S2P1D model might be suitable to describe the rheological behavior of FAM-RAP mixes in the LVE range. If so, could be studied the relationship between the characteristic time of the FAM phase as function of the RAP content in its mix design. Finally, 2S2P1D model could be implemented for the multiscale modelling to link the FAM-RAP mixes to the corresponding asphalt mixtures, in order to provide reasonably good predictions of asphalt mixtures complex moduli with different RAP content.

- Another interesting future development could include the combination of FAM testing with 3D numerical modelling, in order to better understand the micro-mechanical influence of all material phases to the overall response of FAM.

REFERENCES

AASHTO M 320-10UL (2016). "Standard Method of Test for Performance Graded Asphalt Binder". *American Association of State Highway and Transportation Officials*.

AASHTO PP 6 (1994). "Standard Practice for Grading or Verifying the Performance Grade of an Asphalt Binder". *American Association of State Highway and Transportation Officials*.

AASHTO T 85 (2014) "Standard Method of Test for Specific Gravity and Absorption of Coarse Aggregate". *American Association of State Highway and Transportation Officials.*

AASHTO T 164 (2014) "Standard Method of Test for Quantitative Extraction of Asphalt Binder from Hot Mix Asphalt (HMA)". *American Association of State Highway and Transportation Officials.*

AASHTO T 166 (2016). "Standard Method of Test Bulk Specific Gravity of Compacted Asphalt Mixtures using Saturated Surface-Dry Specimens". *American Association of State Highway and Transportation Officials*.

AASHTO T 209 (2019) "Standard Method of Test for Theoretical Maximum Specific Gravity (Gmm) and Density of Asphalt Mixtures". *American Association of State Highway and Transportation Officials.*

AASHTO T 269 (2014). "Standard Method of Test for Percent Air-Voids in Compacted Dense and Open Asphalt Mixtures". *American Association of State Highway and Transportation Officials*.

AASHTO T 308 (2014) "Standard Method of Test for Determining the Asphalt Binder Content of Hot Mix Asphalt (HMA) by the Ignition Method". *American Association of State Highway and Transportation Officials.*

AASHTO T 315-12UL (2012). "Standard Method of Test for Determining the Rheological Properties of Asphalt Binder using a Dynamic Shear Rheometer (DSR)". *American Association of State Highway and Transportation Officials*.

AASHTO TP 4 (2000) "Standard Method for Preparing and Determining the Density of Hot Mix Asphalt (HMA) specimens by means of Superpave Gyratory Compactor". *American Association of State Highway and Transportation Officials*.

AASHTO XXX-12 (2012). "Draft Standard Method of Test for Determining the Low Temperature Rheological Properties of Asphalt Binder using a Dynamic Shear Rheometer (DSR)". *American Association of State Highway and Transportation Officials*.

Abbas, A., Masad, E., Papagiannakis, T., & Shenoy, A. (2007). Modelling asphalt mastic

stiffness using discrete element analysis and micromechanics-based models, *8436*. https://doi.org/10.1080/10298430500159040

Aim, R. B., & Le Goff, P. (1967). Effet de Paroi dans les Empilements Desordonnes de Spheres et Application a la Porosite de Melanges Binaries. *Powder Technology*.

Alavi, M. Z., He, Y., Harvey, J., & Jones, D. (2016). Evaluation of the Combined Effects of Reclaimed Asphalt Pavement (RAP), Reclaimed Asphalt Shingles (RAS), and Different Virgin Binder Sources on the Performance of Blended Binders. *Research Report : UCPRC-RR-2015-06*.

Anderson, D. A., Chris, D. W., Bahia, H. U., Antle, C. E., Dongré, R., Sharma, M. G., & Button, J. (1994). Binder Characterization and Evaluation - Volume 3 : Physical Characterization. *Report SHRP-A-369 Strategic Highway Research Program, Washington*.

Aragão, F. T. S., Kim, Y., Karki, P., & Little, D. N. (2011). Semiempirical, Analytical, and Computational Predictions of Dynamic Modulus of Asphalt Concrete Mixtures. *Transportation Research Record: Journal of the Transportation Research Board*, *2181*(1), 19–27. https://doi.org/10.3141/2181-03

Aragão, F. T. S., Lee, J., Kim, Y. R., & Karki, P. (2010). Material-specific effects of hydrated lime on the properties and performance behavior of asphalt mixtures and asphaltic pavements. *Construction and Building Materials*, *24*(4), 538–544. https://doi.org/10.1016/j.conbuildmat.2009.10.005

Arambula, E., Masad, E., & Martin, A. (2007). Moisture Susceptibility of Asphalt Mixtures with Known Field Performance: Evaluated with Dynamic Analysis and Crack Growth Model. *Transportation Research Record: Journal of the Transportation Research Board*, *2001*, 20–28. https://doi.org/10.3141/2001-03

Arshadi, A., & Bahia, H. (2015). Development of an image-based multi-scale finite-element approach to predict mechanical response of asphalt mixtures. *Road Materials and Pavement Design*, *16*(sup2), 214–229. https://doi.org/10.1080/14680629.2015.1077007

Bhasin, A., Little, D. N., Bommavaram, R., & Vasconcelos, K. (2008). A Framework to Quantify the Effect of Healing in Bituminous Materials using Material Properties. *Road Materials and Pavement Design*, *0629*, 37–41. https://doi.org/10.3166/RMPD.9HS.219-242

Bourbie, T., Coussy, O., & Zinszner, B. (1987). Acoustics of Porous Media. *Journal of Acoustical Society of America*, *91*.

Bücher, J., Wistuba, M. P., Remmler, T., & Wang, D. (2019). On low temperature binder

testing using DSR 4 mm geometry. *Materials and Structures*, *52:113*. https://doi.org/10.1617/s11527-019-1412-3

Cannone Falchetto, A., Montepara, A., Tebaldi, G., & Marasteanu, M. O. (2012). Microstructural and rheological investigation of asphalt mixtures containing recycled asphalt materials. *Construction and Building Materials*, *35*, 321–329. https://doi.org/10.1016/j.conbuildmat.2012.04.016

Cannone Falchetto, A., Montepara, A., Tebaldi, G., & Marasteanu, M. O. (2013). Microstructural Characterization of Asphalt Mixtures Containing Recycled Asphalt Materials, *25*, 45–53. https://doi.org/10.1061/(ASCE)MT.1943-5533.0000544

Cannone Falchetto, A., & Moon, K. H. (2015). Micromechanical – analogical modelling of asphalt binder and asphalt mixture creep stiffness properties at low temperature, *0629*. https://doi.org/10.1080/14680629.2015.1029708

Caro, S., Masad, E., Airey, G., Bhasin, A., & Little, D. (2008). Probabilistic Analysis of Fracture in Asphalt Mixtures Caused by Moisture Damage. *Transportation Research Record: Journal of the Transportation Research Board*, *2057*(Table 1), 28–36. https://doi.org/10.3141/2057-04

Caro, S., Sanchez, D. B., & Caicedo, B. (2015). Methodology to characterise non-standard asphalt materials using DMA testing : application to natural asphalt mixtures. *International Journal of Pavement Engineering*, *16*(1), 1–10.

Castelo Branco, V. T. F. (2008). A unified method for the analysis of nonlinear viscoelasticity and fatigue cracking of asphalt mixtures using the dynamic mechanical analyzer. *PhD Thesis at Texas A&M University*.

Coutinho, R. P. (2012). Utilização da parte fina de misturas asfálticas para avaliação do dano por fadiga.

Delaporte, B., Benedetto, H. Di, Chaverot, P., & Gauthier, G. (2009). Linear Viscoelastic Properties of Bituminous Materials Including New Products Made with Ultrafine Particles. *Road Materials and Pavement Design*, *10:1*, 7–38. https://doi.org/10.3166/RMPD.10.7-38

Dessi, C., Tsibidis, G. D., Vlassopoulos, D., De Corato, M., Trofa, M., D'Avino, G., … Coppola, S. (2016). Analysis of dynamic mechanical response in torsion. *Journal of Rheology*, *60*, 275–287. https://doi.org/10.1122/1.4941603

Di Benedetto, H., Olard, F., Sauzéat, C., & Delaporte, B. (2004). Linear viscoelastic behaviour of bituminous materials : From binders to mixes. *Road Materials and Pavement Design*, 37–41. https://doi.org/10.1080/14680629.2004.9689992

EN 1097-6. (2013). Tests for mechanical and physical properties of aggregates - Part 6: Determination of particle density and water absorption. *European Standard*.

EN 1097-7. (2008). Tests for mechanical and physical properties of aggregates. Determination of the particle density of filler- Pyknometer method. *European Standard*.

EN 12607-1. (2014). Bitumen and bituminous binders - Determination of the resistance to hardening under influence of heat and air - Part 1: RTFOT method. *European Standard*.

EN 12697-26. (2018). Bituminous mixtures. Test methods. Stiffness. *European Standard*.

EN 12697-31. (2007). Bituminous mixtures - Test methods for hot mix asphalt - Part 31: Specimen preparation by Gyratory Compactor. *European Standard*.

EN 12697-6. (2008). Bituminous Mixtures: Test methods for Hot Mix Asphalt Part 6: Determination of bulk density of bituminous specimens. *European Standard*.

EN 13043. (2013). Aggregates for bituminous mixtures and surface treatments for roads, airfields and other trafficked areas. *European Standard*.

EN 13108-1. (2016). Bituminous mixtures. Material specifications. Asphalt Concrete. *European Standard*.

EN 1426. (2007). Bitumen and bituminous binders - Determination of needle penetration. *European Standard*.

EN 1427. (2007). Bitumen and bituminous binders - Determination of the softening point - Ring and Ball method. *European Standard*.

EN 14770. (2012). Bitumen and bituminous binders - Determination of complex shear modulus and phase angle - Dynamic Shear Rheometer (DSR). *European Standard*.

EN 933-1. (2012). Tests for geometrical properties of aggregates. Determination of particle size distribution. Sieving method. *European Standard*.

EN ISO 17892-4. (2016). Geotechnical investigation and testing. Laboratory testing of soil. Part 4: Determination of particle size distribution. *European Standard*.

Farrar, M. J., Sui, C., Salmans, S., & Qin, Q. (2015). Determining the Low-Temperature Rheological Properties of Asphalt Binder Using a Dynamic Shear Rheometer (DSR). *Technical White Paper- Prepared for Federal Highway Administration*.

Ferry, J. D. (1948). Viscoelastic properties of polymer solutions. *Journal of Research of the National Bureau of Standards*, *41*(1), 53–62. https://doi.org/10.1007/BF01534283

Freire, R. A. (2015). Evaluation of the Coarse Aggregate Influence in the Fatigue Damage using

Fine Aggregate Matrices with Different Maximum Nominal Sizes. *Master Degree Thesis Universidade Federal Do Ceara, Fortaleza, Brazil*.

Freire, R. A., Castelo Branco, V. T. F., & Vasconcelos, K. L. (2014). Avaliação da resistência ao trincamento de misturas asfálticas compostas por agregados miúdos com diferentes tamanhos máximos nominais. *Transportes*, *22*(3), 117. https://doi.org/10.14295/transportes.v22i3.791

Gottlieb, M., & Macosko, C. W. (1982). The Effect of Instrument Compliance on Dynamic Rheological Measurements. *Rheologica Acta*, *21*, 90–94.

Gudipudi, P., & Underwood, B. S. (2015). Testing and Modeling of Fine Aggregate Matrix and Its Relationship to Asphalt Concrete Mix. *Transportation Research Record: Journal of the Transportation Research Board*, *2507*, 120–127. https://doi.org/10.3141/2507-13

Gudipudi, P., & Underwood, B. S. (2017a). Development of modulus and fatigue test protocol for fine aggregate matrix for axial direction of loading. *Journal of Testing and Evaluation*, *45 (2)*, 497–508. https://doi.org/https://doi.org/10.1520/JTE20150295

Gudipudi, P., & Underwood, B. S. (2017b). Use of Fine Aggregate Matrix Experimental Data in Improving Reliability of Fatigue Life Prediction of Asphalt Concrete. *Transportation Research Record: Journal of the Transportation Research Board, No. 2631, 2017, Pp. 65–73*. https://doi.org/https://doi.org/10.3141/2631-07

Gudipudi, P., & Underwood, S. (2017c). Use of Fine Aggregate Matrix Experimental Data in Improving Reliability of Fatigue Life Prediction of Asphalt Concrete Sensitivity of this Approach to Variation in Input Parameters. *Journal of Testing and Evaluation*, (June). https://doi.org/10.3141/2631-07

Gundla, A., Gudipudi, P., & Underwood, B. S. (2017). Evaluation of the sensitivity of asphalt concrete modulus to binder oxidation with a multiple length scale study. *Construction and Building Materials*, *152*, 954–963. https://doi.org/10.1016/j.conbuildmat.2017.07.067

Haghshenas, H. F., Nabizadeh, H., Kim, Y., & Santosh, K. (2016). Research on High-RAP Asphalt Mixtures with Rejuvenators and WMA Additives. *Technical Report-University of Nebraska at Lincoln*.

Hashin, Z. (1983). Analysis of Composite Materials — A Survey. *Journal of Applied Mechanics*, *50*, 481–505.

He, Y., Alavi, M. Z., Jones, D., & Harvey, J. (2016). Proposing a solvent-free approach to evaluate the properties of blended binders in asphalt mixes containing high quantities of reclaimed asphalt pavement and recycled asphalt shingles, *114*, 172–180.

Im, S., You, T., Ban, H., & Kim, Y. R. (2017). Multiscale testing-analysis of asphaltic materials considering viscoelastic and viscoplastic deformation. *International Journal of Pavement Engineering*, *18*(9), 783–797. https://doi.org/10.1080/10298436.2015.1066002

Isailović, I., & Wistuba, M. P. (2018). Sweep test protocol for fatigue evaluation of asphalt mixtures. *Road Materials and Pavement Design*, *0*(0), 1–14. https://doi.org/10.1080/14680629.2018.1438305

Izadi, A. (2012). Quantitative Characterization of Microstructure of Asphalt Mixtures to Evaluate Fatigue Crack Growth. *Thesis at University of Texas at Austin*.

Izadi, A., Motamed, A., & Bhasin, A. (2011). Designing Fine Aggregate Mixtures to Evaluate Fatigue Crack-Growth in Asphalt Mixtures. *Report 161022-1 Center for Transportation Research The University of Texas*, *7*(1), 54.

Kanaan, A. I., Ozer, H., & Al-Qadi, I. L. (2014). Testing of Fine Asphalt Mixtures to Quantify Effectiveness of Asphalt Binder Replacement Using Recycled Shingles. *Transportation Research Record: Journal of the Transportation Research Board*, *2445*, 103–112. https://doi.org/10.3141/2445-12

Karki, P. (2010). Computational and experimental characterization of Bituminous composites based on experimentally determined properties of constituents. *Thesis at University of Nebraska at Lincoln*.

Karki, P., Bhasin, A., & Underwood, B. S. (2016). Fatigue Performance Prediction of Asphalt Composites Subjected to Cyclic Loading with Intermittent Rest Periods, (2576), 72–82. https://doi.org/10.3141/2576-08

Karki, P., Kim, Y.-R., & Little, D. N. (2015). Dynamic Modulus Prediction of Asphalt Concrete Mixtures Through Computational Micromechanics. *Transportation Research Record: Journal of the Transportation Research Board*, *2507*, 1–9. https://doi.org/10.3141/2507-01

Kim, Y.-R., & Little, D. N. (2005). Development of Specification-Type Tests to Assess the Impact of Fine Aggregate and Mineral Filler on Fatigue Damage, *7*(2).

Kim, Y.-R., Little, D., & Song, I. (2003). Effect of Mineral Fillers on Fatigue Resistance and Fundamental Material Characteristics: Mechanistic Evaluation. *Transportation Research Record*, *1832*(1), 1–8. https://doi.org/10.3141/1832-01

Kim, Y. R. (2003). *Mechanistic Fatigue Characterization and Damage Modeling of Asphalt Mixtures*. PhD Thesis at Texas A&M Univ. College Station.

Kim, Y. R., Little, D. N., & Lytton, R. L. (2002). Use of Dynamic Mechanical Analysis (DMA)

to evaluate the fatigue and healing potential of asphalt binders in sand asphalt mixtures. *J. Assoc. Asphalt Paving Techno.*, *71*, 176–206.

Kim, Y. R., Little, D. N., & Lytton, R. L. (2003). Fatigue and Healing Characterization of Asphalt Mixtures. *Journal of Materials in Civil Engineering*, *15*(1), 75–83. https://doi.org/10.1061/(ASCE)0899-1561(2003)15:1(75)

Laukkanen, O.-V. (2015). Low-temperature rheology of bitumen and its relationship with chemical and thermal properties. *Thesis at Aalto University*.

Lu, X., Uhlback, P., & Soenen, H. (2016). Investigation of bitumen low temperature properties using a dynamic shear rheometer with 4 mm parallel plates. *International Journal of Pavement Research and Technology*. https://doi.org/10.1016/j.ijprt.2016.08.010

Mangiafico, S., Di Benedetto, H., Sauzéat, C., & Olard, F. (2013). Influence of reclaimed asphalt pavement content on complex modulus of asphalt binder blends and corresponding mixes : experimental results and modelling. *Road Materials and Pavement Design*, *14 (1)*, 37–41. https://doi.org/10.1080/14680629.2013.774751

Marasteanu, M. (1999). Inter-conversions of the linear viscoelastic functions used for the rheological characterization of asphalt binders. *Thesis in Civil Engineering at Pennsylvania State University*.

Martono, W., Bahia, H. U., & D'Angelo, J. (2007). Effect of Testing Geometry on Measuring Fatigue of Asphalt Binders and Mastics. *Journal of Materials in Civil Engineering*, *19*(9), 746–752. https://doi.org/10.1061/(ASCE)0899-1561(2007)19:9(746)

Masad, E., Bulut, R., Little, D., & Lytton, R. L. (2006). Characterization of HMA moisture damage using surface energy and fracture properties. *Journal of the Association of Asphalt Paving Technologists*, *75*, 713–754.

Masad, E., Muhunthan, B., Shashidhar, N., & Harmanet, T. (1999). Internal Structure Characterization of Asphalt Concrete using Image Analysis. *Journal of Computing in Civil Engineering*, *13*, 88–95.

Miranda-Arguello, F., Loria-Salazar, L., & Aguiar-Moya, J. P. (2014). Dynamic Mechanic Analyzer (DMA) shear test implementation for measurement of G * in Fine Asphalt Mixes, (506), 2511–2524.

Motamed, A., Bhasin, A., & Izadi, A. (2012). *Fracture Properties and Fatigue Cracking Resistance of Asphalt Binders- Report 161122-1*.

Nabizadeh, H. (2015). Viscoelastic, Fatigue Damage, and Permanent Deformation

Characterization of High RAP Bituminous Mixtures Using Fine Aggregate Matrix (FAM). *Thesis at University of Nebraska at Lincoln*.

Nabizadeh, H., Haghshenas, H. F., Kim, Y.-R., & Aragão, F. T. S. (2017). Effects of rejuvenators on high-RAP mixtures based on laboratory tests of asphalt concrete (AC) mixtures and fine aggregate matrix (FAM) mixtures. *Construction and Building Materials 152*, 65–73.

NCHRP-459. (2001). *Characterization of Modified Asphalt Binders in Superpave Mix Design*. *National Academy Press Washington D.C.* https://doi.org/10.1016/B978-0-12-809289-7.00002-6

Ng, A. K. Y., Vale, A. C., Gigante, A. C., Faxina, A. L., & Ph, D. (2018). Determination of the Binder Content of Fine Aggregate Matrices Prepared with Modified Binders. *Journal of Materials in Civil Enginee*, *30*(4), 1–12. https://doi.org/10.1061/(ASCE)MT.1943-5533.0002160.

Olard, F. (2003). Comportement Thermomécanique des Enrobés Bitumineua à Basses Températures. Relations entre les propriétés du liant et de l'enrobé. *PhD Thesis Université de Lyon*.

Olard, F., & Di Benedetto, H. (2003). General "2S2P1D" Model and Relation Between the Linear Viscoelastic Behaviours of Bituminous Binders and Mixes. *Road Materials and Pavement Design*, *4*(2), 185–224. https://doi.org/10.1080/14680629.2003.9689946

Olard, F., Di Benedetto, H., Eckmann, B., & Triquigneaux, J. (2003). Linear Viscoelastic Properties of Bituminous Binders and Mixtures at Low and Intermediate Temperatures. *Road Materials and Pavement Design*, *4:1*, 77–107. https://doi.org/10.1080/14680629.2003.9689941

Palvadi, N. S. (2011). *Measurement of material properties related to self-healing based on continuum and micromechanics approach*. Thesis at Texas University.

Palvadi, N. S., Bhasin, A., & Little, D. N. (2012). Method to Quantify Healing in Asphalt Composites by Continuum Damage Approach. *Transportation Research Record: Journal of the Transportation Research Board*, *2296*(1), 86–96. https://doi.org/10.3141/2296-09

Pouget, S., Sauzéat, C., Di Benedetto, H., & Olard, F. (2010). Road Materials and Pavement Design From the Behavior of Constituent Materials to the Calculation and Design of Orthotropic Bridge Structures. *Road Materials and Pavement Design 11- Sup 1*, 111–144. https://doi.org/10.1080/14680629.2010.9690329

Reed, J. S. (1988). *Introduction to the Principles of Ceramic Processing*. John Wiley & Sons.

Riccardi, C. (2017). *Mechanistic Modeling of Bituminous Mortars to Predict Performance of Asphalt Mixtures Containing RAP*. PhD Thesis at TU Braunschweig and University of Florence.

Riccardi, C., Cannone Falchetto, A., Losa, M., & Wistuba, M. (2016). Modeling of the rheological properties of asphalt binder and asphalt mortar containing recycled asphalt material. *Transportation Research Procedia*, *14*(10), 3503–3511. https://doi.org/10.1016/j.trpro.2016.05.317

Riccardi, C., Cannone Falchetto, A., Losa, M., & Wistuba, M. P. (2018). Development of simple relationship between asphalt binder and mastic based on rheological tests. *Road Materials and Pavement Design*, *19*(1), 18–35. https://doi.org/10.1080/14680629.2016.1230514

Riccardi, C., Cannone Falchetto, A., Wang, D., & Wistuba, M. P. (2017). Effect of cooling medium on low-temperature properties of asphalt binder. *Road Materials and Pavement Design*, 1–22. https://doi.org/10.1080/14680629.2017.1389072

Riccardi, C., Cannone Falchetto, A., & Wistuba, M. P. (2018). Experimental Investigation of Rutting in the Different Phases of Asphalt Mixtures. In *RILEM 252-CMB 2018* (pp. 105–110). Springer International Publishing. https://doi.org/10.1007/978-3-030-00476-7

Rieger, J. (2001). The glass transition temperature Tg of polymers—Comparison of the values from differential thermal analysis (DTA, DSC) and dynamic mechanical measurements (torsion pendulum). *Polymer Testing*, *20*, 199–204.

Roberts, F. L., Kandhal, P. S., Brown, E. R., Lee, D. Y., & Kennedy, T. W. (1996). *Hot Mix Asphalt Materials, Mixture Design, and Construction*. National Asphalt Paving Association Education Foundation.

Sánchez, D. B., Grenfell, J., Airey, G., & Caro, S. (2017). Evaluation of the Degradation of Fine Asphalt- Aggregate Mixtures containing High Reclaimed Asphalt Pavement Contents. *Road Materials and Pavement Design N.18*, *0629*, 91–107. https://doi.org/10.1080/14680629.2017.1304250

Sayegh, G. (1965). Variation des modules de quelques bitumes purs et enrobés bitumineux. *PhD Thesis at Université de Paris*.

Schröter, K., Hutcheson, S. A., Shi, X., Mandanici, A., & Mckenna, G. B. (2006). Dynamic shear modulus of glycerol : Corrections due to instrument compliance. *The Journal of Chemical Physics*, *125*. https://doi.org/10.1063/1.2400862

Sousa, P. C. D. E. (2010). Automated Protocol for Analysis of Dynamic Mechanical Analyzer

Data from Fine Aggregate Asphalt Mixes. *PhD Thesis*, (Texas A&M University).

Sousa, P., Kassem, E., Masad, E., & Little, D. (2013). New design method of fine aggregates mixtures and automated method for analysis of dynamic mechanical characterization data. *Construction and Building Materials*, *41*, 216–223. https://doi.org/10.1016/j.conbuildmat.2012.11.038

Sui, C., Farrar, M. J., Harnsberger, P. M., Tuminello, W. H., & Turner, T. F. (2010). New Low-Temperature Performance-Grading Method Using 4-mm Parallel Plates on a Dynamic Shear Rheometer. *Transport Reseach Record*, *2207*, 43–48. https://doi.org/10.3141/2207-06

Sui, C., Farrar, M. J., Tuminello, W. H., & Turner, T. F. (2010). New Technique for Measuring Low-Temperature Properties of Asphalt Binders with Small Amounts of Material. *Transport Reseach Record*, *2179*, 23–28. https://doi.org/10.3141/2179-03

Tabatabaee, H., Velasquez, R., Arshadi, A., & Bahia, H. U. (2012). Modeling of Asphalt Mixtures Contraction and Expansion Due to Thermal Cycling Investigation of Low Temperature Cracking in Asphalt Pavements National Pooled Fund Study – Phase II Task 5. *University of Wisconsin- Madison*.

Tiouajini, S., Di Benedetto, H., Sauzéat, C., & Pouget, S. (2011). Approximation of Linear Viscoelastic Model in the 3 Dimensional Case with Mechanical Analogues of Finite Size. *Road Materials and Pavement Design 12(4)*, 897–930. https://doi.org/10.1080/14680629.2011.9713899

Toufar, W., Born, M., & Klose, E. (1976). *Beitrag zur Optimierung der Packungsdichte Polydisperse Körniger Systeme Freiberger Forschungsheft A 558*. VEB Deutscher Verlag fur Grundstoffindustrie.

Toufar, W., Klose, E., & Born, M. (1977). *Berechnung der Packungsdichte von Korngemischen*. Aufbereitungs-Technik.

Underwood, B. S., & Kim, Y. R. (2011). Experimental investigation into the multiscale behaviour of asphalt concrete. *International Journal of Pavement Engineering*, *12*(4), 357–370. https://doi.org/10.1080/10298436.2011.574136

Underwood, B. S., & Kim, Y. R. (2013). Effect of volumetric factors on the mechanical behavior of asphalt fine aggregate matrix and the relationship to asphalt mixture properties. *Construction and Building Materials*, *49*, 672–681. https://doi.org/10.1016/j.conbuildmat.2013.08.045

Underwood, B. S., & Kim, Y. R. (2013a). Mechanistic Behaviors of Fine Aggregate Matrix and

its Relation to Asphalt Mixture Behaviors. In *Transportation and Development Inst. Airfield and Highway Pavement Conference June 12, 2013*.

Underwood, B. S., & Kim, Y. R. (2013b). Microstructural Association Model for Upscaling Prediction of Asphalt Concrete Dynamic Modulus. *Journal of Materials in Civil Engineering*, *25*, 1153–1161. https://doi.org/10.1061/(ASCE)MT.1943-5533.0000657.

Underwood, B. S., & Kim, Y. R. (2013c). Microstructural Investigation of Asphalt Concrete for Performing Multiscale Experimental Studies. *International Journal of Pavement Engineering*, *14*(5), 498–516. https://doi.org/10.1080/10298436.2012.746689

Valenta, R., Sejnoha, M., & Zeman, J. (2018). Macroscopic constitutive law for Mastic Asphalt Mixtures from multiscale modeling. *International Journal for Multiscale Computational Engineering*.

Vasconcelos, K. L., Bhasin, A., & Little, D. N. (2010). Influence of Reduced Production Temperatures on the Adhesive Properties of Aggregates and Laboratory Performance of Fine Aggregate-Asphalt Mixtures. *Road Materials and Pavement Design*, *11:1*, 47–64. https://doi.org/10.3166/RMPD.11.47-64

Vasconcelos, K. L., Bhasin, A., Little, D. N., & Lytton, R. L. (2011). Experimental Measurement of Water Diffusion through Fine Aggregate Mixtures. *Journal of Materials in Civil Engineering*. https://doi.org/10.1061/(ASCE)MT.1943-5533.0000190

Vavrik, W. R., Huber, G., Pine, W. J., Carpenter, S. H., & Bailey, R. (2002). Bailey Method for Gradation Selection in Hot-Mix Asphalt Mixture Design. *Transportation Research CIRCULAR, E-C044*.

Vavrik, W. R., Pine, W. J., Huber, G., Carpenter, S. H., & Bailey, R. (2001). The Bailey Method of Gradation Evaluation: The Influence of Aggregate Gradation and Packing Characteristics on Voids in the Mineral Aggregate, 132–175.

Wang, D., Cannone Falchetto, A., Alisov, A., Schrader, J., & Riccardi, C. (2019). An Alternative Experimental Method for Measuring the Low Temperature Rheological Properties of Asphalt Binder by using 4-mm Parallel Plates on Dynamic Shear Rheometer. *Transportation Research Board Annual Meeting January 13-17, 2019 Washington, D.C.*

Wang, D., Cannone Falchetto, A., & Riccardi, C. (2019). Effect of Glass Transition Temperature and Normal Shift Factor on Low Temperature Properties of Asphalt Binder. *Transportation Research Board Annual Meeting January 13-17, 2019 Washington, D.C.*

Williams, M. L., Landel, R. F., & Ferry, J. D. (1955). The Temperature Dependence of Relaxation Mechanisms in Amorphous Polymers and Other Glass-Forming Liquids. *J A*

Chem Soc, *77 (14)*, 3701–3707. https://doi.org/10.1021/ja01619a008

Wistuba, M. P. (2016). The German segmented steel roller compaction method – state-of-the-art report. *International Journal of Pavement Engineering*, *17*, 81–86. https://doi.org/10.1080/10298436.2014.925555

You, T., Masad, E. A., Al-rub, R. K. A., Kassem, E., & Little, D. N. (2014). Calibration and Validation of a Comprehensive Constitutive Model for Asphalt Mixtures. *Transportation Research Record*, *2447*(02), 13–22. https://doi.org/10.3141/2447-02

Yusoff, N. I. M., Mounier, D., Marc-Stéphane, G., Hainin, M. R., Airey, G. D., & Di Benedetto, H. (2013). Modelling the rheological properties of bituminous binders using the 2S2P1D Model. *Construction and Building Materials*, *38*, 395–406. https://doi.org/10.1016/j.conbuildmat.2012.08.038

Yusoff, N. I., Mounier, D., & Airey, G. D. (2014). The 2S2P1D: An Excellent Linear Viscoelastic Model. *UNIMAS E-Journal of Civil Engineering*, *5*.

Zeng, M., Bahia, H. U., Zhai, H., Anderson, M. R., & Turner, P. (2001). Rheological Modeling of Modified Asphalt Binders and Binders. *Asphalt Paving Technology: Association of Asphalt Paving Technologists-Proceedings of the Technical Sessions 70*, 403–441.

Zhu, J., Alavi, M. Z., Harvey, J., Sun, L., & He, Y. (2017). Evaluating fatigue performance of fine aggregate matrix of asphalt mix containing recycled asphalt shingles. *Construction and Building Materials*, *139*, 203–211. https://doi.org/10.1016/j.conbuildmat.2017.02.060

Zollinger, C. J. (2005). Application of Surface Energy Measurements to Evaluate Moisture Susceptibility of Asphalt and Aggregates. *Master Degree Thesis at Texas A&M University*.

ANNEXES

ANNEX A: Mastercurves

- *Mastercurves of B_11, M_111, FAM_111 and Mix_111- Paragraph 3.4*
- *Mastercurves of B_21, M_211, FAM_211 and Mix_211*

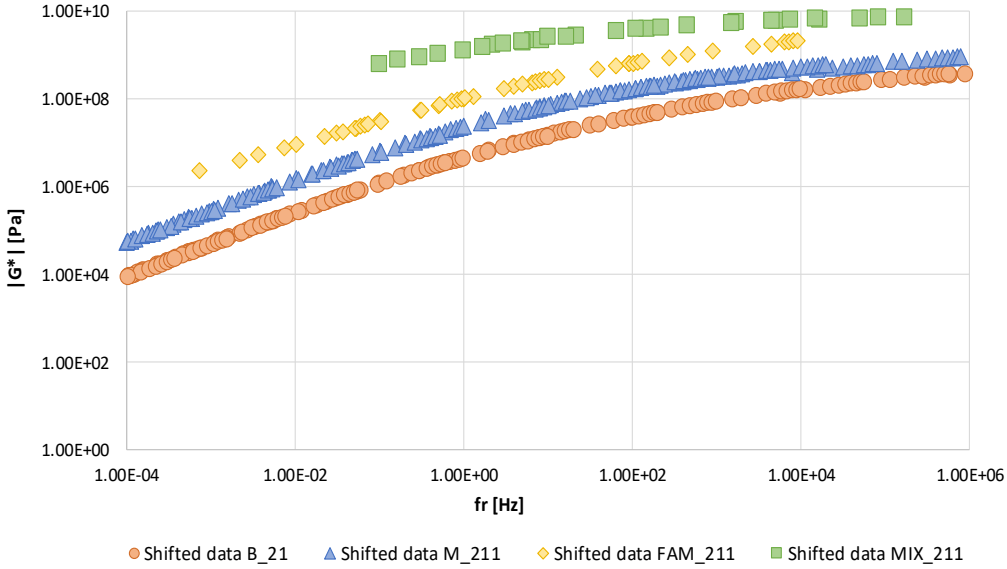

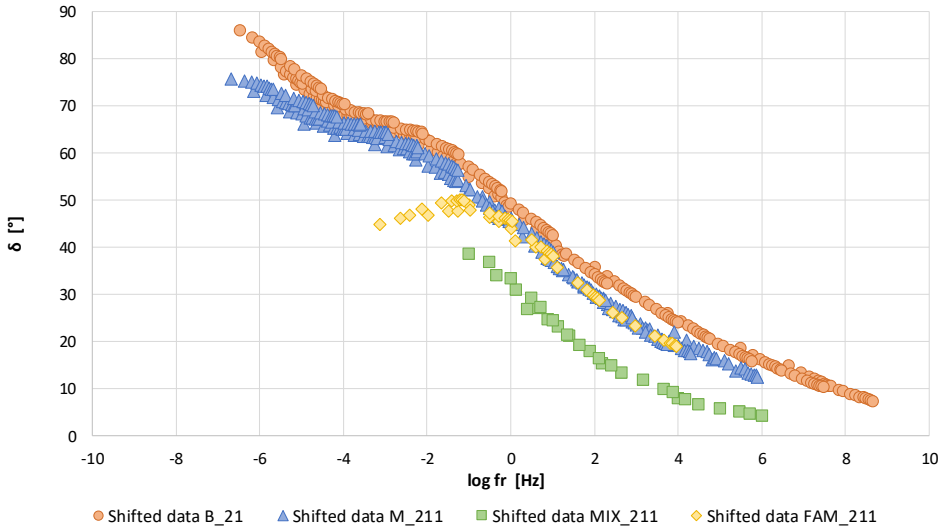

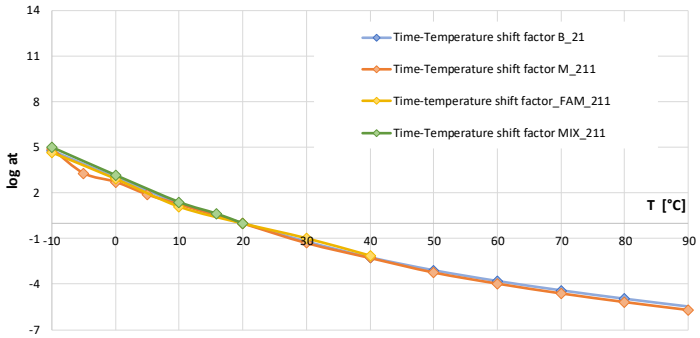

- *Mastercurves of B_32, M_321, FAM_321 and Mix_321*

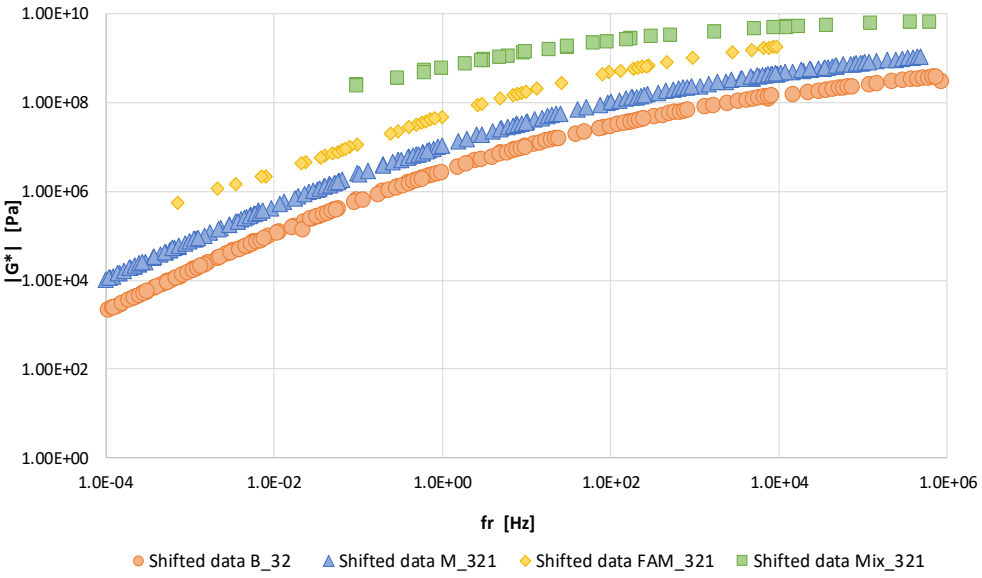

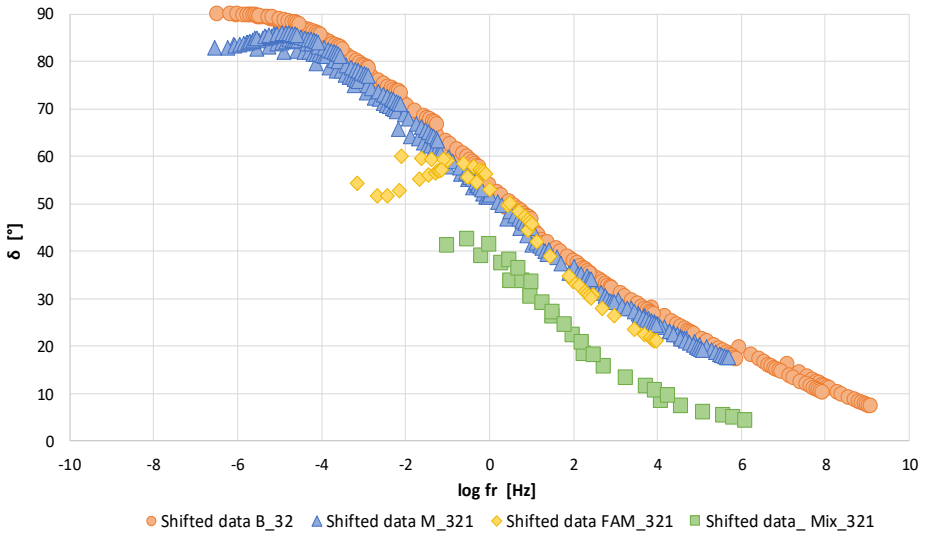

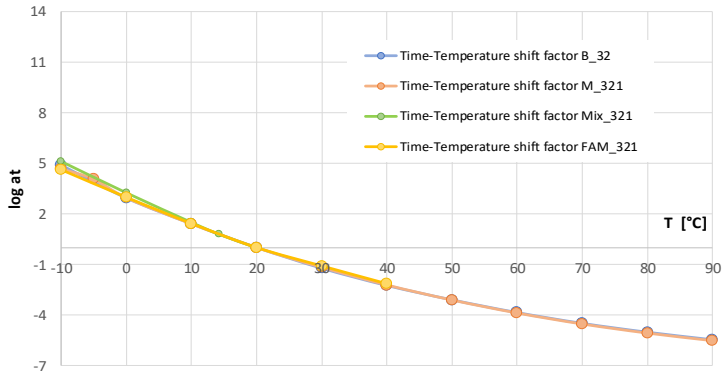

- *Mastercurves of B_42, M_421, FAM_421 and Mix_421*

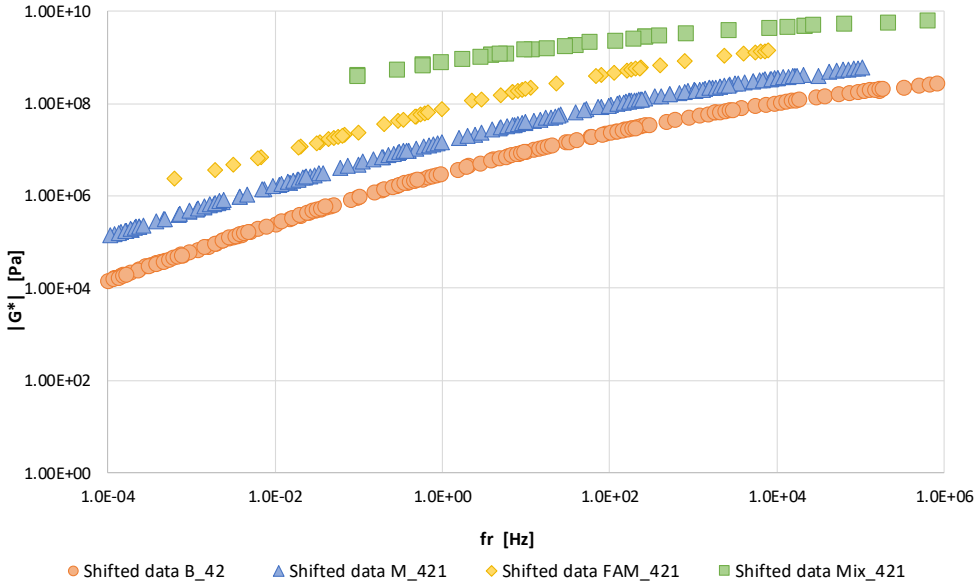

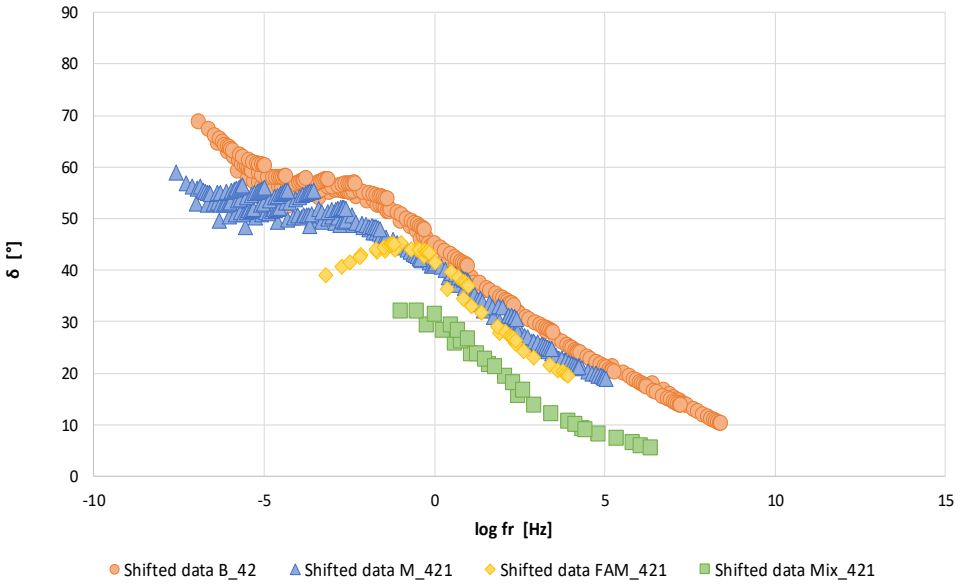

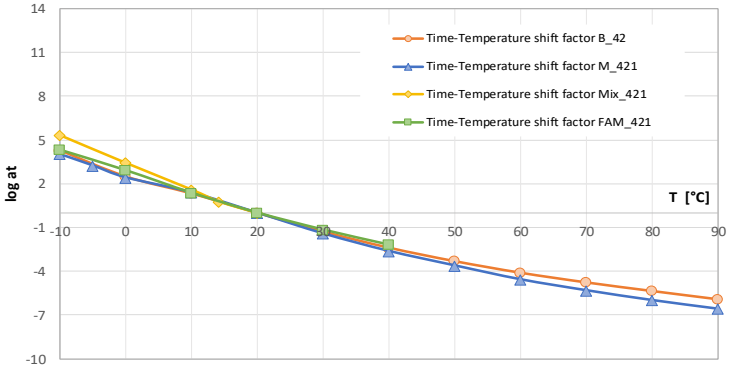

ANNEX B: Black diagrams

- *Binders*

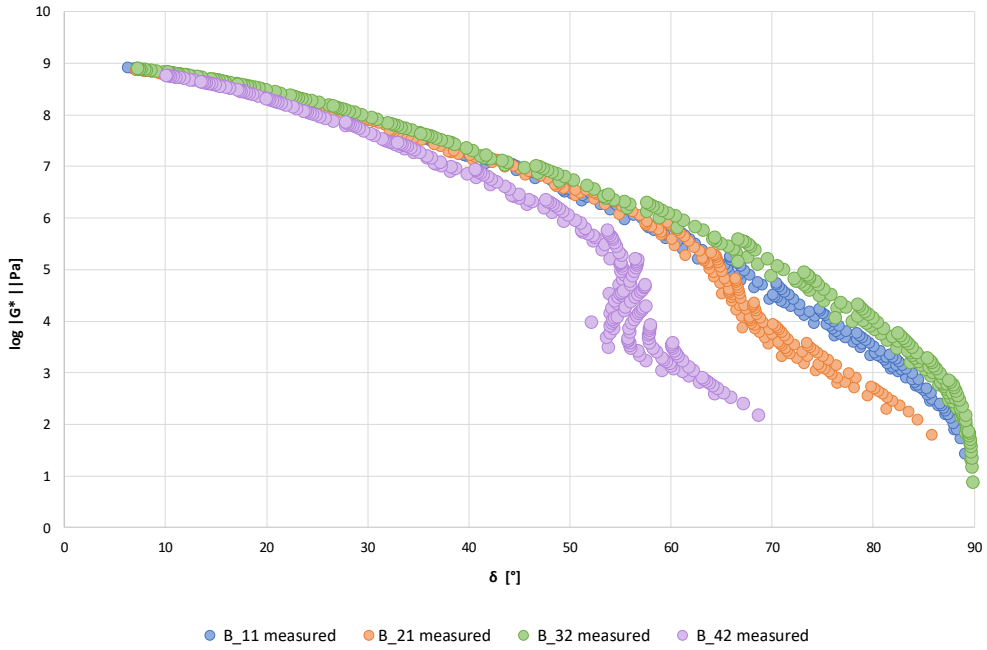

- *Mastics*

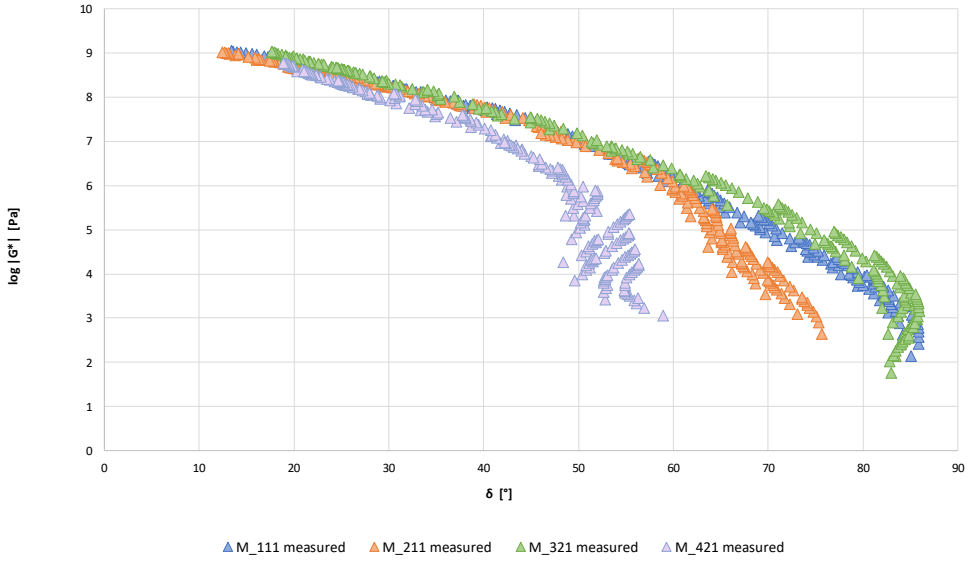

- *FAM*

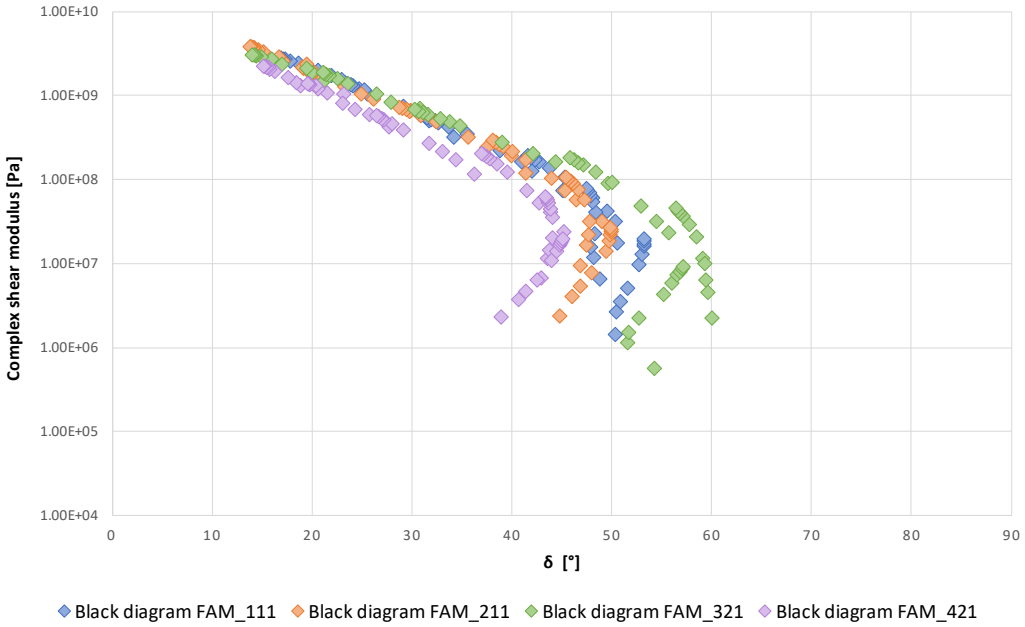

- *Asphalt mixtures*

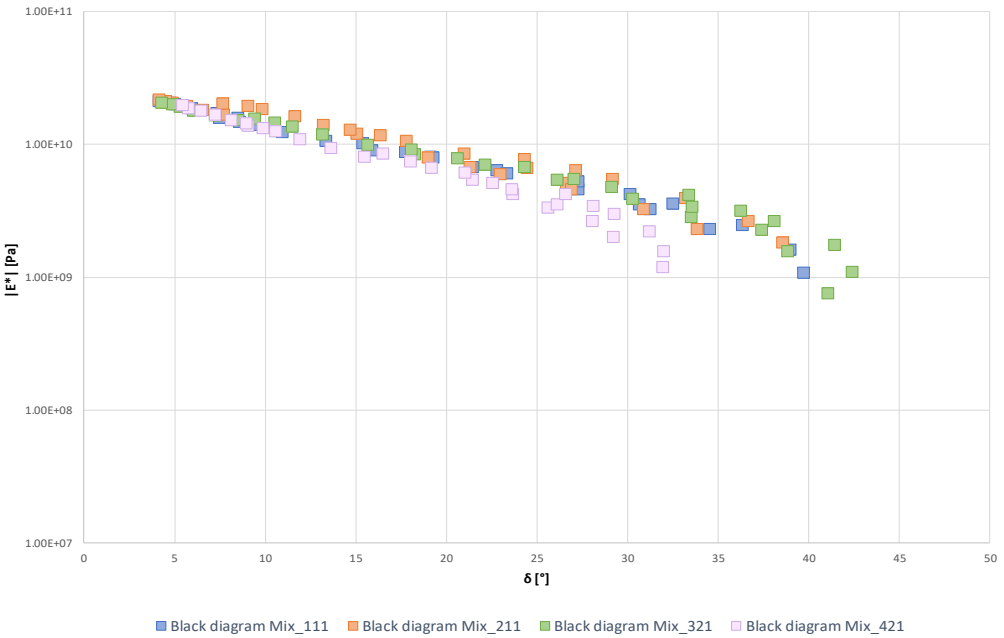

ANNEX C: Cole- Cole normalized- binder parameters

- *Cole-Cole normalized with δ, k, h and β parameters fixed from binder phase of B_11, M_111, FAM_111 and Mix_111*

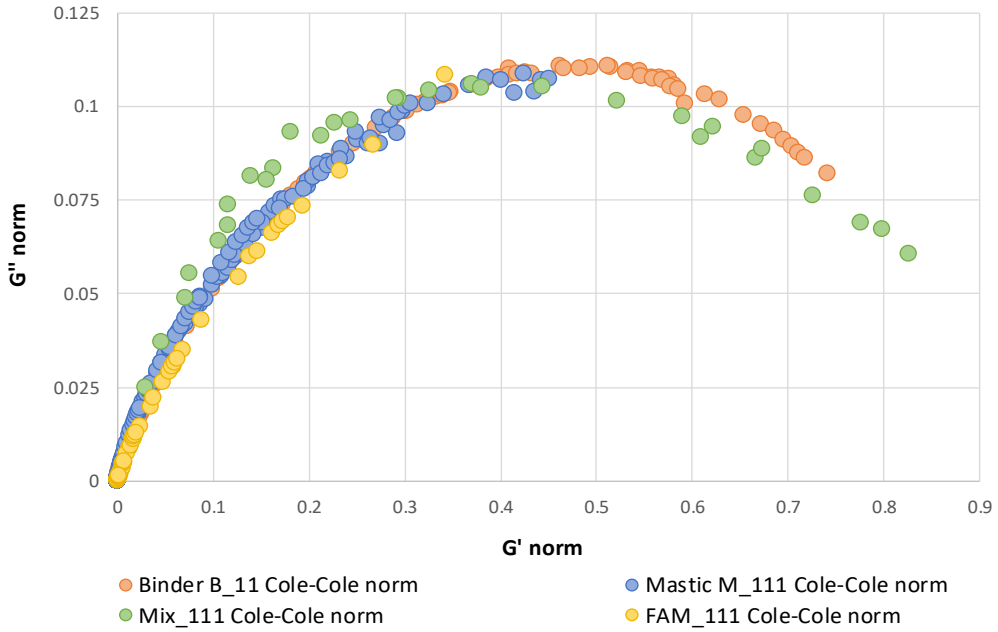

- *Cole-Cole normalized with δ, k, h and β parameters fixed from binder phase of B_21, M_211, FAM_211 and Mix_211- Paragraph 4.1*

- *Cole-Cole normalized with δ, k, h and β parameters fixed from binder phase of B_32, M_321, FAM_321 and Mix_321*

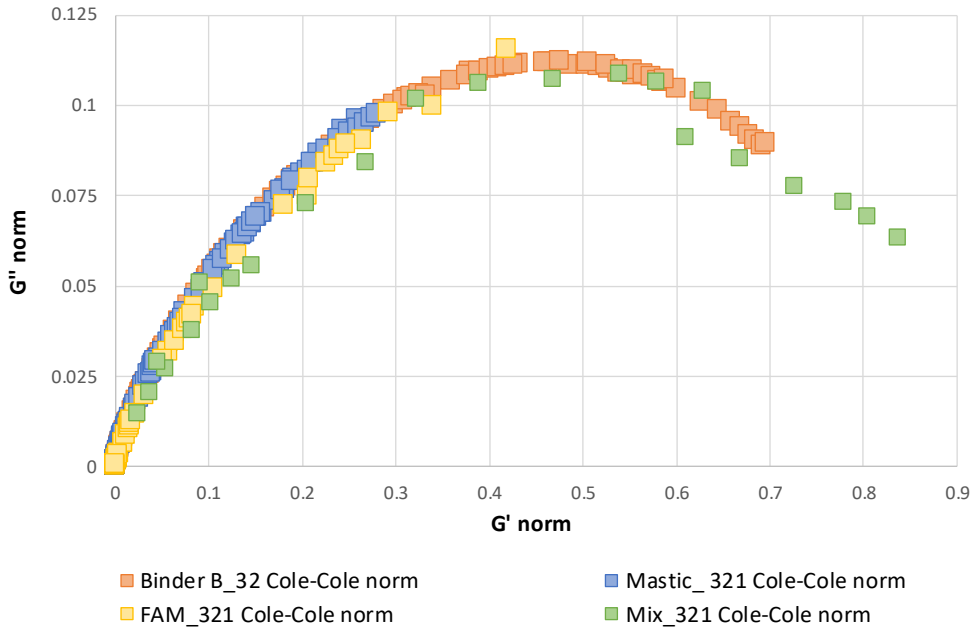

- *Cole-Cole normalized with δ, k, h and β parameters fixed from binder phase of B_42, M_421, FAM_421 and Mix_421*

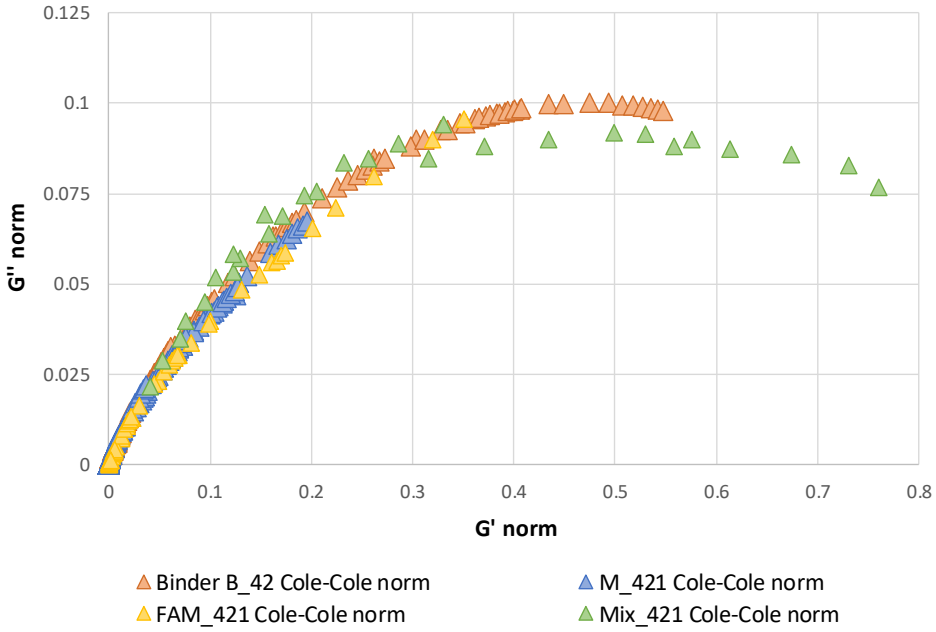

ANNEX D: Cole- Cole normalized- FAM parameters

- *Cole-Cole normalized with δ, k, h and β parameters fixed from FAM phase of FAM_111 and Mix_111*

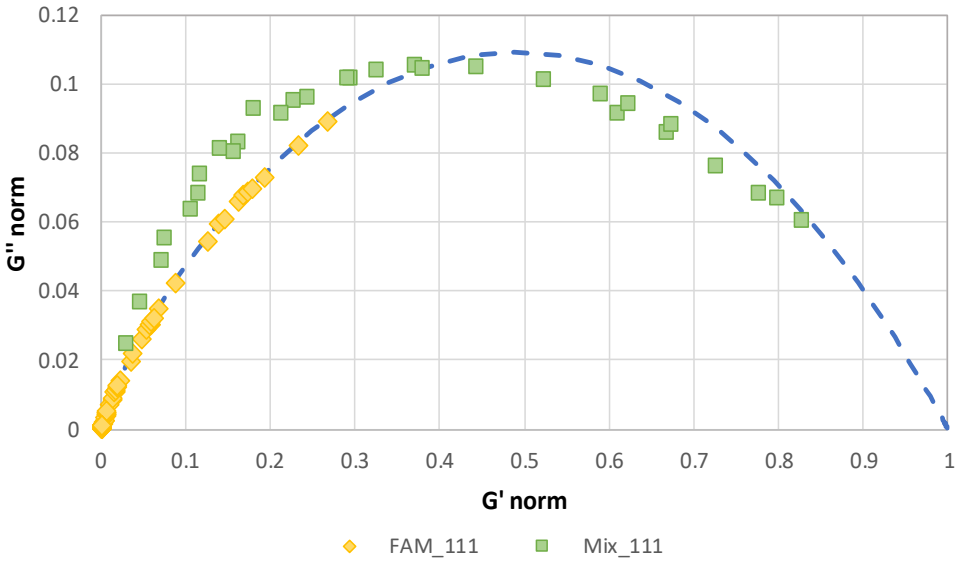

- *Cole-Cole normalized with δ, k, h and β parameters fixed from FAM phase of FAM_211 and Mix_211- Paragraph 5.1*

- *Cole-Cole normalized with δ, k, h and β parameters fixed from FAM phase of FAM_321 and Mix_321*

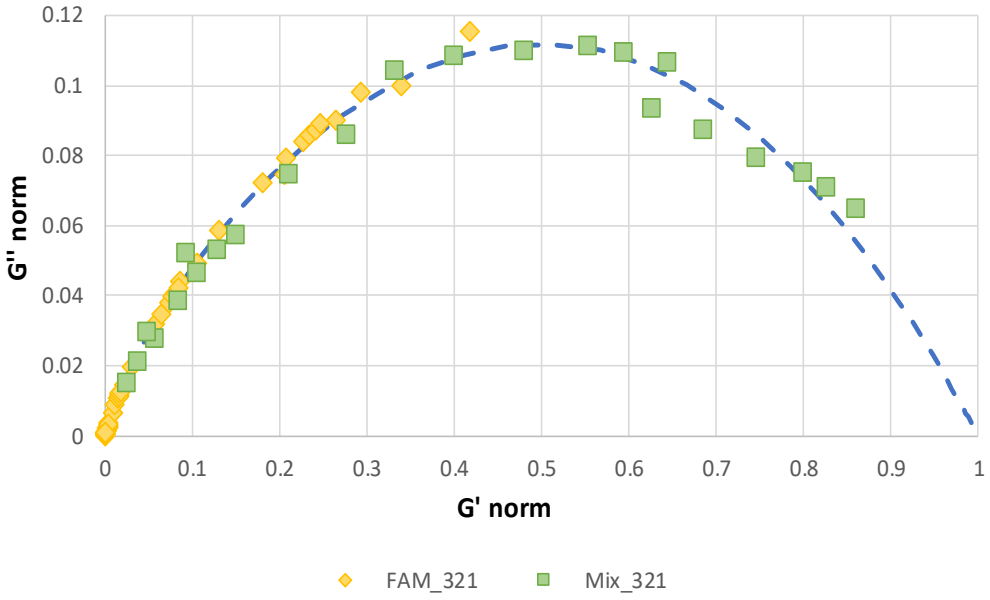

- *Cole-Cole normalized with δ, k, h and β parameters fixed from FAM phase of FAM_421 and Mix_421*